

Contents

6.1	Introduction	245
6.2	Stratigraphic Mapping with Petrophysical Logs	245
6.2.1	Log Shape and Electrofacies.....	246
6.2.2	Examples of Stratigraphic Reconstructions	249
6.2.3	Problems and Solutions.....	251
6.3	Seismic Stratigraphy	254
6.3.1	The Nature of the Seismic Record.....	255
6.3.2	Constructing Regional Stratigraphies.....	263
6.3.3	Seismic Facies	268
6.3.4	Seismic Geomorphology	272
6.4	Directional Drilling and Geosteering	276
6.5	Older Methods: Isoleth Contouring	278
6.6	Mapping on the Basis of Detrital Composition	280
6.6.1	Clastic Petrofacies	280
6.6.2	Provenance Studies Using Detrital Zircons	288
6.6.3	Chemostratigraphy	290
6.7	Paleocurrent Analysis	292
6.7.1	Introduction.....	292
6.7.2	Types of Paleocurrent Indicators	293
6.7.3	Data Collection and Processing	297
6.7.4	The Bedform Hierarchy.....	299
6.7.5	Environment and Paleoslope Interpretations.....	300
References	305

6.1 Introduction

In the introduction to this chapter in the 2000 edition of *“Principles of sedimentary basin analysis”* I said (p. 249):

The art of basin mapping is one of reconstructing paleogeography and fill geometry from very limited evidence. Being skilled at data synthesis, interpretation, and extrapolation is of prime importance. Maps drawn only from outcrop data are rarely sufficiently accurate or useful for subsurface predictions, because they do not contain an adequate, three-dimensional distribution of data points.

This statement now qualifies as a historically interesting comment, because the maturation of sequence stratigraphy and developments in reflection-seismic methods have caused a complete change in the practice of basin mapping. In 2000, seismic stratigraphy had assumed considerable importance, but a reliance on scattered exploration wells was still essential. Sequence methods have advanced substantially since then, and now comprise a comprehensive set of predictive tools for the tracking of stratigraphic units in the surface and subsurface. The basic methods, including an introduction to the topic of seismic facies, are described in Chap. 5. Modern, sophisticated, digital methods for the processing and display of seismic data have made the work of the subsurface geologist immeasurably easier. These new methods include an increasingly common use of three-dimensional seismic data volumes, from which cross-sections in any orientation, and stratigraphically horizontal seismic maps can readily be constructed, enabling the three-dimensional visualization of complex stratigraphic objects. Such objects reflect the depositional, structural and diagenetic processes by which stratigraphy is constructed, and this new ability for three-dimensional visualization has led to the growth of an entirely new tool, that of **seismic geomorphology**—the study of ancient landscapes and depositional systems based on 3-D seismic data. Petrophysical and core data are essential in providing the “ground truthing” of seismic interpretations, such as confirming complex correlations and providing necessary lithofacies and biostratigraphic detail, but in many cases they no longer

provide the primary data set from which the subsurface geophysicists and geologists do their work.

Seismic data are used to generate and extend a stratigraphic synthesis across a broad project area. Older methods, such as facies and isopach mapping, and paleocurrent analysis (mainly useful for surface work) do not provide this level of detail, and are useful mainly in order to explore regional basinal trends, including the direction of paleoslope, differential subsidence patterns, and regional facies trends. These methods are included in this chapter for completeness, because not all mapping projects have access to seismic data.

6.2 Stratigraphic Mapping with Petrophysical Logs

6.2.1 Log Shape and Electrofacies

Well-log data are used for stratigraphic correlation and for lithologic interpretation. They may also be used directly for facies mapping purposes. As noted briefly in Sect. 2.4, various combinations of logs can be employed in crossplots to yield lithologic information. These relationships can be converted into computer algorithms, and where log data are digitized and stored in data banks, a powerful automated mapping technique becomes available. Digital log data can also be displayed and manipulated using interactive computer graphics routines, a facility that permits easy comparisons for stratigraphic correlation purposes, plus checking for accuracy, and for the normalizing of logs made at different times using different hole conditions, and many other purposes. Well-log service companies have devoted considerable energy to devising and marketing automated processing and display techniques for use in basin analysis and petroleum development, but all such techniques suffer from the limitation that petrophysical responses are very location-specific. The techniques cannot be used without much initial careful calibration to local petrographic and groundwater conditions.

An early example of the use of petrophysical log data for mapping purposes was given by McCrossan (1961). He constructed a resistivity map for the lower and middle Ireton Formation of central Alberta that can be used to predict the proximity to reefs (Fig. 6.1). The Ireton is an Upper Devonian basinal shale that drapes against the reefs. Calcareous content and thus resistivity increase close to the reefs because of the presence of reef talus. The resistivity data therefore provide a useful analogue paleogeographic map.

The recognition of characteristic log “shapes” and distinctive vertical-profile character in siliciclastic deposits (**electrofacies**) may be a useful tool for correlation purposes (Figs. 6.2 and 6.3). Regardless of their lithology, facies or environment, lithologic units typically have a recognizable

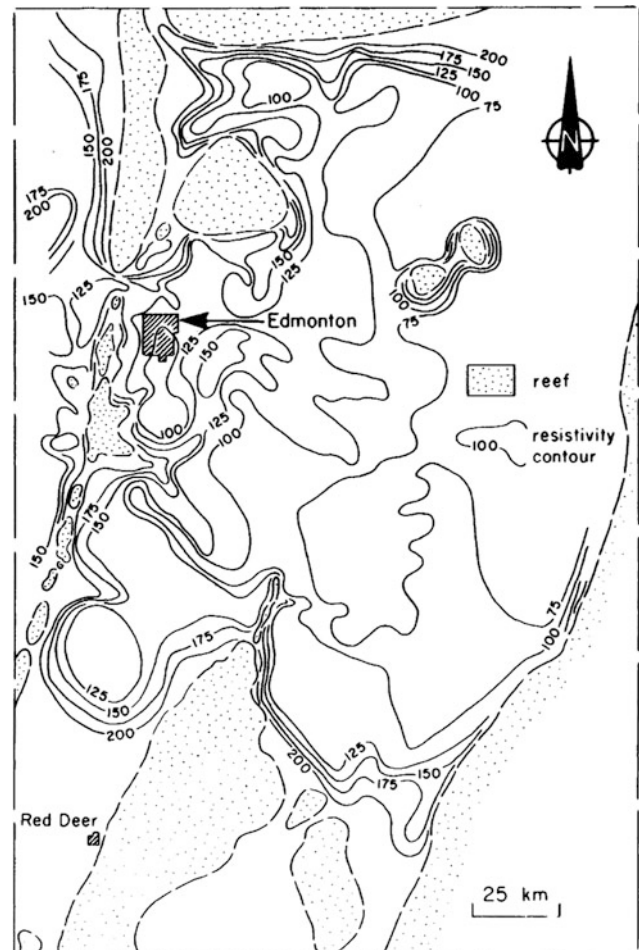


Fig. 6.1 Resistivity map of the Ireton Formation (Devonian), central Alberta. High values indicate an increase in carbonate content adjacent to reef bodies (McCrossan 1961)

profile on petrophysical logs, which enables them to be traced and correlated from well to well. The ease and reliability of this mapping technique depends on how rapidly lithologic units change in thickness and facies laterally. Where there is considerable lateral variability, as in channelized deposits such as fluvial systems and submarine fans, it may be difficult or impossible to correlate reliably between drill holes. Much depends on hole spacing. Figure 6.2 is an example of a lithologic succession that shows little change from hole to hole, over distances of several kilometres, which permits every major unit to be defined and correlated on the stratigraphic cross section. By contrast, in Fig. 6.3, with greater well spacing, several units thin, change lithology or thin out altogether across the section, which makes correlation more difficult. The use of log shape analysis to interpret vertical facies successions and characterize certain sedimentary environments is described in Sect. 3.5.10.

The application of sequence-stratigraphic techniques, including the identification of systems tracts, may

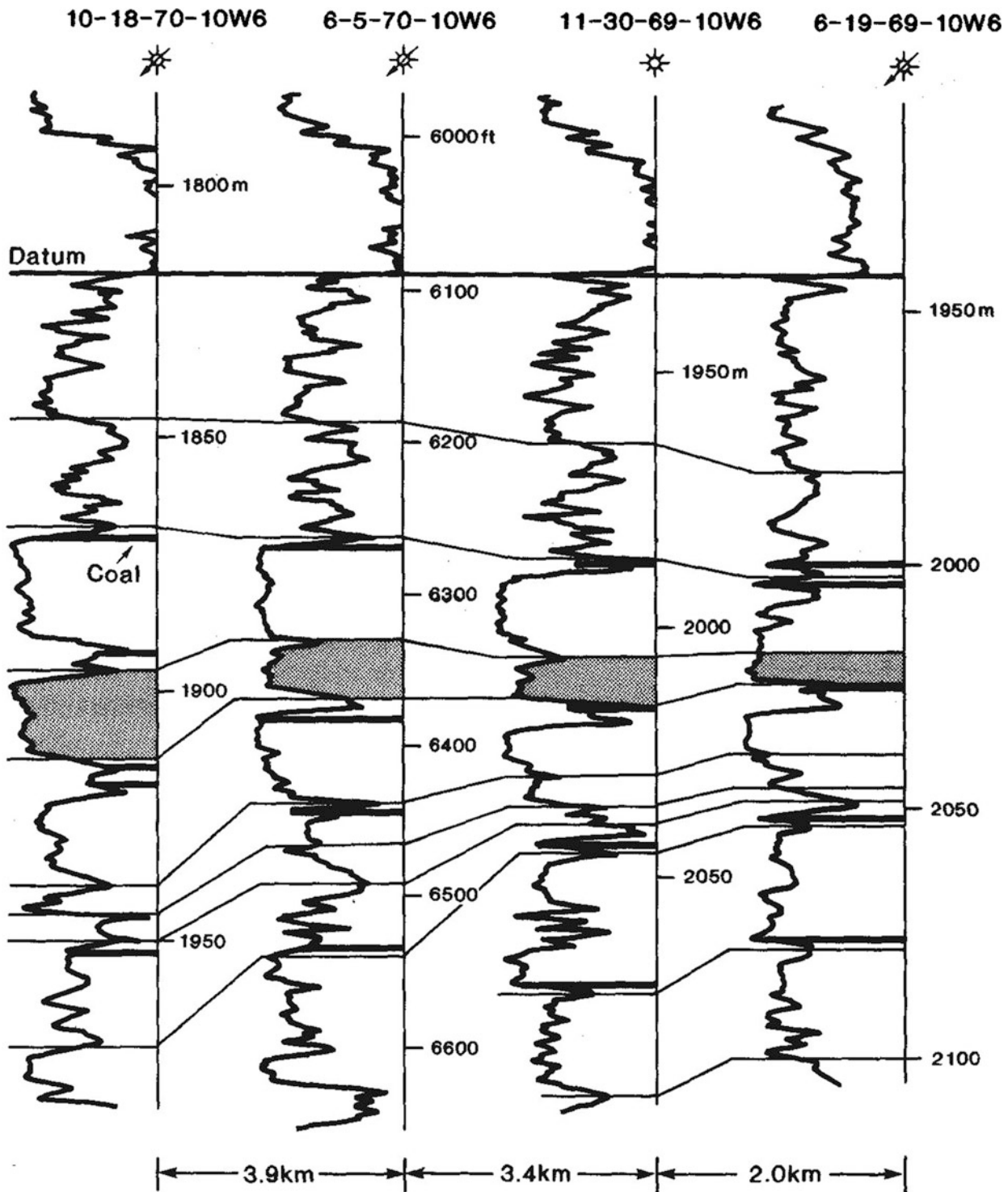


Fig. 6.2 A suite of gamma-ray logs, showing how log-shape may be used to carry out subsurface lithostratigraphic correlation (Cant 1992)

considerably improve the practice of log correlation because of their predictive value. The various elements of many standard sequence models commonly have distinctive lithologies and geometries, and typically occur in the same vertical succession, which provides useful clues for

interpretation and correlation (Chap. 5). For example, incised valleys that commonly cut down into highstand deposits may consist of distinctive coarse channel-fill deposits incised into layered, fine-grained shelf deposits; sequence boundaries in clastic successions are commonly

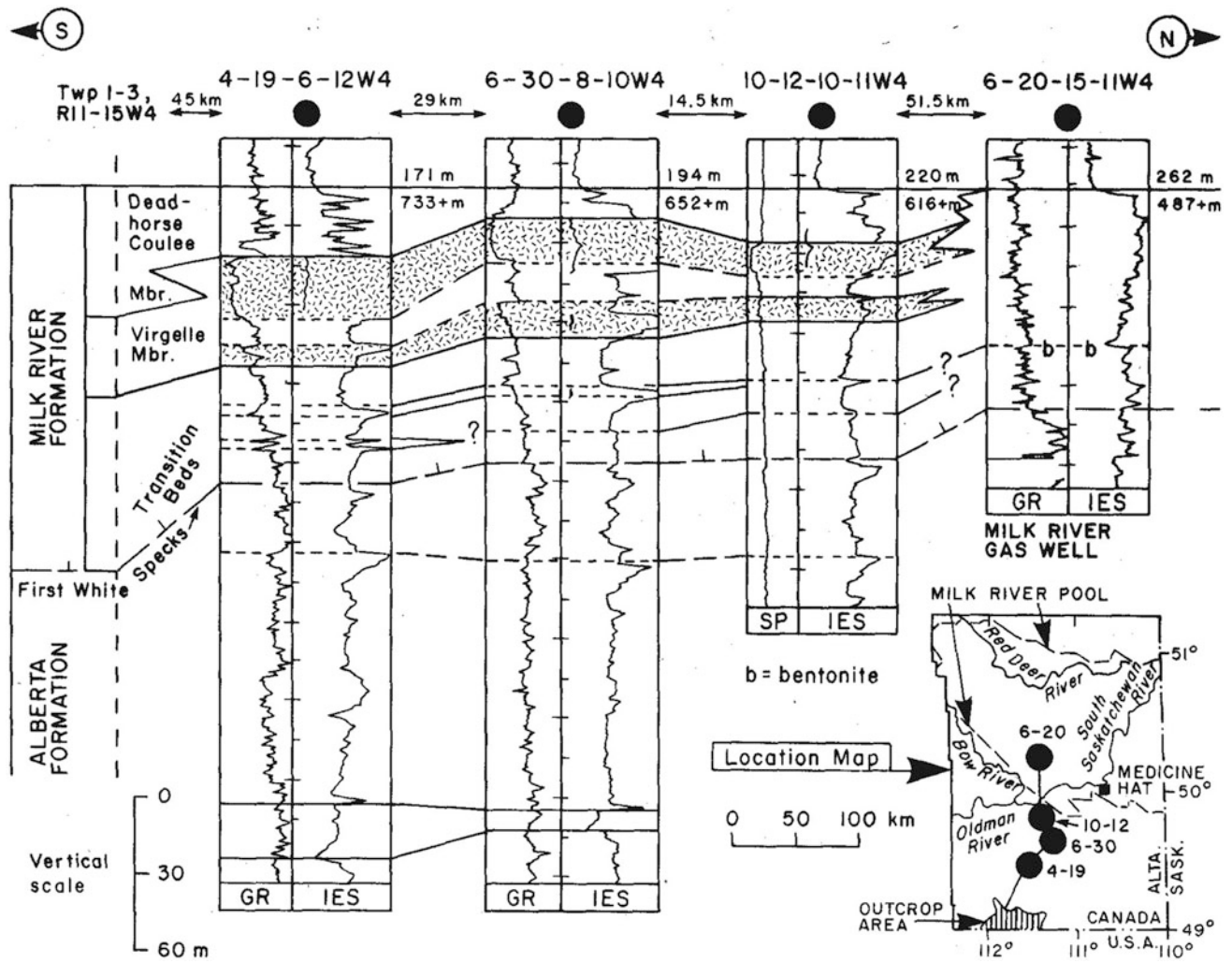


Fig. 6.3 Use of gamma ray (GR), spontaneous potential (SP), and induction electric survey (IES) logs to correlate subsurface sections. This diagram shows that where lithostratigraphic units retain similar

thickness and lithology they can readily be correlated using geophysical logs. Cretaceous, Alberta (Myhr and Meijer-Drees 1976)

marked by widespread coarse-grained deposits; maximum flooding surfaces may be recognized by widespread “hot” (radioactive) shales (usually detected by the use of high readings on the gamma-ray log) or by condensed deposits, and so on.

Log shape analysis may be a useful aid for interpreting depositional environment (Figs. 3.61–3.63). The analysis depends on the distinctiveness of the vertical profile through a sandstone body, and our ability to interpret this profile in terms of depositional processes and environment. The well-known bell-shaped gamma ray or spontaneous-potential log response yielded by a typical fluvial fining-upward cycle, is a classic example (Visher 1965). The study of an interpreted subsurface point-bar sandstone by Berg (1968) is an early example of the application of these ideas to a practical exploration problem.

Despite the dramatic increase in the volume and quality of reflection-seismic data, the correlation of petrophysical logs

is still the best means to construct a sequence-stratigraphy for any stratigraphic volume that has an adequate network of exploration holes. For example, the huge data-base of well-logs stored by the Alberta government in Calgary has enabled A.G. Plint and his students and colleagues to extend parts of the high-resolution sequence framework of the Cretaceous succession over the entire province of Alberta and to extend it southward into Montana, where it can be tied into American work on the same part of the stratigraphic record. Shank and Plint (2013) constructed a network of petrophysical log-correlation cross-sections of the Cardium Alloformation (Turonian-Coniacian) across the entire province, and Walaszczyk et al. (2014) tied this framework into the biostratigraphic and sequence framework of Montana, from whence it can be related to the cyclostratigraphic research underway across the Rocky Mountains states, using the so-called HiRES techniques first developed by Kauffman (1986, 1988). As discussed in Sect. 8.11, Locklair and

Sageman (2008) and Sageman et al. (2014) are developing a tightly constrained astrochronological time scale for equivalent rocks in the latter area.

6.2.2 Examples of Stratigraphic Reconstructions

Three modern examples of the use of petrophysical log correlation are discussed in this section. In the first, core and log data are used to provide a facies classification of the shallow-marine Bakken Formation in Saskatchewan where log correlation is made considerably easier by the recognition of key sequence surfaces and systems tracts. In the second example, a new model for the Marcellus Shale of New York shows how the correct choice of datum and the application of a new depositional model not only clarifies the stratigraphy but provides useful information for the understanding of the distribution of organic-rich shales, the source of the shale gas in this unit. In the last example, log shape

analysis is used to map the complex pattern of facies that constitute a Tertiary fluvial system in Texas.

The Bakken Formation is a marine siliciclastic unit of Upper Devonian and Lower Carboniferous age that extends across the Williston Basin (mainly North and South Dakota, Saskatchewan, southeastern Alberta and Montana,). In recent years, fracking operations in this unit in North Dakota have turned that state into one of the leading US producers of oil, gas and gas liquids. In this section we refer to a core and petrophysical log study of the unit carried out across southern Saskatchewan (Angulo and Buatois 2012). The formation has been subdivided into three members: lower and upper organic-rich black shale members and a middle member of dolomitic siltstone and sandstone, which constitutes the main hydrocarbon reservoir. Further subdivisions of the middle member are shown in Fig. 6.4. The three members may be traced on petrophysical logs throughout the Williston Basin, with the upper and lower members characterized by unusually high gamma-ray readings, reflecting

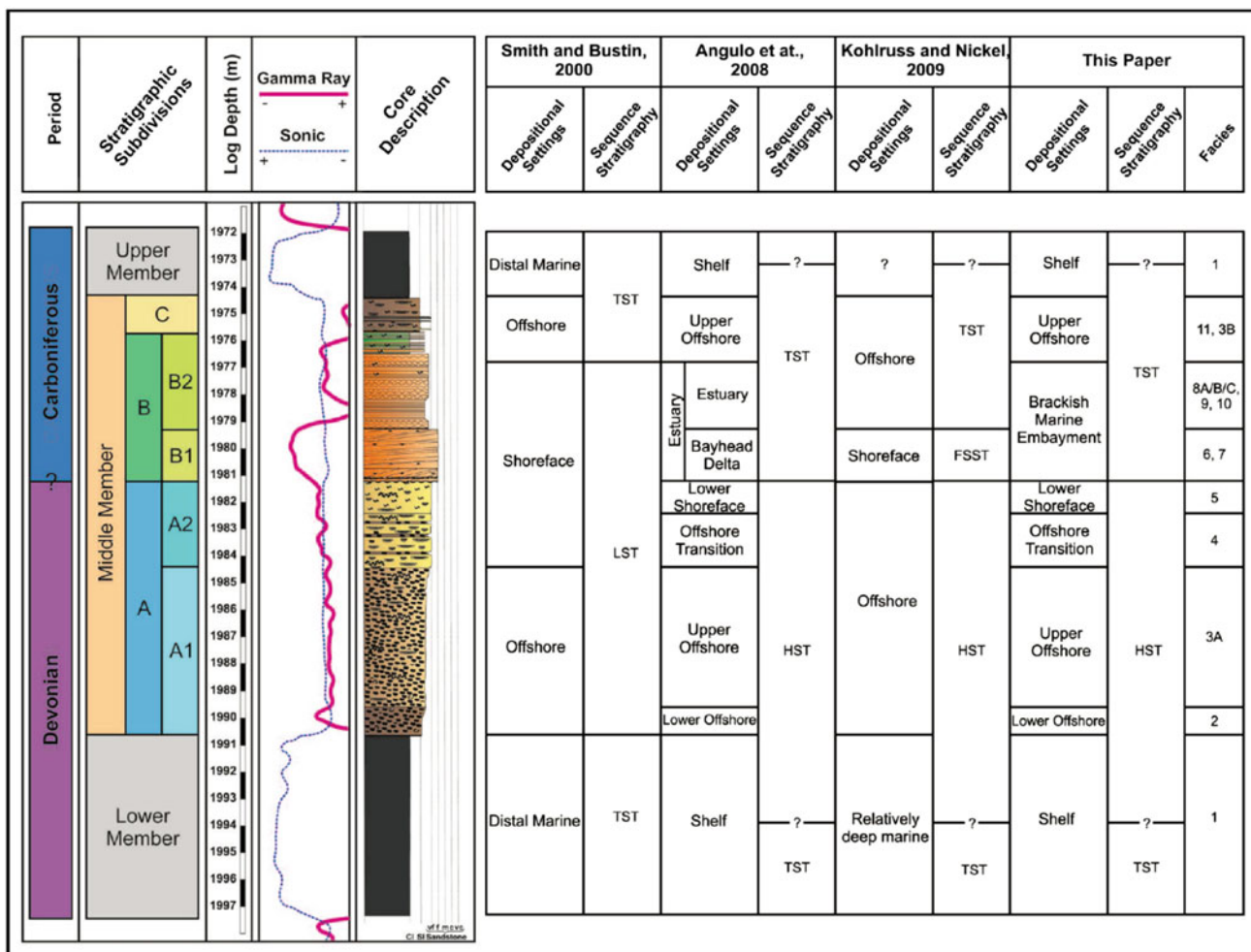


Fig. 6.4 Core and log characteristics and stratigraphic subdivision of the Bakken Formation of southern Saskatchewan (Angulo and Buatois 2012). AAPG © 2012, reprinted by permission of the AAPG whose permission is required for further use

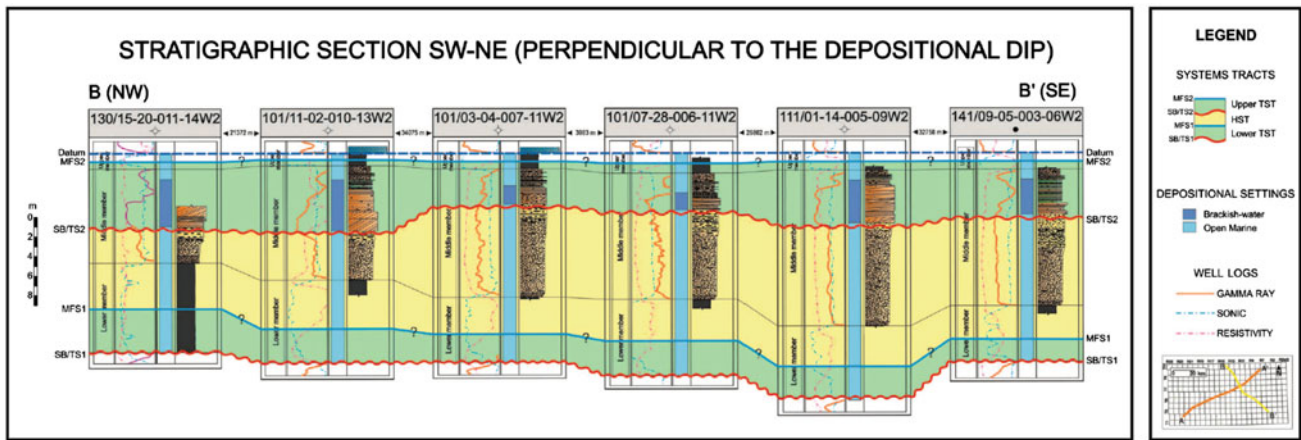


Fig. 6.5 Stratigraphic cross-section through the Bakken Formation, Saskatchewan (Angulo and Buatois 2012). AAPG © 2012, reprinted by permission of the AAPG whose permission is required for further use

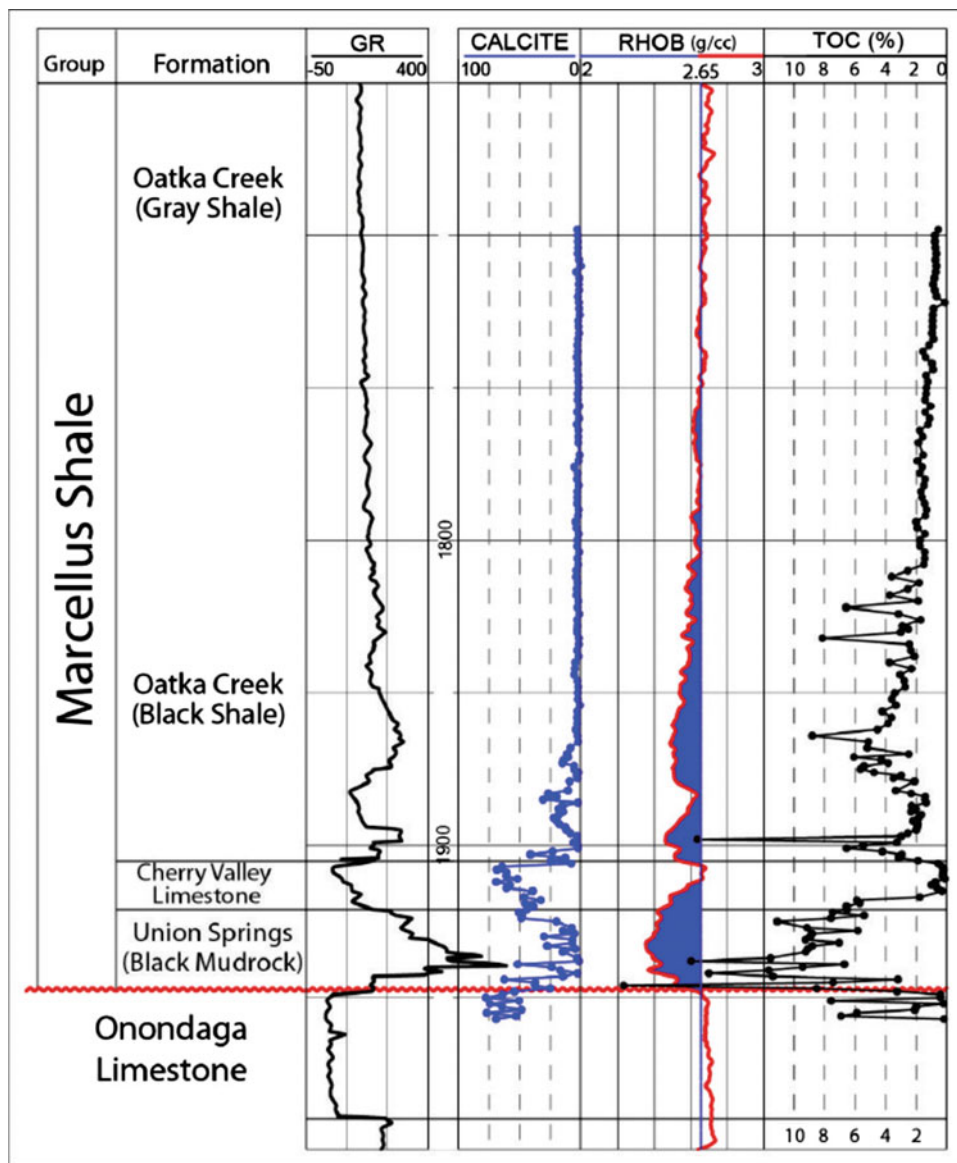
the concentration of radioactive elements in the organic shales. Eleven lithofacies types have been recognized by Angulo and Buatois (2012), falling into two broad facies associations, open-marine, and brackish-water marginal-marine. As shown in Fig. 6.4, a sequence analysis demonstrates that the lower member and the lower part of the middle member comprises a regressive (transgressive to highstand) systems tract, with a sequence boundary occurring at the base of a brackish-marine shoreface sandstone in the middle of the middle member, and the upper part of the Bakken Formation interpreted as a transgressive systems tract. Figure 6.5 shows how core and petrophysical-log data may be used to correlate these units across Saskatchewan. The distinctive deflections and shapes of the gamma ray, sonic and resistivity logs through each of these members are apparent from this diagram.

The second example described here is a re-analysis of the basin setting and configuration of the stratigraphic section that contains the important gas bearing unit, the Marcellus Shale (Smith and Leone 2014). Well logs were first calibrated against calculated values for total organic carbon and calcium carbonate obtained from core analyses (Fig. 6.6). Earlier basin models had suggested that the Marcellus Shale was a distal component of the Catskill clastic wedge that downlapped westward into an anoxic basin up to 250 m deep constituting the Appalachian foreland basin. However, the stratigraphic setting of nearby outcrops of similar organic-carbon-rich rocks suggests that they were deposited in shallow water over the basin forebulge in water depths probably less than 50 m. Instead of basing stratigraphic interpretations on the concept of a basal downlap surface, Smith and Leone (2014) used markers higher in the section as datum and constructed a different stratigraphic model (Fig. 6.7). In this model organic shales thin but become more organic rich westward as they interbedded with progressively

thicker carbonate units. This configuration led to a different depositional model. Instead of a deep anoxic basin in which the organic shales were deposited, the authors suggested the occurrence of seasonal anoxia in a shallow-water basin, with recycling of nutrients delivered from the Catskill “delta” complex. The richest organic shales are those further to the west, the most distal from the clay influx from the delta. They onlap multiple unconformities westward onto a tectonically positive forebulge. In an eastward direction they are interbedded with turbidites derived from the Appalachian orogen. For other examples of petrophysical (and seismic) mapping of fine-grained rocks, the reader is referred to Bohacs et al. (2002).

The third example discussed briefly here demonstrates how petrophysical log correlation and the analysis of log shape was used to document the stratigraphy of a coastal clastic system and identify and map the array of lithofacies constituting the deltaic-barrier-lagoon system within which these deposits were formed (Zeng et al. 1996). Figure 6.8 is a dip-oriented cross-section through two progradational shelf-shoreface-coastal successions separated by a surface of transgression. Fourteen sandstone units have been identified and correlated across the study area. These show considerable lateral persistence, but display significant differences in log shape across the area. Facies analysis of each sandy depositional unit was derived from SP log character (and sometimes from resistivity log shape) and sandstone geometry. Some sidewall cores provided information on grain size and mineral identification. No conventional cores were available for this study. SP log patterns for 11 sandy units in the middle of the modeled section distinguished three major log facies: blocky, upward fining, and mixed (Fig. 6.9). These patterns were used to group sandy units developed in similar depositional environments. The distribution of these patterns in within three of the sandstone units is shown in the

Fig. 6.6 Calibration of petrophysical logs against compositional data derived from core analyses, Marcellus Shale, New York (Smith and Leone 2014). AAPG © 2014, reprinted by permission of the AAPG whose permission is required for further use



maps in Fig. 6.9, and sandstone thickness, measured from SP log response, is shown in Fig. 6.10. The thicknesses and relative arrangements of the various facies, with supplementary information on lithology from sidewall cores, were then used to make paleoenvironmental interpretations for each of the sandy units identified in the cross-section. Three of the resulting maps are shown in Fig. 6.11.

6.2.3 Problems and Solutions

There are several difficulties inherent in the use of petrophysical logs for stratigraphic work, which stem from the fact that drill holes necessarily represent a very limited sample of the rocks under study (the same problems arise with the use of outcrop sections for correlation except in

areas of exceptional exposure, where correlations may be “walked out” on the ground). Even with the very close well spacing that characterize enhanced recovery projects (a few hundred metres) it is commonly the case that the lateral dimensions of lithofacies units may be less than the distance between wells, which means that correlations may be unreliable, and attempts to characterize and model lithofacies architecture for production purposes subject to wide margins of error (Martin 1993). An example is illustrated in Fig. 6.12, which shows three different approaches to the correlation of a suite of fluvial sand bodies in the subsurface where well spacing averages 1.54 km. This example is discussed by Miall (2014a, Sect. 2.3.2), as part of a general discussion of the difficulty of carrying out facies modeling in the subsurface. In other environments where lateral variability is not so marked, stratigraphic correlations may be

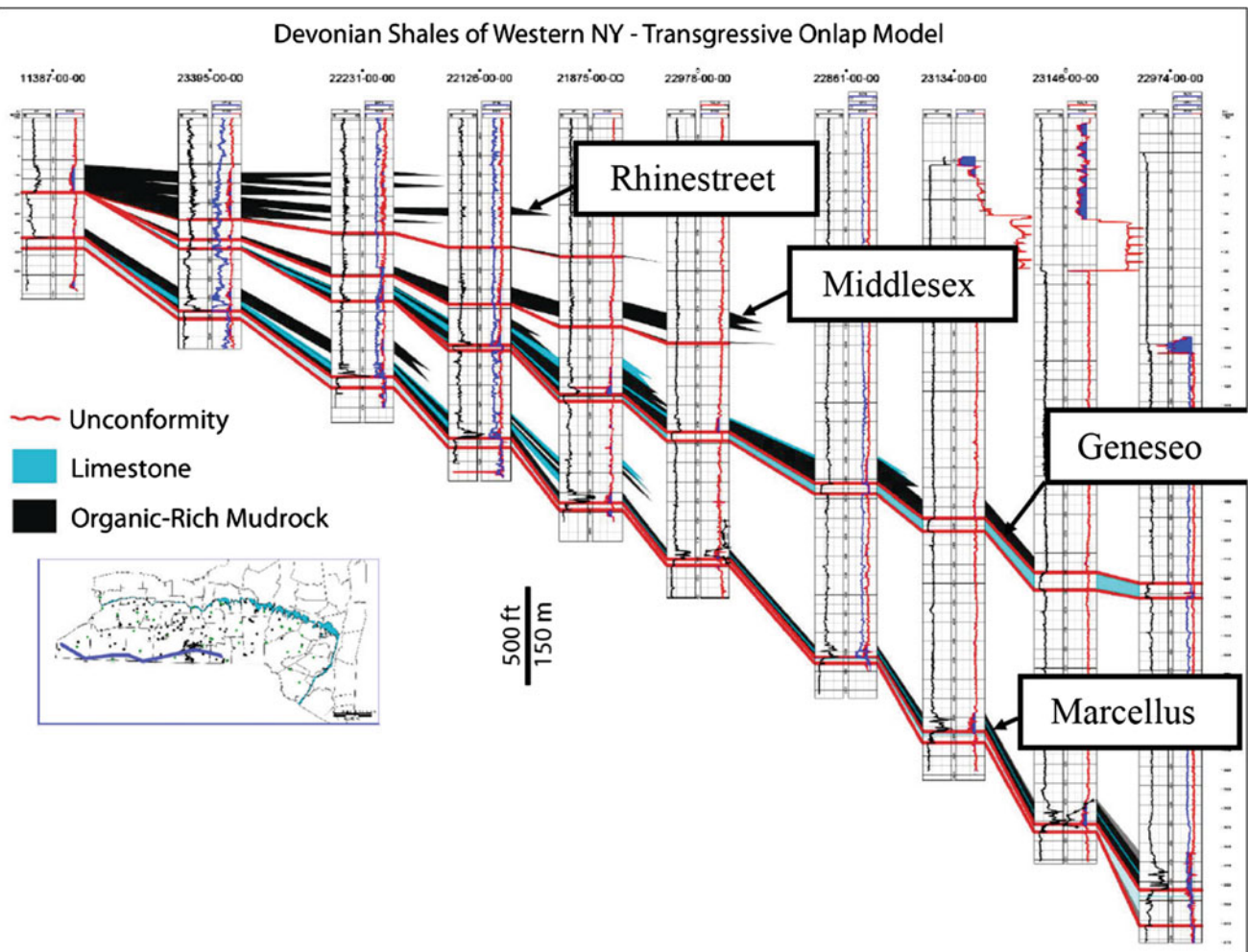


Fig. 6.7 A cross-section through the Marcellus and other distal parts of the Catskill complex in western New York State showing the westward change in facies and thicknesses toward the onlap of the

basin forebulge (Smith and Leone 2014). AAPG © 2014, reprinted by permission of the AAPG whose permission is required for further use

more reliable. The example of a complex facies mosaic illustrated in Figs. 6.8, 6.9, 6.10 and 6.11 shows where a degree of certainty may be assumed from the reconstructions showing that the extent of most of the facies units is considerably greater than well spacings, which range up to 5 km. In the case of some open-marine facies, such as transgressive sand bodies or turbidites, correlations of individual units over even greater distances may be possible.

Log correlation is usually guided by the identification of key surfaces and units that display characteristic log responses, and may be aided by biostratigraphic, chemostratigraphic, or other tools, some of which are discussed later in this chapter. The development of sequence stratigraphy has made an enormous difference to the work of subsurface stratigraphic correlation. Sequence models have a predictive power that can help to clarify what might otherwise be very confusing vertical and lateral lithofacies relationships. Key surfaces, such as subaerial erosion surfaces,

maximum flooding surfaces, or transgressive sands, may be traceable for many kilometres and may serve to vertically align well sections in arrangement that reveal the larger stratigraphic architecture. Much may depend on the choice of the datum on which to hang correlations.

In stratigraphic work the choice of datum may be key to the successful resolution of stratigraphic complexity. This is a surface selected because of its assumed original horizontality. Lining up sections by aligning a key surface at a horizontal datum removes structural disturbance from a section, and may move facies volumes and their interpreted depositional environments into relationships that make their interpretation much simpler. Bhattacharya (2011) provided an extensive discussion on this point, and provided many examples of how confusing facies and stratigraphic reconstructions can be clarified by the appropriate choice of datum and the application of the appropriate sequence model. Several examples follow. He noted that in marine deposits,

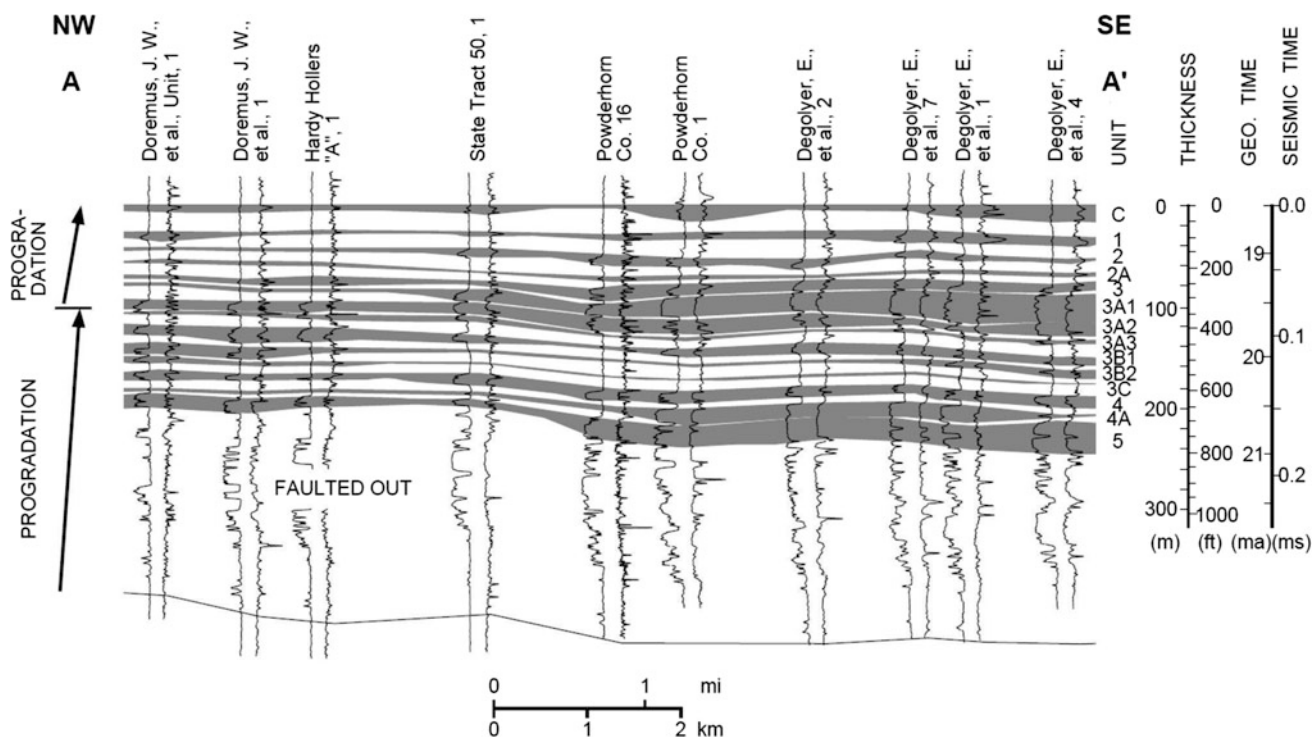


Fig. 6.8 Dip-oriented stratigraphic cross-section through a Miocene coastal deltaic system in the Powderhorn field, Texas, showing the definition of a series of sand-dominated lithostratigraphic units,

grouped into two progradational successions (Zeng et al. 1996, Fig. 4, p. 21). AAPG © 1996, reprinted by permission of the AAPG whose permission is required for further use

stratigraphic packages exhibiting significant depositional dip are extremely common. These are termed **clinoforms**, a term coined by Rich (1951). They range in scale from the dipping units at the front of deltas, typically as little as a few metres in amplitude where the delta progrades into shallow water, to the shelf clinoforms developed where a continental margin is building into an ocean, with vertical amplitudes up to several kilometres. Reconstructing clinoforms from outcrop or petrophysical data is extremely difficult because the depositional dip may be less than 1° . In fact, it was not until the advent of seismic stratigraphy that earth scientists fully appreciated the ubiquitous nature of the clinoform architecture in the stratigraphic record. Figure 6.13 illustrates the importance of correlating correctly. The reconstruction shown in Fig. 6.13a is based on traditional lithostratigraphic principles, using a prominent facies change as a marker and datum. However, Fig. 6.13b is the correct interpretation, in which units of gradually changing lithofacies with a significant depositional dip prograded from left to right.

What may be the first reconstruction of clinoform architecture to be based on petrophysical data is illustrated in Fig. 6.14. Earlier mapping of the reefal Woodbend Group (Upper Devonian) in central Alberta by McCrossan (1961) had suggested the presence of depositional dips in the Ireton Formation, a mixed shale-limestone unit which was recognized as constituting the talus deposits flanking prominent

reef carbonate units. However, it was the later work of Oliver and Cowper (1963, 1965) that specifically identified the three depositional environments of Rich (1951)—the undaform, clinoform and fondoform. Their reconstruction (Fig. 6.14) is based on the correlation of picks in resistivity logs. Thin, resistive beds are carbonate talus units deposited on the flanks of the reef. In this study, the top of the Ireton Formation was selected as the datum, but Bhattacharya (2011) argued that in some cases selecting an underlying surface as the datum is necessary for the correct reconstruction to be recognized. He made this point by presenting a redrawing of the seismic reflections within a modern delta (Fig. 6.15). The clinoform architecture of the delta is obvious from the original cross-section, in which every surface dips seaward, showing offlapping clinoform wedges and a dipping modern depositional surface (Fig. 6.15a). But if one were to imagine that each reflection was a pick on a petrophysical log and that the picks were correlated based on a flattening of the top surface, the architecture becomes severely distorted, with some beds actually dipping landward (Fig. 6.15b).

The evolving interpretation of the Wapiabi Formation in southern Alberta demonstrates the difficulty in making the appropriate reconstruction when several different types of criteria could be used to guide correlations. This example (Fig. 6.16) actually makes use of outcrop sections in an area where walking out correlations was not possible, but the

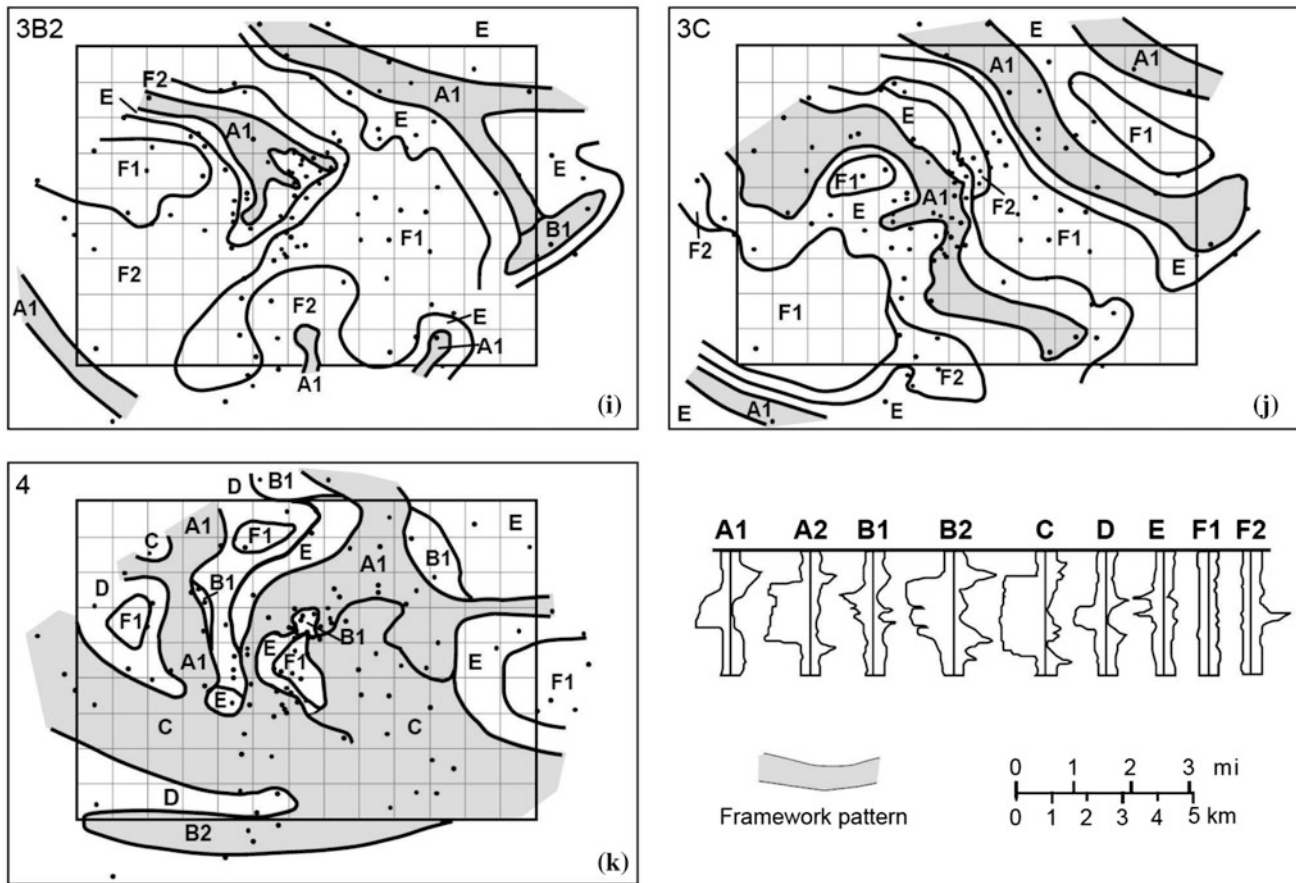


Fig. 6.9 SP log patterns of three of the sandy depositional units identified in Fig. 6.4. Log shapes at each location are identified at lower right: *A1* fining upward, *A2* fining upward with shoulder, *B1* coarsening upward, *B2* coarsening upward and blocky, *C* blocky, *D* fingerlike,

E serrate, *F1* straight with low resistivity, *F2* straight with high resistivity (Zeng et al. 1996, part of Fig. 5, p. 23). AAPG © 1996, reprinted by permission of the AAPG whose permission is required for further use

problems are identical to those encountered in the subsurface. In the first reconstruction (Fig. 6.16a) the top of the Chungo Member is used as datum. The Chungo Member constitutes a coarsening-upward and shallowing-upward succession in which diachronous and interfingering facies changes are indicated, but a clinoform architecture is not suggested or implied. In the second attempt (Fig. 6.16b) the top of the shoreface sandstones within the Chungo Member is used as datum, but this reconstruction provides no easily interpreted facies architectures. The third configuration (Fig. 6.16c) returns to the use of the top of the Chungo Member as the datum, and this time the clinoform configurations are specifically addressed in the suggested unit correlations. Given that the progradation of the Chungo shoreface must represent significant elapsed time, this implies a substantial time break above the fluvial Chungo preceding the Nomad transgression. Bhattacharya (2011, p. 130) reported that ancillary chronostratigraphic data supports this third reconstruction.

The reader is referred to Sect. 8.9 and to Bhattacharya's (2011) paper for further discussion of these issues, including

the problems inherent in the mapping, correlation and chronostratigraphic interpretation of coastal fluvial and shallow-marine systems and incised valleys, and the use of supplementary correlation criteria, including coal seams and (particularly useful) bentonite beds. In Sect. 8.10 we discuss the use of Wheeler diagrams to illustrate correlations in terms of elapsed time—a technique that, in throwing light on chronostratigraphic relations, may raise important questions about sedimentation rates, timing, and the correlation of lithofacies units through areas of stratigraphic uncertainty.

6.3 Seismic Stratigraphy

Seismic stratigraphy is the study of stratigraphic units defined on the basis of their seismic characteristics (Cross and Lessenger 1988; Hart 2013).

An introduction to the use of seismic facies to map depositional systems and systems tracts is provided in Sect. 5.4. Problems of sequence definition are discussed in Sect. 7.7. In this section the practical methods of sequence

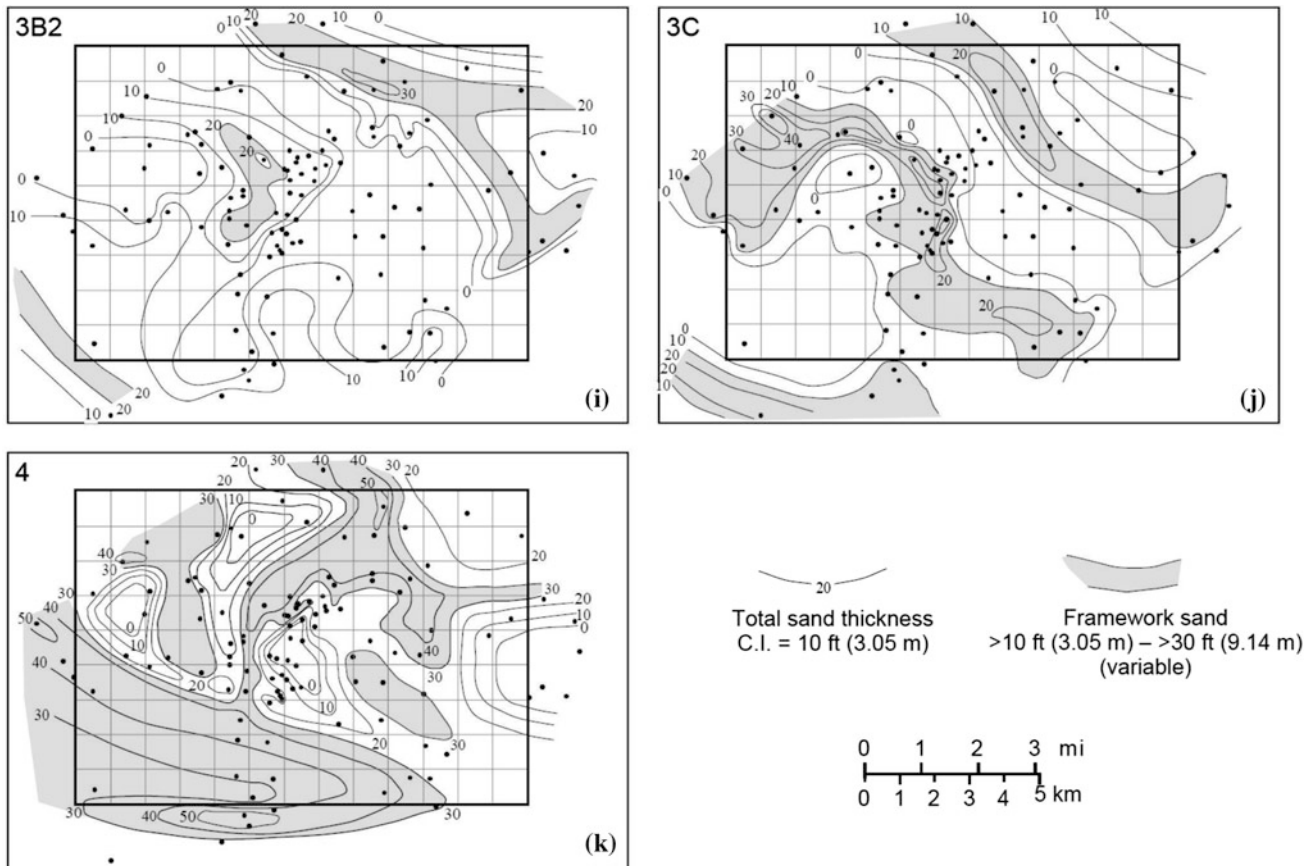


Fig. 6.10 Total sandstone thickness of sandy depositional units (Zeng et al. 1996, part of Fig. 6, p. 26). AAPG © 1996, reprinted by permission of the AAPG whose permission is required for further use

correlation and mapping are described and illustrated. This section does not deal with data processing, which is a very specialized field beyond the scope of the stratigraphic practitioner (see Veeken 2007, for an extensive introduction). The examples selected for discussion here make use of seismic data that has already received the necessary processing to highlight the relevant stratigraphic detail. If necessary, reference may be made back to the original articles from which the examples used here have been derived.

6.3.1 The Nature of the Seismic Record

A seismic reflection is generated at the interface between two materials with different acoustic properties. The latter is described as **acoustic impedance** and is given by the product of density and velocity. The larger the difference in impedance between two lithologies, the stronger the reflection. Where a soft lithology lies on a harder one, the reflection polarity is positive and is normally represented by a waveform deflection to the right, colored to render it more visible. Where the reverse situation applies, the polarity of the deflection is to the left (left blank). This is the origin of the familiar variable-area **wiggle traces**. Colors are now

commonly used to exaggerate amplitude and other differences, and these may emphasize major facies variations.

A seismic wave trace recorded at a geophone represents the modification of a source pulse by reflection from various layers below the surface. The nature of each wavelet depends on the nature of the impedance contrasts at each bed contact. An example of a synthetic seismogram illustrating the production of a seismic signal is shown in Fig. 6.17. Such seismograms are time sections; that is, their long axis is proportional to time, not depth. Complex calculations must be performed to convert time to depth. This is because seismic velocities generally increase downward as rock density increases and porosity diminishes because of mechanical compaction, pressure solution and cementation. An empirical relationship, known as the **Faust equation**, has been demonstrated between seismic velocity and the depth and age of rock units (Sharma 1986):

$$V = 46.5(ZT)^{1/6} \text{ m/s,}$$

where V is seismic velocity, Z is depth of burial, and T is geological age in years.

It is important to remember that the seismic technique cannot resolve small-scale stratigraphic anomalies or very

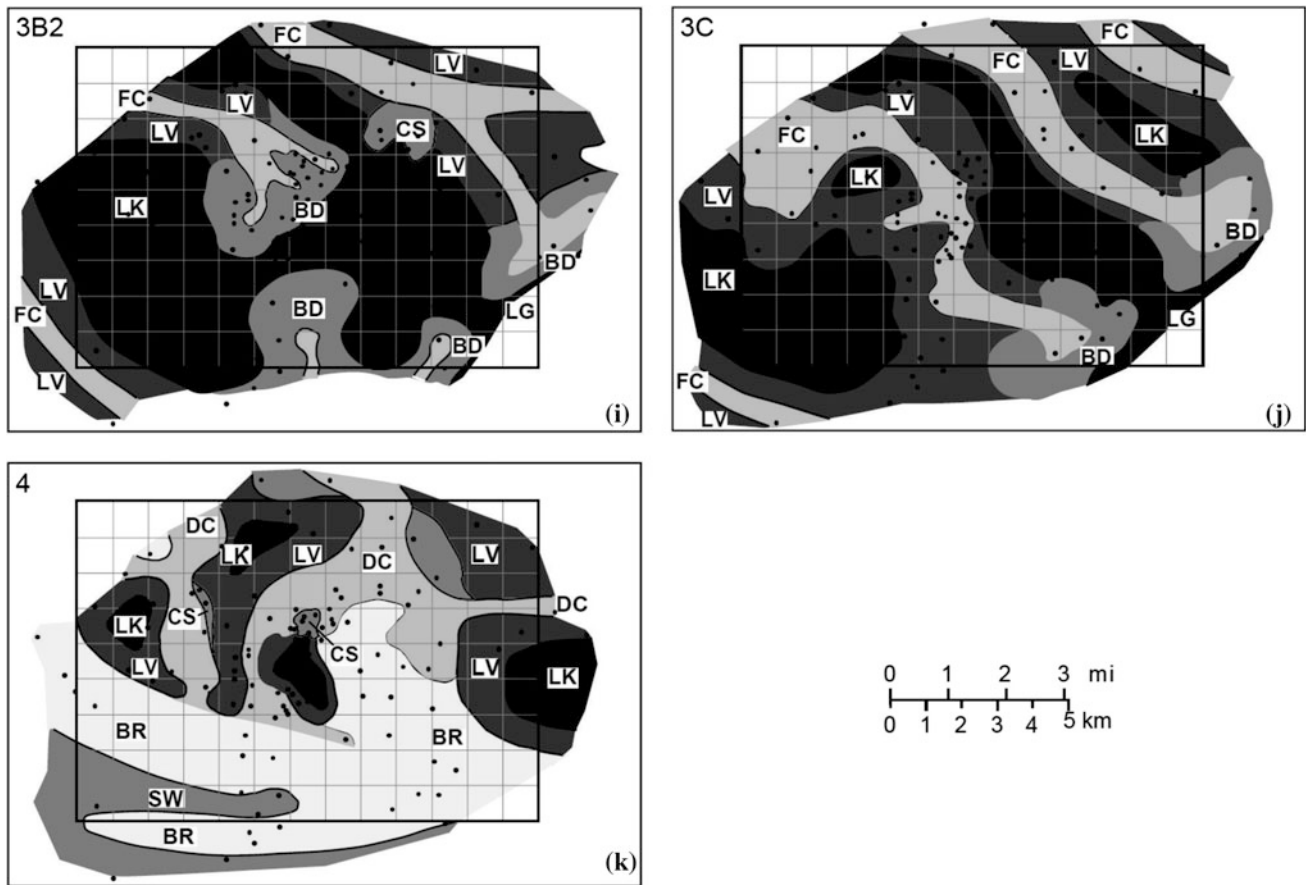


Fig. 6.11 Environmental interpretation of sandy depositional units. Symbols for various panel are as follows. Barrier bar/lagoon system (e, f): *BC* barrier core, *IF* inlet fill, *IN* inlet, *FTD* flood-tidal delta, *ETD* ebb-tidal delta, *LG* lagoon. Coastal stream plain (a–c, g, i, j): *FC* fluvial channel, *LV* levee, *CS* crevasse splay, *AC* abandoned channel, *FP* flood plain, *LK* lake, *BD* bayhead delta. Wave-dominated delta (d, h, k): *DC*

distributary channel, *LV* levee, *CS* crevasse splay, *AC* abandoned channel, *DP* delta plain, *LK* lake, *SPL* strand plain, *SW* swale, *BR* beach ridge (Zeng et al. 1996, part of Fig. 7, p. 27). AAPG © 1996, reprinted by permission of the AAPG whose permission is required for further use

thin beds, and that the resolution decreases with depth, as seismic velocity increases. A general rule is that two reflecting horizons must be a minimum of about 1/4 of a wavelength apart if they are to be resolvable in a typical seismic section (Sheriff 1985). Thus, at shallow depths in loosely consolidated sandstones and mudstones, a typical seismic velocity would be on the order of 1800 m/s, and the typical frequency would be around 60 Hz. One quarter wavelength is therefore 7.5 m. Resolution is much poorer in older and deeper formations. Consider, for example, a Paleozoic carbonate section, with a seismic velocity of 4500 m/s and a frequency of 15 Hz. The thinnest unit resolvable in this situation would be 75 m. This lower limit is much larger (thicker) than many of the important facies details that can be seen in outcrops and high-resolution petrophysical logs, as shown dramatically in Fig. 7.1. High-resolution techniques are available for studying sediments at shallow depths and are becoming widely used in detailed studies of stratigraphic architecture in modern environments (Bouma et al. 1987);

but they are not yet available for the study of deep-basin structure and stratigraphy.

Published seismic sections show a series of vertical wave traces, each representing the recording made at a shot point. These are usually located about 25 to 50 m apart. Each trace is obtained by combining (**stacking**) the records of many adjacent geophones. The vertical scale of the section is **two-way travel time**, not depth. For each time horizon, depth varies according to velocity, as noted previously, so that, unless corrected, the structure revealed on a section may be spurious. For example, a mass of high-velocity rock, such as a dense carbonate reef or channel fill, may overlie what looks like a gentle anticline. This is a case of **velocity pull-up**, where the more rapid acoustic transmission through the dense material returns reflections from the underlying layers sooner than occurs on either side. Computer processing can produce a depth-corrected section if accurate velocity information is available, typically by making use of sonic petrophysical logs. This is discussed briefly below.

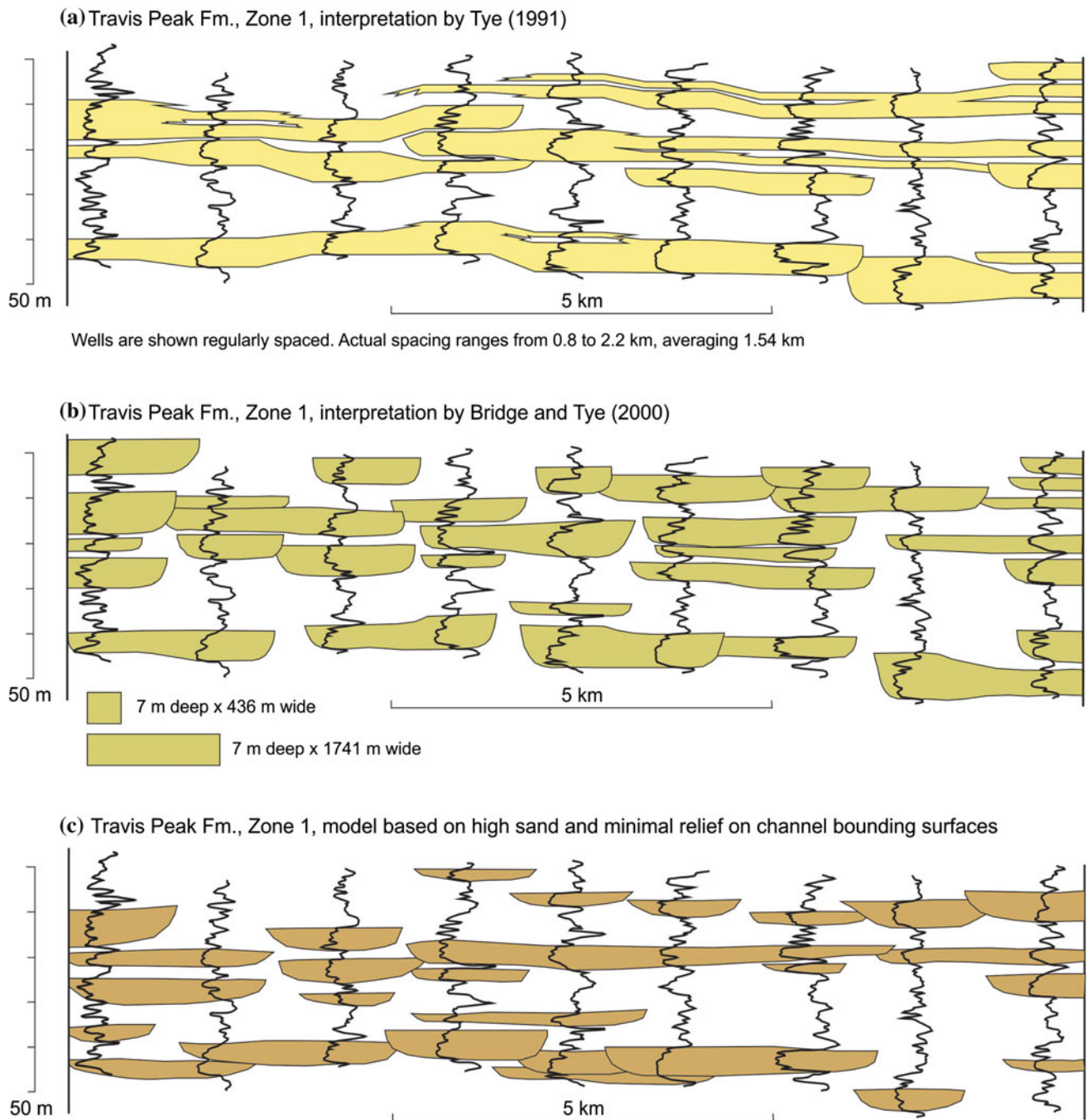


Fig. 6.12 Three interpretations of the braided-fluvial deposits of the Travis Peak Formation, Zone 1 (Early Cretaceous, East Texas). **a** Initial interpretation, by Tye (1991), based on detailed core and isopach mapping study. Arbitrary equal well-spacing is used in this and the subsequent diagrams; **b** A reinterpretation by Bridge and Tye (2000), based on assumptions of narrower channel belts. Rectangular boxes at the base of this panel indicate range of channel-belt sizes predicted

from estimated bankfull depth, using the equations of Bridge and Mackey (1993). Their own model, shown here, does not make use of this range of values; **c** An alternative model developed by the present writer (Miall 2006), based on two basic guidelines for interpreting petrophysical logs: **a** channels normally have flat bases, and **b** the main sand bodies are indicated only by blocky-shaped, low-value gamma ray signatures (from Miall 2014a, Fig. 2.16)

It is important to remember that it is contacts that produce reflections, not rock bodies as such. For example, tight, cemented sandstone and dense, nonporous carbonate have higher impedances than most mudrocks, so that a contact of

one of these with an overlying mudstone will yield a strong positive reflection. Conversely, a gas-filled sandstone has a very low impedance. Where it is overlain by a mudstone there will be a strong negative deflection. This appears as a

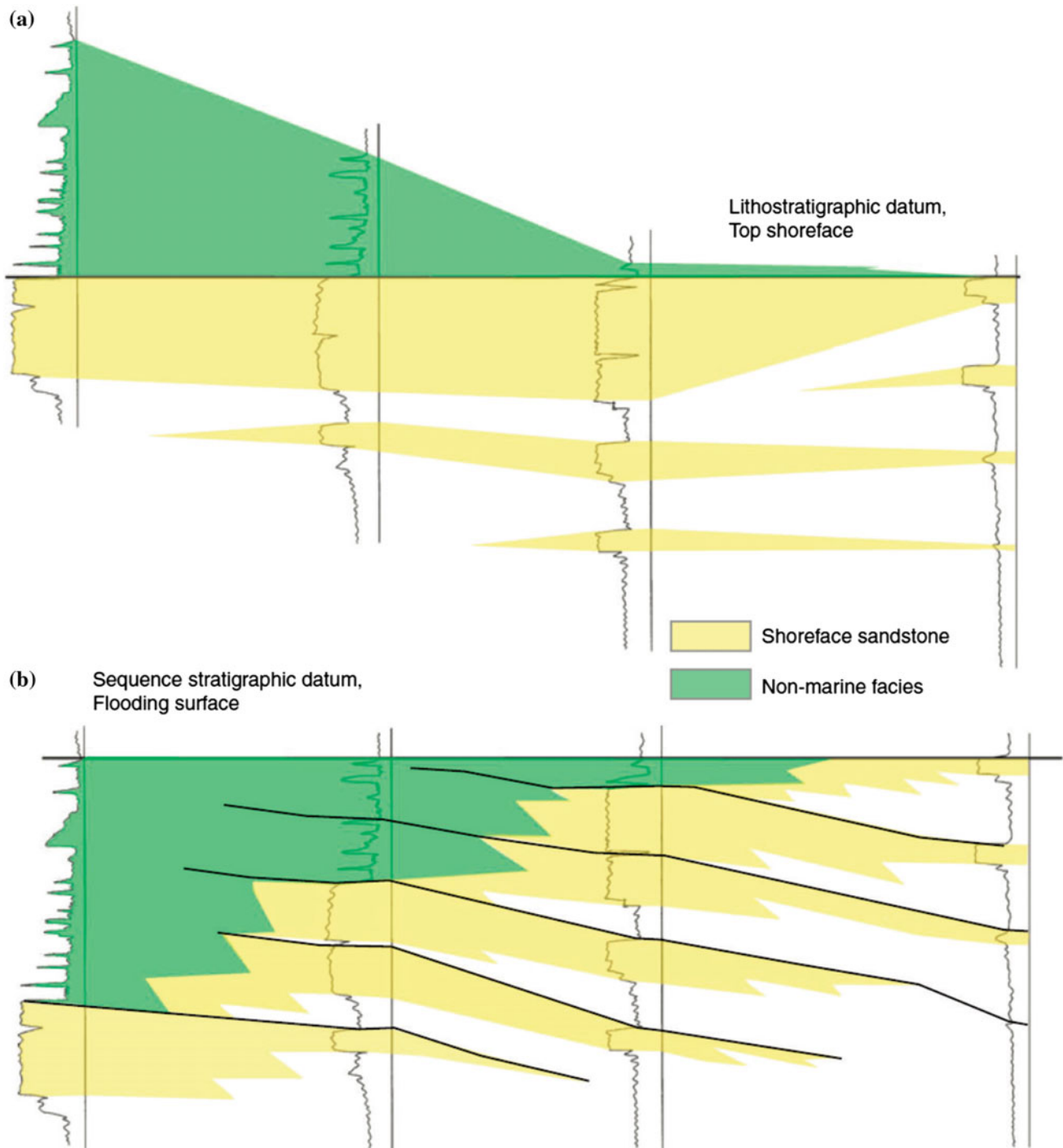


Fig. 6.13 An example of how the choice of datum for the correlation of petrophysical logs can obscure or clarify depositional relationships. **a** In this reconstruction the assumption is made that the top of the marine sandstone constitutes a time line. **b** The presence of significant

lateral facies change and the presence of a depositional dip characterizes this reconstruction. The succession constitutes a clinoform set within which facies change laterally from nonmarine to shoreface to offshore (Bhattacharya 2011, Fig. 5, p. 127)

blank area in the seismic record, and is the basis of the **bright-spot technique** for locating gas reservoirs. However, there are many conditions where interbedded units may have contrasting lithology but very similar impedances, so that they yield little or no seismic reflections. Examples would

include a contact between a tight sandstone and a porous carbonate and a very porous oil- or water-saturated sandstone and a mudstone.

A very important assumption, first emphasized by Vail et al. (1977), and reemphasized by Cross and Lessenger

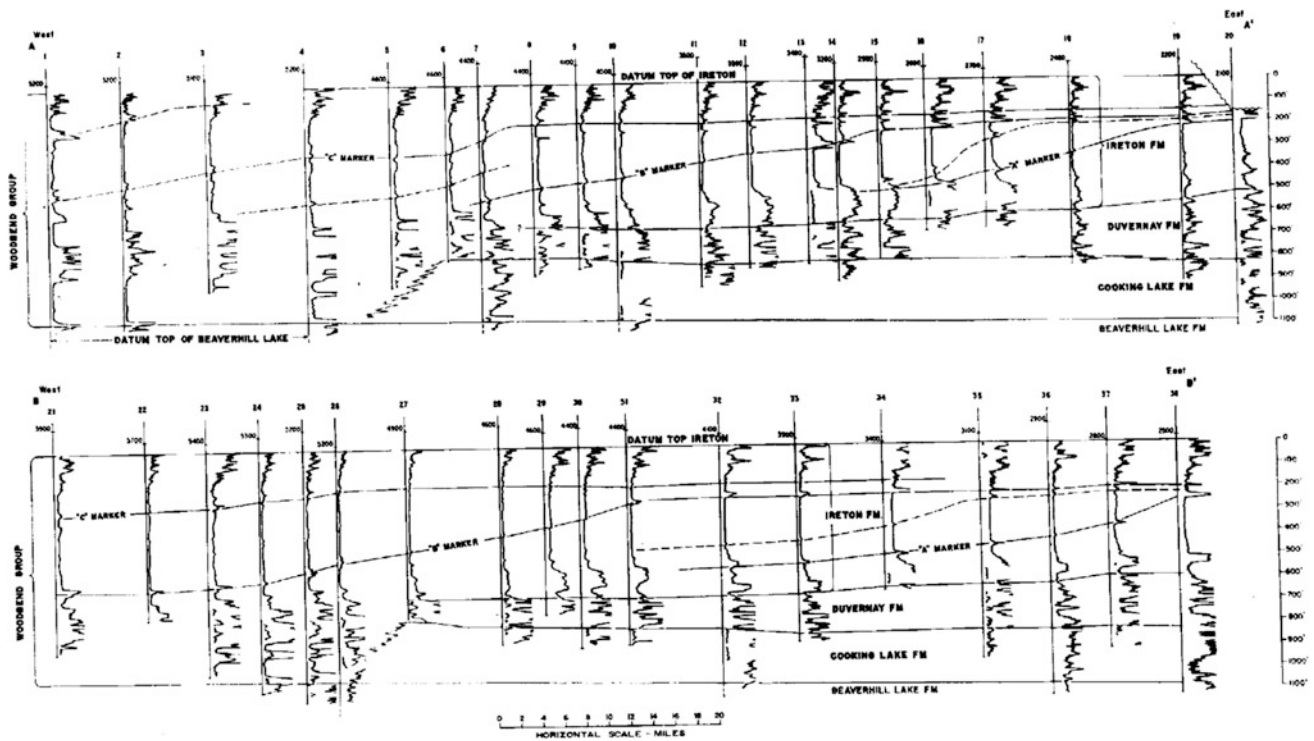


Fig. 6.14 This is one of the first reconstructions of clinoform stratigraphy based on petrophysical log correlation (Oliver and Cowper 1965, Fig. 4, p. 1414). AAPG © 1965, reprinted by permission of the AAPG whose permission is required for further use

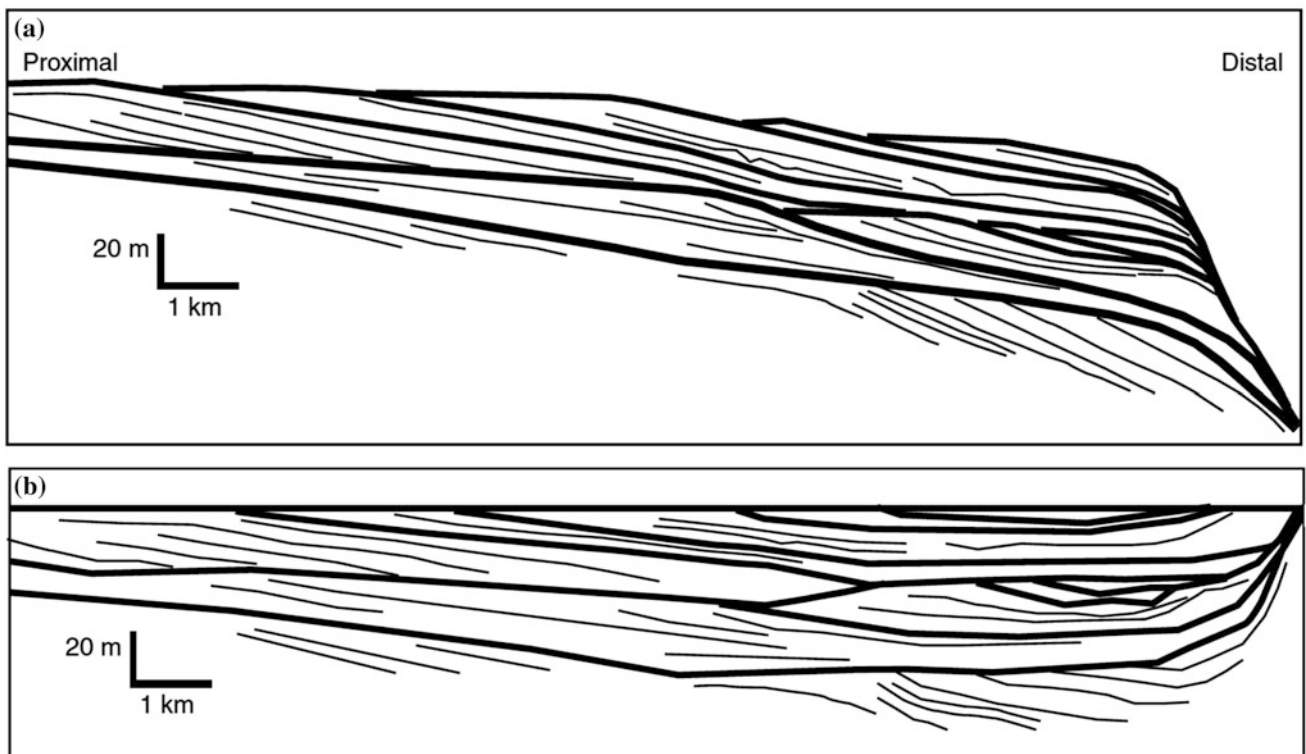


Fig. 6.15 a Seismic reflection through a modern shelf-edge delta (Rhône delta, Mediterranean Sea), showing a clear clinoform architecture. b Flattening the top surface of the delta, a common practice in the subsurface correlation of deposits if this type, results in a severe distortion of the internal geometry of the beds (Bhattacharya 2011, Fig. 10, p. 134)

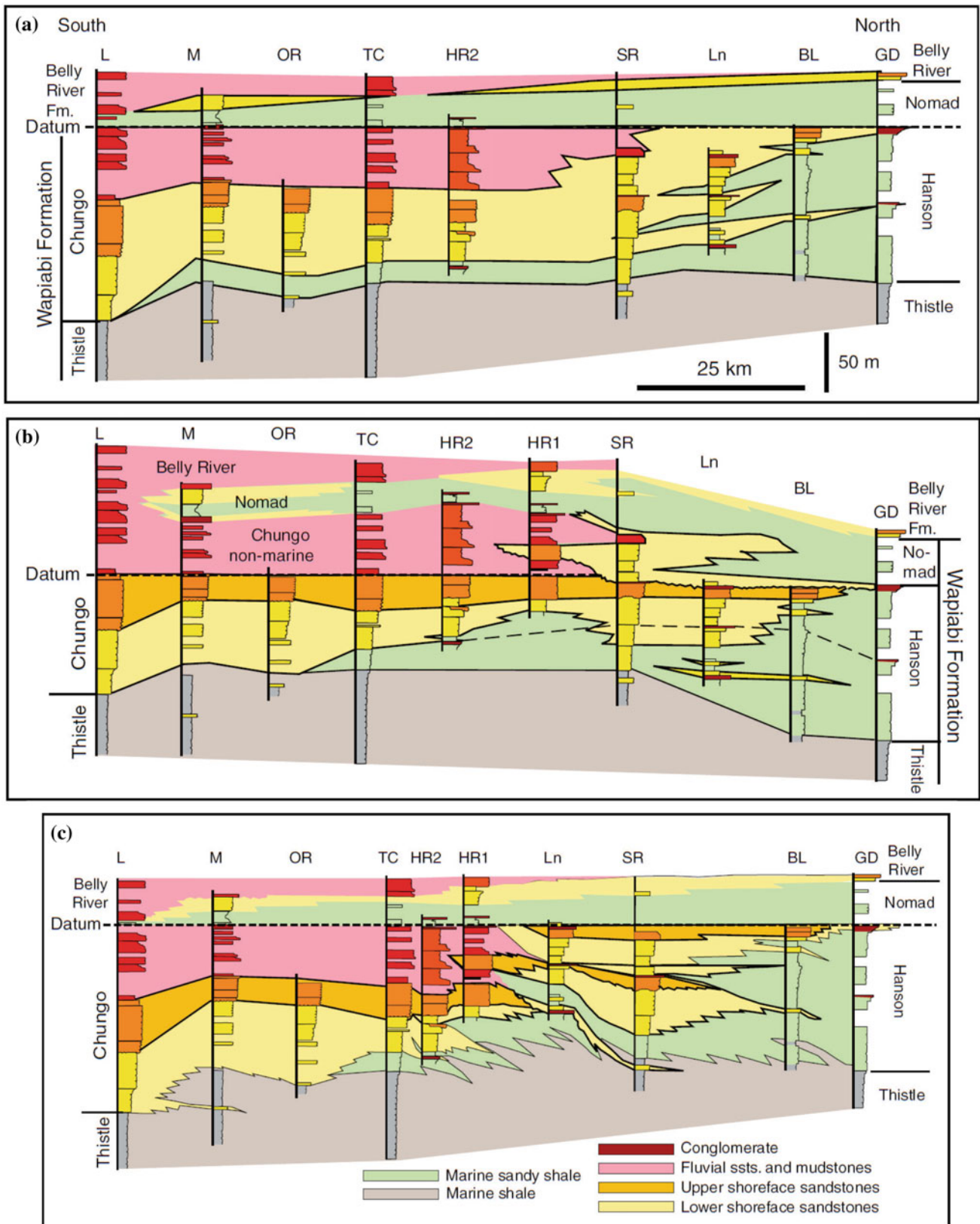
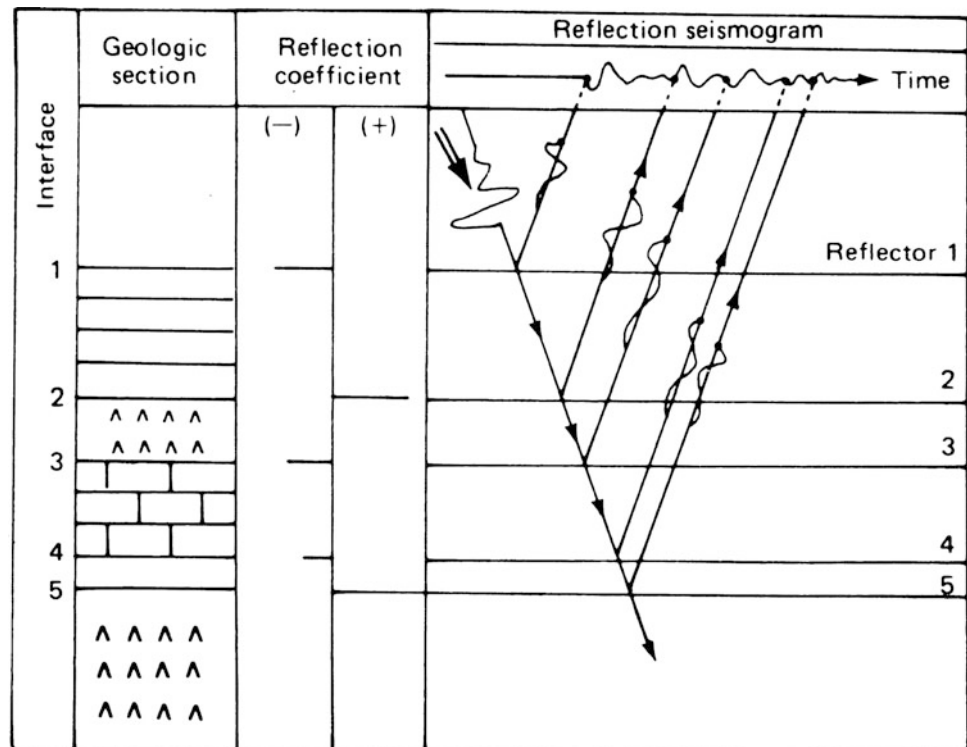


Fig. 6.16 Three different stratigraphic reconstructions of the Upper Cretaceous Wapiabi Formation in Alberta. These outcrop sections are tens of kilometres apart. **a** From Rosenthal et al. (1984); **b** From

Rosenthal and Walker (1987); **c** From Leckie et al. (1994). See text for discussion and explanation

Fig. 6.17 Synthetic reflection seismogram generated from a simple geological section. At each interface the input wavelet is modified by the reflection effects (Sharma 1986)



(1988), and Hart (2013) is that in most cases seismic reflections from conformable bedding surfaces are chronostratigraphic (isochronous) in nature. Facies contacts are diachronous, but they are too gradual to yield reflections. Facies changes may be deduced from subtle lateral changes in reflection characteristics within a single bed. The assumption that continuous seismic reflections represent “time lines” is of profound importance in the study of basin structure and stratigraphy and the analysis of stratigraphic sequences (Chap. 5).

Imagine an angular unconformity with lateral facies changes in the overlying unit and a gently dipping, truncated sequence of different units below. The seismic reflection from the unconformity could vary from strongly positive to strongly negative, with some areas completely invisible. This would be a difficult reflection to follow accurately on seismic records.

Seismic records are also complicated by **multiples** and **diffractions**. Multiples are reflections from a shallow layer that are reflected downward again from a near surface level such as the base of the weathering zone. This internal reflection is then redirected toward the surface from the original point and appears in the seismic record as a parallel layer several tenths of a second lower down in the section. Multiples may be strong enough to obscure deep reflections, but they are now relatively easy to remove by processing. Diffractions are reflections from steeply dipping surfaces, such as faults, channel margins, and erosional relief on an

unconformity. Their appearance in the record often occurs because seismic waves are not linear, laser-like energy beams but spherical wave fronts. The pulse from each shot point therefore sees reflection events over a circular region (the **Fresnel zone**), the diameter of which can be shown by calculation to range from about 100 to 1200 m, depending on depth and wavelength. A reflection on the periphery of the wave front will be seen later than one at the same depth directly below the shot point and, if at a high angle from the horizontal, may produce complex internal reflections. The resulting diffraction patterns may be very pronounced. They are a useful indicator of a steep reflecting event but may confuse other reflections and can be removed by a processing routine called **migration**, which repositions the reflections in their correct spatial position. The circular reflection area also accounts for the fact that diffractions can be produced by reflectors off the line of section, for example, if the seismic line skirts past a reef body or a buried fault line scarp.

The seismic record can be considerably improved, and interpretation facilitated by the use of two special techniques, the construction of **synthetic seismograms**, and the use of **vertical seismic profiling** (VSP) (Hardage 1985). Synthetic seismograms are generated by the conversion of sonic and density data from petrophysical logs into a series of reflection coefficients (see Sect. 2.4 for a discussion of petrophysical logs). Vertical seismic profiling is the recording and analysis of seismic signals received from a geophone lowered downhole. Signals generated at the

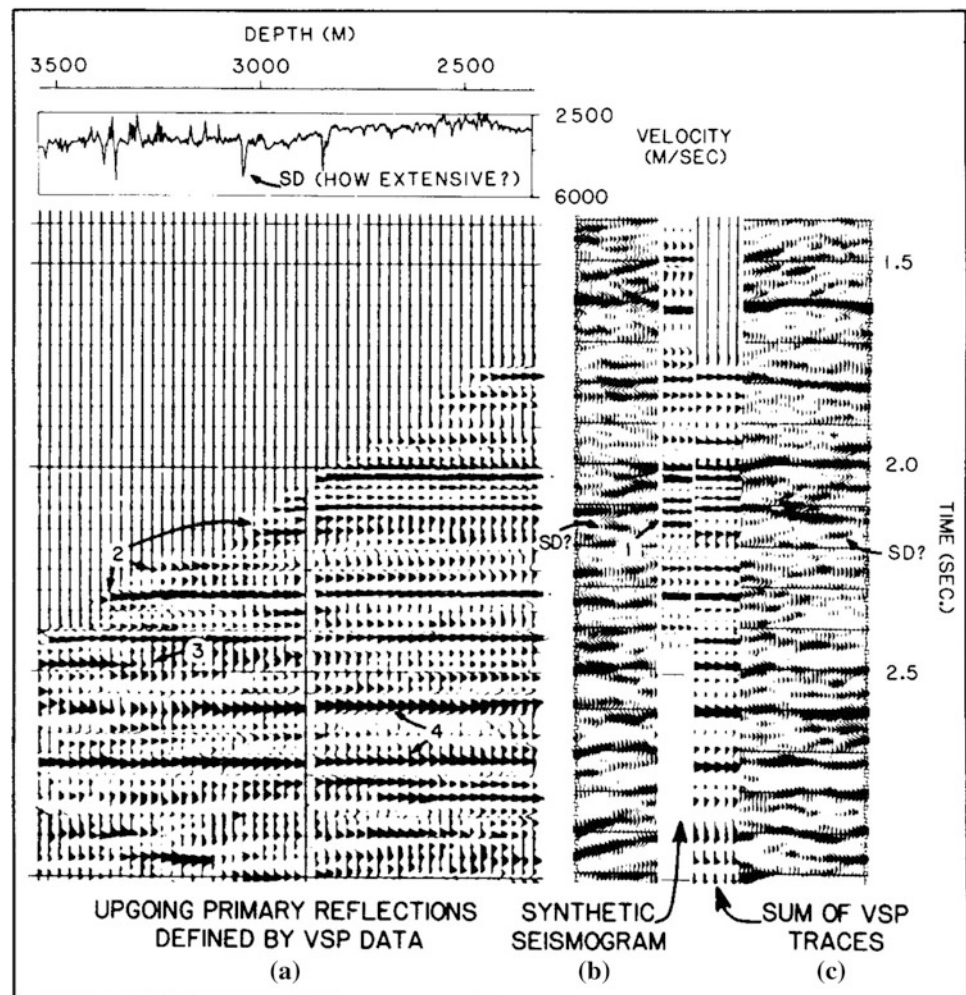
surface are recorded as they descend and as they return to the surface. The geophone is moved in increments, the length of each being set at less than half the shortest wavelength of the signals being analyzed. A new recording is made at each position. A comparison between synthetic, VSP, and field recorded data is shown in Fig. 6.18. Both synthetic and VSP data are extremely valuable for the purposes of calibrating the seismic record. For example, they enable a detailed record of seismic velocities to be generated that can be used to produce depth-corrected cross sections. However, the VSP technique is far superior for various reasons. It can, for example, be used to extend the calculations below the total depth (TD) of the well, which synthetic seismograms cannot (Fig. 6.18). The synthetic method relies on well log data, which only reflect conditions immediately adjacent to the hole. In the case of poor hole conditions or seismic reflectors having a very small horizontal extent (less than one Fresnel zone), the synthetic method may not provide a record typical of the area. For example, in Fig. 6.18 there is a discontinuous calcareous sandstone (denoted by the letters SD) at a depth of about 3070 ft. It is visible as a strong reflector at about

2.15 s in the synthetic seismogram, but not on the VSP trace, indicating that the bed does not extend very far from the borehole. Other possible occurrences of the bed are shown by the letters SD on the field record. VSP data are now routinely used to improve subsurface imaging around critical boreholes, to carry out precise time-depth conversions, and to remove multiples.

One of the most important features of **seismic stratigraphy**, as first described by Vail et al. (1977), is the concept of **seismic facies**, defined to mean an areally restricted group of seismic reflections whose appearance and characteristics are distinguishable from those of adjacent groups (Sangre and Widmier 1977). This is introduced in Sect. 5.2.2, and discussed in some detail below (Sect. 6.3.3).

A revolutionary advance in seismic methods is the use of **three-dimensional seismic data**. According to Davies et al. (2004b) the first commercial 3-D survey was run in the North Sea in 1975, but it was not until the mid-1980s that the power of the new tool became more widely known (Brown 1985, 1986). Developments in computer processing and visualization were necessary before this could happen.

Fig. 6.18 Comparison of VSP data with a synthetic seismogram and that produced by normal surface field recording. The surface section is split in two at the location of a well down which the synthetic record and the VSP traces were generated. At left is shown the VSP traces and above is the sonic log of the well. Total well depth is at 2.41 s. Notes: 1 Calcareous sandstone (see text); 2 Curvature of VSP reflections implies structural dip; 3 Termination of reflection implies presence of a fault near the borehole; 4 VSP data from below TD (Hardage 1985)



A tight grid of seismic lines is run across an area at line spacings of a few tens of meters (25 m is typical). By correlation of key reflectors from line to line this permits the plotting of horizontal seismic sections at selected depths. Correlation of key reflectors can be carried out by computers using automatic tracking techniques, and this provides a facility for plotting seismic maps of selected stratigraphic horizons. Where the structure is simple or can be removed by suitable processing routines the resulting plots display areal amplitude variations for a single stratigraphic horizon, which may be highlighted by the use of false colours. These variations depend on lithology, so that the sections may reveal detailed subsurface facies variations that can readily be interpreted in terms of depositional environment and paleogeography. Channels, sand bars, and other depositional features may be clearly delineated. For example, Zeng et al. (1996) explored the potential for individual depositional elements to be revealed by 3-D seismic by developing synthetic models based on petrophysical data (see Figs. 6.8, 6.9, 6.10 and 6.11 and discussion in Sect. 6.2.2).

One of the most important aspects of 3-D data is the three-dimensional visualization it provides of depositional systems. This is a hugely important development. Traditionally, 2-D cross-sections have been used to illustrate proximal-distal variability in stratigraphy and interpreted depositional systems. Typically, thicknesses and facies undergo significant changes from basin-margin to basin-centre, and dip-oriented 2-D cross-sections have been the preferred way to illustrate this. However, sediment-dispersal is a three-dimensional process—long-shore drift, geostrophic currents, diverging distributaries on deltas and submarine fans, are all examples of where significant sediment transport may take place out of the plane of such 2-D sections. For example, Moscardelli et al. (2012) discuss this important point with respect to a suite of shelf-margin deltas in Trinidad (a paper to which we refer below). In addition, orthogonal, linear subsidence or rotational subsidence on an axis parallel to the basin margin may not be the norm for any given basin, an important attribute that is difficult to capture with 2-D sections. Interpretations of the timing of important stages in sequence development, and quantitative modeling of a basin, such as source-to-sink calculations, may be in significant error if these three-dimensional characteristics of the basin cannot be fully taken into account.

Processing and interpretation of 3-D data require the use of sophisticated computer workstations and interactive graphics. Color display and plotting are essential. Savit and Changsheng (1982) provided an early example of the application of these ideas; the latest edition of the classic memoir by Brown (2011) brings them up to date. Hart (2013) offered a very useful review of modern seismic-stratigraphic methods and potential. Many examples of the interpretation of depositional features, such as

channels and bars, from horizontal seismic sections have now been published (Posamentier 2000). Henry Posamentier has led the introduction of an entire new subdiscipline, termed **seismic geomorphology**, which uses horizontal seismic sections to explore and interpret entire depositional systems (Posamentier 2000; Posamentier and Kolla 2003; Davies et al. 2004a, 2007; Sect. 6.3.4). Chronostratigraphic interpretations of 3-D seismic volumes may be constructed using techniques of “computational seismic chronostratigraphy” (Stark et al. 2013), as discussed in Sect. 8.10.2.

6.3.2 Constructing Regional Stratigraphies

The use of conventional 2-D seismic-reflection data to provide reconnaissance information in frontier basins has been standard practice since shortly after the end of the First World War. Since 1968, the year the *Glomar Challenger*, the first ship of the Deep Sea Drilling Project set sail, marine seismic has been a standard, essential component of the global effort to map the geology of the continental margins and deep oceans. Seismic data are calibrated against well and core records. In the case of onshore and offshore frontier exploration, the seismic data are correlated to the first suites of exploration drill holes. Seismic stratigraphy revolutionized the practice of petroleum exploration and development when it was introduced in the late 1970s, a development credited mainly to Peter Vail and his colleagues at Exxon Corporation, (Vail et al. 1977) and to Bert Bally at Shell (see, in particular, Bally 1987).

What follows are five examples of what has become standard subsurface methodology. Reconnaissance 2-D seismic is used first, in the exploration of new frontier basins, and the first exploration drill holes are tied into the seismic data in order to provide calibrations of lithologies, biostratigraphic ages, and depth-to-sonic velocity relationships. Prominent seismic reflections are labeled and codified (commonly, important reflectors are shown in distinctive colours) and are traced throughout the study area using the loop-correlation method, whereby horizons are followed as far as possible around an area using intersecting survey lines, ultimately bringing the correlation back to its starting point to ensure that the correlations have not inadvertently shifted into a different stratigraphic level. Further ideas about the workflow to be used in basin analysis are provided in Sect. 1.5.

Figure 6.19 illustrates a seismic line from the West Antarctic Rift System, a series of marine rift basins located between the Antarctic Peninsula and the Ross Sea. Earlier seismic and drilling activity had provided the basis for the stratigraphic subdivisions shown on this section, which provides a clear picture of the subsurface stratigraphy and structure of the area. Seismic facies and structural relations in this and other sections may be interpreted in terms of the

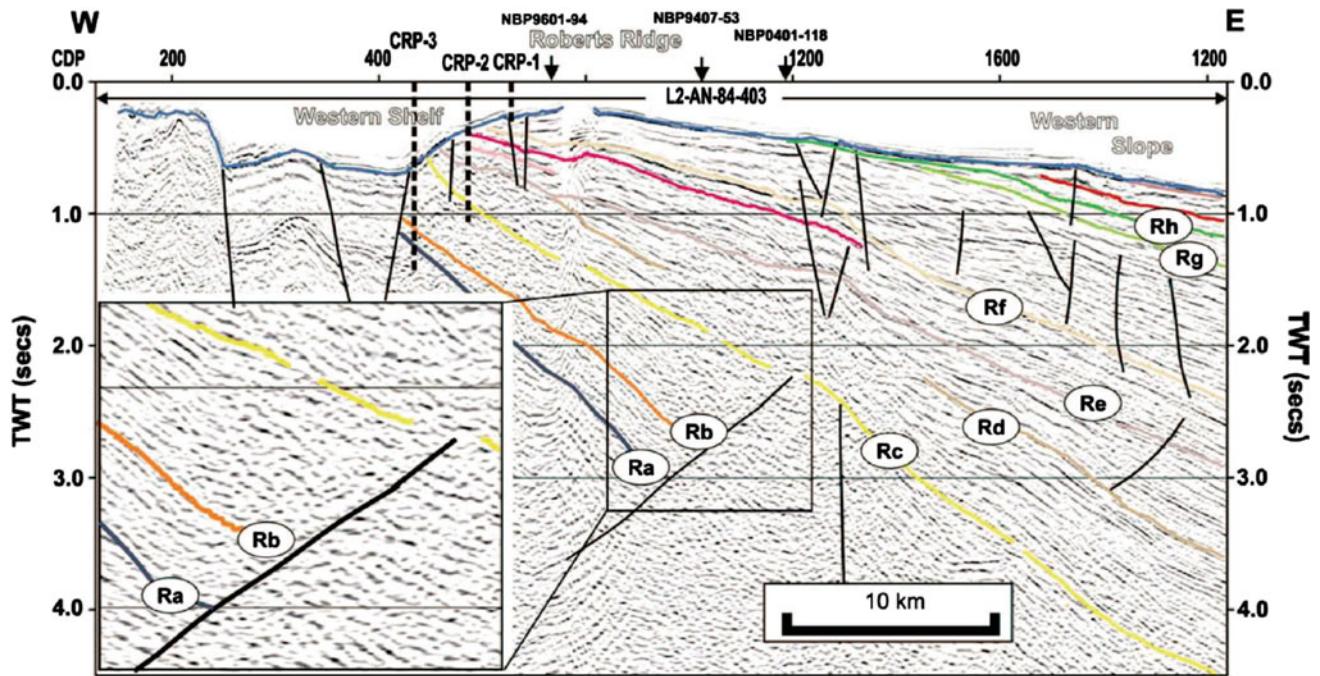


Fig. 6.19 Seismic stratigraphy of the Antarctic margin. This section shows rift architecture close to the western edge of the Victoria Land Basin (Western Shelf). *Inset* shows close-up view of the principal seismic facies of the Early Rift (navy blue—Ra to yellow—Rb reflectors) and Main Rift (yellow—Rb to purple-grey—Rc successions). Thermal relaxation phase: Purple reflectors and Rf–Rg reflectors.

In the Early Rift section, mainly concordant, moderately continuous, high amplitude events with some low-angle clinoforms pass downdip into a chaotic seismic fabric adjacent to the half-graben-bounding fault. In the Main Rift section, mainly concordant events of similar character to the underlying section dominate, and are continuous across the top of earlier extensional topography (Fielding et al. 2008, Fig. 2, p. 13)

phases of development of the rifts basins: early rift, main phase, and thermal-relaxation phase. The illustrated section follows what is now standard practice, to use different colours for the key reflectors. Initially this adheres to the empirical approach necessary for building a stratigraphic reconstruction directly from the data and free of regional assumptions or other biases. Eventually these colour-coded reflections are used as the basis for stratigraphic subdivision. Many of them will subsequently be defined as sequence boundaries or other important surfaces.

As described by Fielding et al. (2008, p. 13), based on an interpretation of the section shown here as Fig. 6.19:

In the area of Roberts Ridge, the Early Rift interval forms an eastward-thickening wedge that is abruptly truncated against the first major basement-offsetting fault. Within the Early Rift section, the principal seismic facies are 1. irregular to chaotic, discontinuous, moderate to high amplitude reflections in the updip area, passing downdip into 2. mainly concordant, parallel to somewhat irregular, semi-continuous reflections of moderate to high amplitude and moderate frequency, with local development of clinoform sets, in turn passing into 3. chaotic to reflection-free facies in the immediate hanging wall region of the half-graben-bounding fault.

Wherever possible, the calibration between petrophysical logs or cores and seismic data should be clearly shown. Core and log data help to clarify the interpretation of seismic

facies, and both together may be used in the definition of the sequence stratigraphy and regional tectonic reconstructions. Figure 6.20 is an example from a very complex area, the Sigsbee Knolls area, on the continental slope off Texas, in the northwest Gulf of Mexico. Vast amounts of clastic debris have been shed into the Gulf since the Jurassic, with many major depositional systems having prograded southward, extending the continental margin by tens of kilometres during that time interval. The Brazos-Trinity slope system, which developed during the Pleistocene, is one of the last of these depositional phases. It represents the distal end of a nonmarine-shallow-marine and shelf-edge delta system, the source for which lay within the Brazos-Trinity watersheds, that extend northwestward across Texas and into New Mexico (Pirmez et al. 2012). The Sigsbee Knolls is an area along the continental slope where evaporites of Jurassic age rise in multiple complex diapiric bodies to form topographic highs on the sea floor, between which clastic sediment is ponded in multiple intra-slope basins. The sediment influx is controlled by the shifting deltaic depositional systems to the north, by the modifications to the basins by salt tectonics, and by sea-level changes. Steep, local intra-basin slopes created by salt activity are thought to be capable of triggering local sediment gravity flows. Considerable exploration work has been carried out in this broad area because

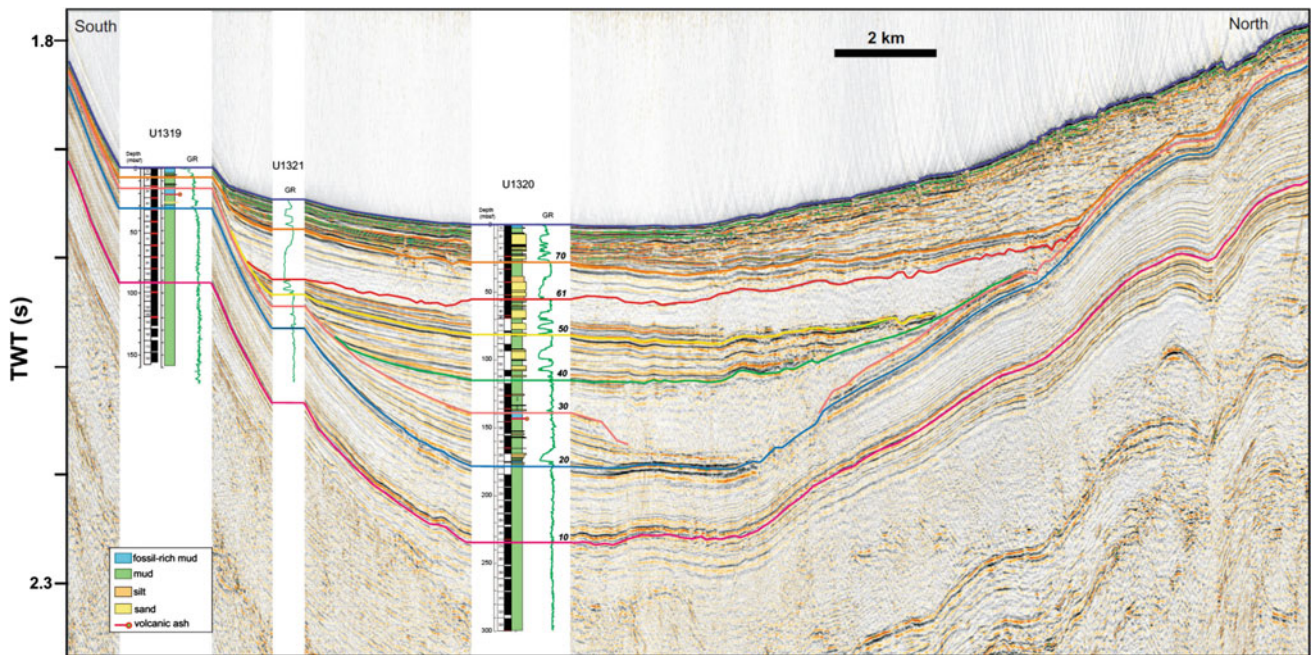


Fig. 6.20 Seismic section through the Brazos-Trinity depositional system (Pleistocene) in an intraslope basin off the Texas margin continental shelf. High-resolution 2D seismic data are correlated to relevant well logs, showing key surfaces, and positions of cores. Logs are plotted in depth scaled using an average velocity; note the good

relationship between the key mapped horizons and major lithologic changes. Core columns contain, from left to right: (with respective core number), core recovery (black recovered, white/blue no core, red core interval with gas expansion), and lithologic column (with legend key to colors) (Pirmez et al. 2012, Fig. 4, p. 16)

the deep-water sands deposited by these depositional systems have proved to be very hydrocarbon rich. Local stratigraphic variability is therefore considerable, and explorationists must rely on, and reconcile, multiple data sets in order to generate reliable regional reconstructions.

The reflectors seen in Fig. 6.20 may be traced throughout the area. According to Pirmez et al. 2012, p. 115):

Each key horizon is mappable throughout the area and has distinguishing geometric or seismic facies characteristics. Horizon 10 separates laterally continuous, moderate- to high-amplitude reflectors below, from a laterally continuous low-amplitude to transparent unit above. Horizon 20 is defined on the basis of onlapping reflections above it, observed particularly in Basin IV [Fig. 6.20] and Basin ... Horizon 20 can be traced to Basin II, where it shows conformable reflections above and below. Horizon 30 is a laterally continuous reflector defined by onlapping reflections above it in all basins; locally it is truncated by an acoustically transparent unit [Fig. 6.20]. Horizons 40, 50, and 60 are laterally continuous horizons that mark a vertical change in seismic facies. Horizon 40 is an erosional surface locally near the exit of Basin II ... Horizon 61 [Fig. 6.20] is an erosional surface with onlapping reflections above. It is a very weak reflection and is mappable only in Basin IV. Horizon 70 is well defined in Basin IV, where it forms a baselap surface at the base of a fan wedge sourced from the eastern channel [Fig. 6.20].

This example of basin analysis is discussed further in Sect. 8.10.1, where some of the details of the advanced chronostratigraphic dating and correlation techniques are briefly summarized.

The third example discussed briefly here is a regional study of the Cretaceous Chalk in the Norwegian portion of the North Sea's Central Graben (from Gennaro et al. 2013). As the authors noted (p. 236), "In the last decade, the classical paradigm of chalk as a monotonous and flat-lying deposit has been significantly revised and increasing evidence from seismic data has revealed the role that bottom currents have on chalk deposition. These currents sculpted the chalk sea-floor relief creating important topographic features such as channels, drifts and valleys." Sediment gravity flows and contourites composed of chalk have been mapped, and there is increasing evidence for syndepositional tectonic activity. The stratigraphic subdivisions and petrophysical and seismic character of the Chalk are shown in Fig. 6.21. These are based on seismic facies characteristics and the mapping of reflection terminations. Examples of the regional stratigraphic architecture are illustrated in Fig. 6.22, and an enlarged portion of this section, showing facies characteristics in more detail, is shown in Fig. 6.23.

Detailed mapping of the thicknesses and facies variations of the sequences identified in this study have been interpreted in terms of three tectonic phases, pre-inversion, syn-inversion and post-inversion. Although the details of this study are not relevant for our present purposes, it is of interest to note how the seismic data illustrates the onlap of the top Narve and top Thud reflectors onto anticlinal highs in Fig. 6.22. These features of the seismic architecture are

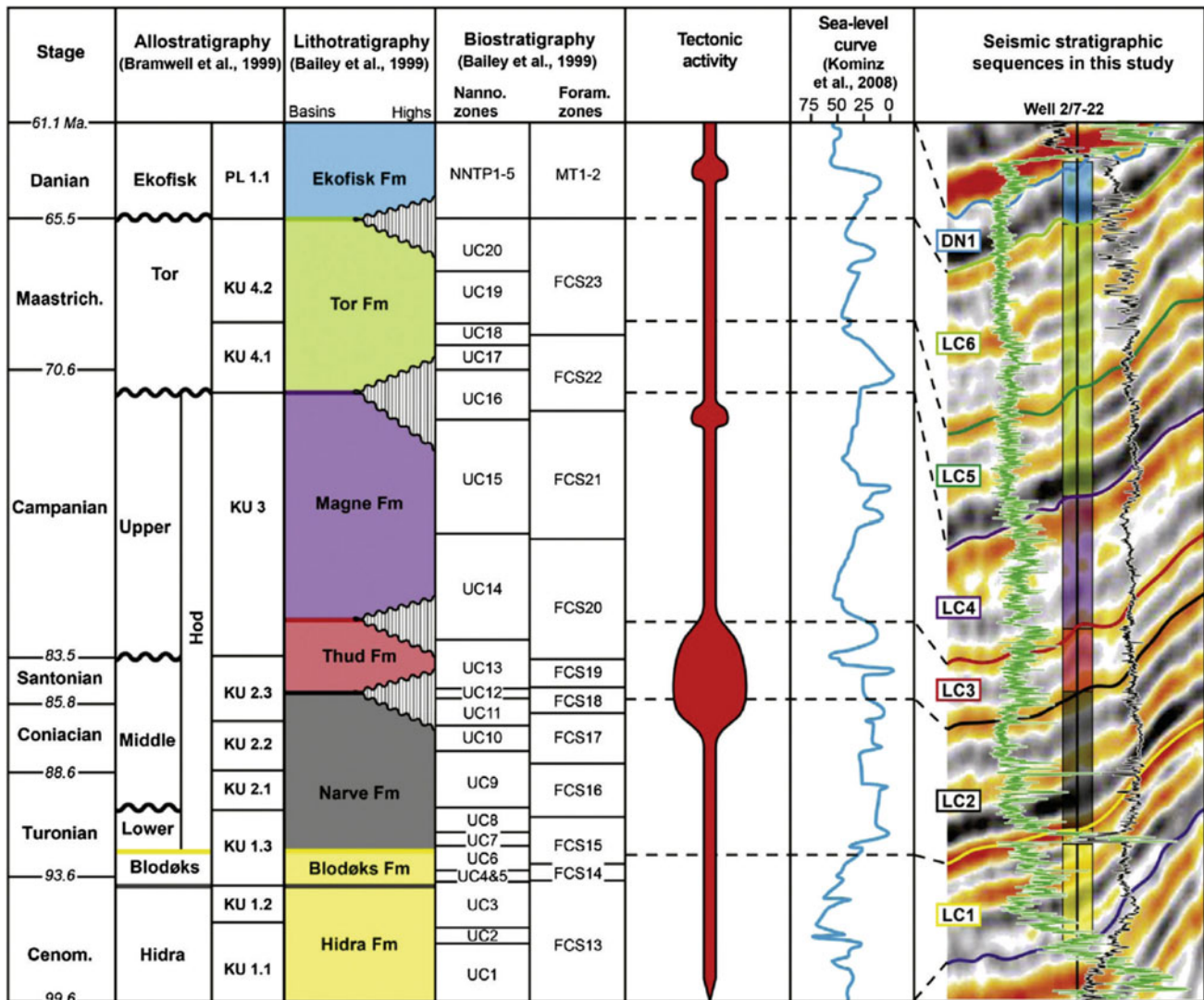


Fig. 6.21 Allostratigraphic and lithostratigraphic subdivision of the Chalk Group in the southern Norwegian sector of the North Sea and the corresponding seismostratigraphic units used in this study. The graph on the tectonic activity indicates the relative magnitude of the tectonic

inversion. The tectonic activity is considered to be continuous, but with culminations. *Green* well curve, gamma ray log increasing from *left to right*; *black* well curve, sonic log increasing from *right to left* (Gennaro et al. 2013, Fig. 2, p. 238)

interpreted as the result of syndepositional uplift during the inversion phase, following which erosion of the resulting highs provided a source for allochthonous chalk during the post-inversion phase.

One of the more important improvements in the seismic-reflection technique has been the development of the ability to image the complex structures associated with diapiric salt, including the edges and underlying boundaries of salt bodies and the stratigraphy beneath. A description of the processing techniques that have permitted this are beyond the scope of this book, but include the use of what is termed “pre-stack migration”. Traditionally, seismic traces are stacked to form a single trace, and then undergo migration to restore distortion caused by varying seismic velocities. With the increased processing speed and power of modern

computer methods, it is now possible to migrate each trace before combining, or “stacking” them, which preserves considerably more detail. An example is shown in Fig. 6.24. It is this breakthrough in processing that has permitted deep-water exploration of pre-salt structure and stratigraphy in such basins as the Gulf of Mexico and the deep offshore Atlantic Ocean off Brazil, Angola, etc.

The final example in this section touches on one of the most frequently encountered seismic facies, that of the complex clinoform set. The example illustrated (Fig. 6.25) is from the Barents shelf margin, located between northern Norway and Svalbard. An active phase of subsidence commenced in the mid-Eocene as rifting accompanied the opening of the Norwegian-Greenland Sea. High relief, a narrow shelf and an abundant sediment supply led to the

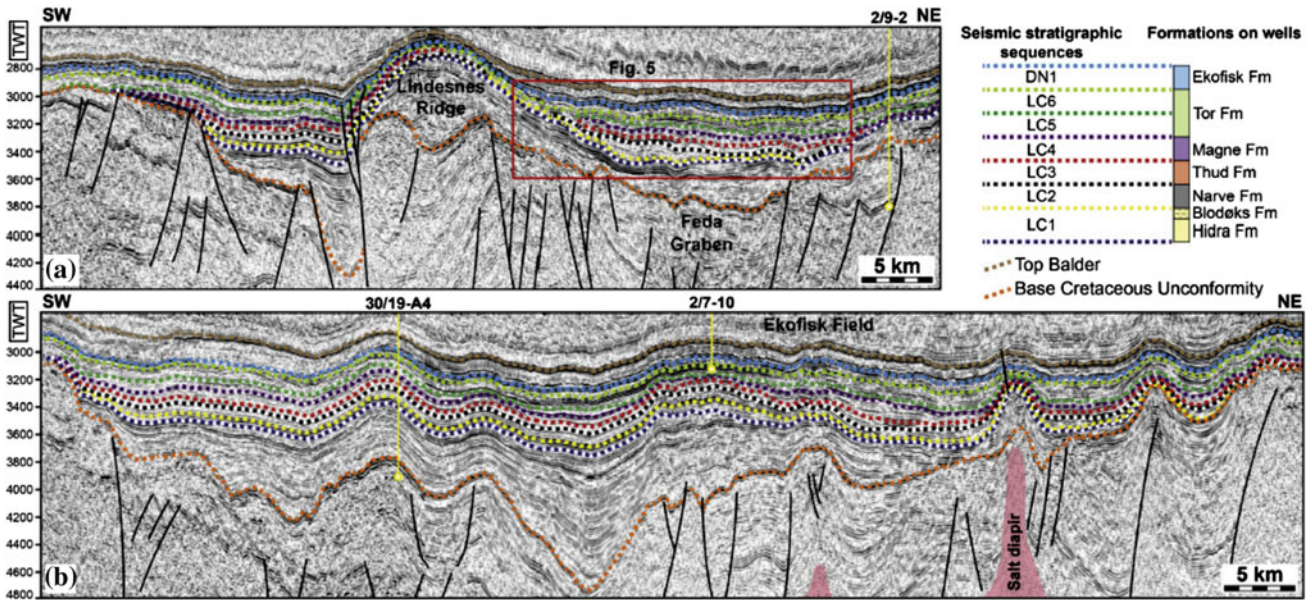


Fig. 6.22 Seismic sections of the southern Norwegian Central Graben with interpreted intra-Chalk seismic sequences LC1 to DN1. Regional structural elements and tectonic lineaments are also indicated. The

rectangular areas labeled Fig. 5 is reproduced here as Fig. 6.23 (Gennaro et al. 2013, part of Fig. 4, p. 242)

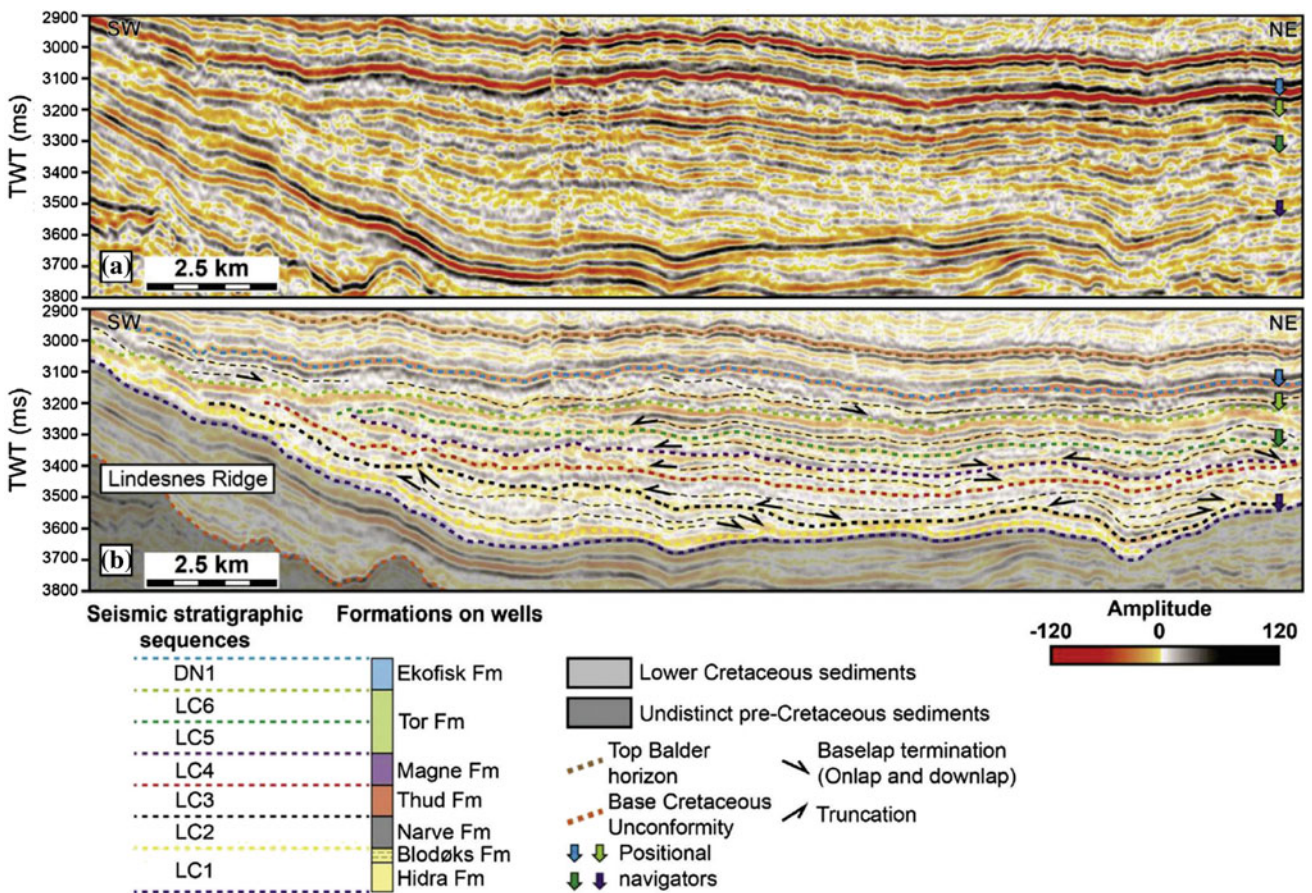


Fig. 6.23 Reflection configuration and terminations within the seismic units of the Chalk Group. **a** Uninterpreted and **b** interpreted 3D seismic profile (Gennaro et al. 2013, Fig. 5, p. 244)

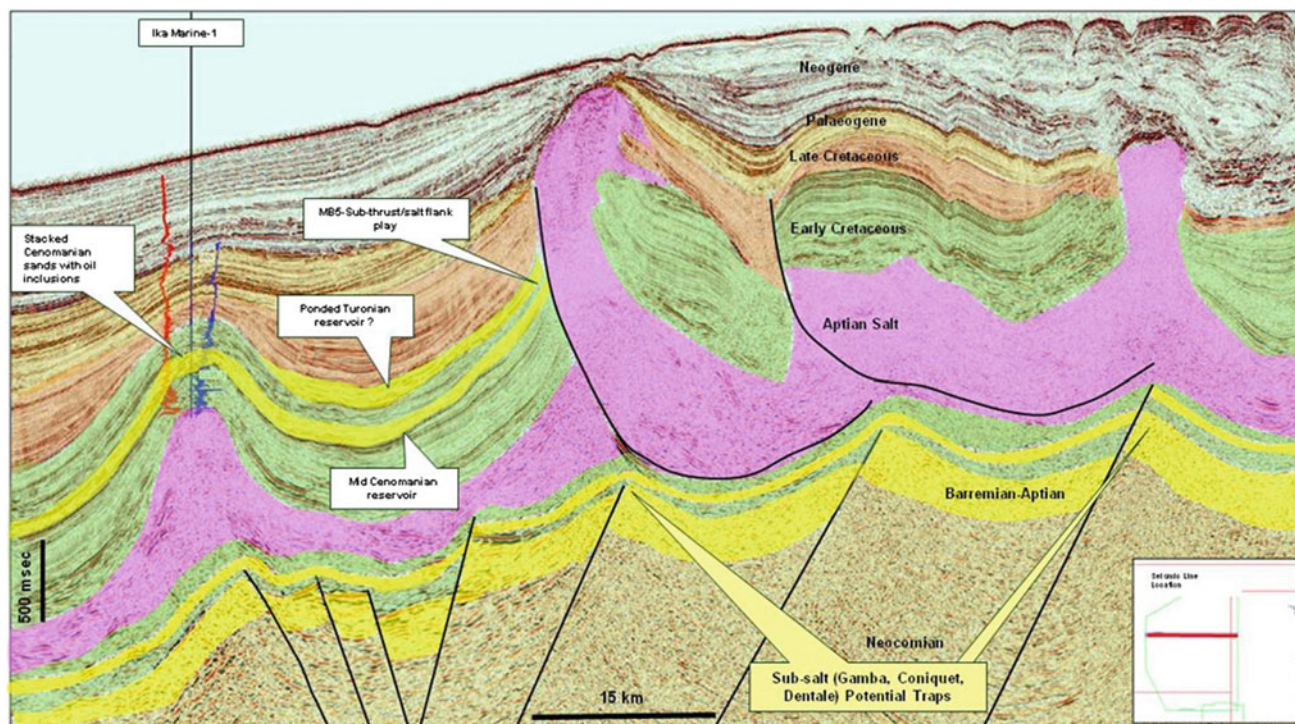


Fig. 6.24 An interpreted seismic line from offshore Gabon, showing the extremely complex structure and stratigraphy associated with diapiric salt (from Presalt.com; a seismic line from joint exploration by Ophir and Petrobras)

development of thick prograding clinoform sets within which slumping and subsidence remobilized large volumes of sand to form injectites. A single well with two short cores has been drilled within the study area, although not along the line of the illustrated section. The major stratigraphic subdivisions that may be recognized in this section consist of prograding clinoform units on the continental slope, consisting of re-sedimented shelf deltaic and other marine sediment. These units pass down into what are labeled as “depositional units” that have been interpreted as submarine fan complexes. Analysis of the architecture of these clinoforms provides considerable information about the history of subsidence and sea-level, a subject touched on in the next section.

6.3.3 Seismic Facies

The early work on seismic stratigraphy, in the 1970s, provided many useful broad generalizations about stratigraphic architecture that focused on large-scale geometric features, particularly the nature of reflection terminations (Sect. 5.2.2). These were illustrated in what is by now the classic diagram shown in Fig. 5.8, and constitute the larger scale elements of what is termed **seismic facies**, a term defined to mean “areally restricted group[s] of seismic reflections whose appearance and characteristics are distinguishable from those of adjacent groups” (Sangree and Widmier 1977). Reflection amplitude

and continuity are additional elements of seismic facies that have become increasingly important as processing and visualization power have improved. The concept of seismic facies is most usefully applied where the primary data consists of 2-D cross-sections, for which stratigraphic and sedimentological interpretations may not be immediately obvious. But the ground-truthing of seismic facies in terms of lithofacies may be difficult in the absence of well data (particularly cores) in key locations, because few seismic facies have unique interpretations (clinoform facies are the simplest to interpret directly). This problem is much less acute where 3-D data are available, because of the essential attribute of the 3-D volume that entire depositional systems may be visualized.

The other essential aspect of seismic-stratigraphic data, particularly 3-D data, is the scale of features that can now be imaged in their entirety. Complete depositional systems may be sliced and viewed in any vertical orientation and at different horizontal levels, over horizontal dimensions of tens of kilometres. This is orders of magnitude greater than even the best outcrop sections, which means that we can now “see” things that have never been seen before. This is particularly the case with deep-marine depositional systems, such as submarine fans and contourite drifts, for which outcrop data has mostly been very scrappy. The first depositional models for these features (Mutti and Ricci-Lucchi 1972; Walker 1978) were based on limited outcrop data and,

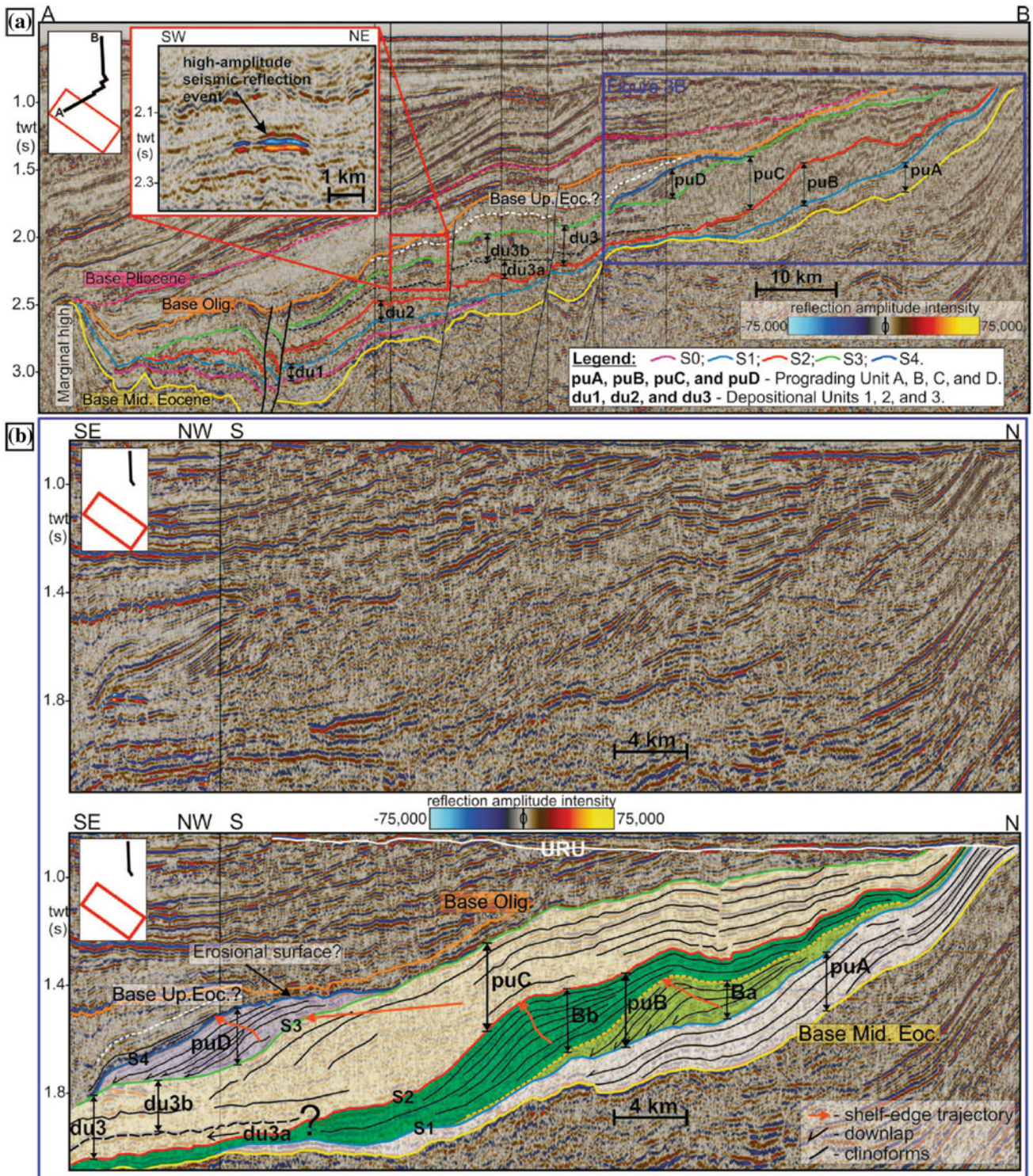


Fig. 6.25 Clinoform sets of Eocene-Oligocene age on the margin of the Barents Shelf. **a** In this section, three deep-water depositional units (1–3) pass up dip into prograding units, four of which (units A–D) have been mapped. **b** Uninterpreted and interpreted sections showing Prograding units A–D in the northern part of the study area (the

section outlined by the *blue rectangle* in the upper-right portion of diagram A) (Safronova et al. 2014, Fig. 3, p. 520). AAPG © 2014, reprinted by permission of the AAPG whose permission is required for further use

as has become apparent, provide very little real guidance for the interpretation of the large submarine channel and fan systems that form important reservoirs in many deep-water base-of-slope frontier basins, in part because of the enormous variability we now know exists in the size, shape and composition of submarine fans. This point can readily be appreciated by comparing these early, simple models, with the realities of a wide array of modern fans surveyed using side-scan sonar technology, summary details of which were assembled by Bouma et al. (1985).

Davies et al. (2004b) discussed the practicalities and pitfalls of the use of 3-D seismic data. The knowledge and experience of both geophysics and geology are required, in order to fully understand what can be done with processing, and the limitations inherent in the seismic method (geophysics) and the realities of stratigraphy and of sedimentological interpretation (geology). A common error is the attempt at direct interpretation of clastic lithofacies from reflection strength and continuity. There are many criteria that govern this feature of seismic facies (fluid content and diagenetic modification being obvious ones), and all of these need to be taken into account.

Facies models and sequence models provide guidance for the interpretation of the real world (Chaps. 4 and 5). It would be an ideal world if seismic facies could be categorized in the same way. Many researchers have provided categorizations of the seismic facies in their project areas, but as several authors have noted (e.g., Futral et al. 2012), calibration between seismic attributes and lithofacies is to a considerable extent basin specific, and so generalizations must be accorded a considerable latitude for inherent variability. Two seismic-facies classification tables are shown here (Figs. 6.26 and 6.27).

The first illustration (Fig. 6.26) shows a facies classification for a mixed carbonate-clastic continental-margin assemblage in the Philippines. The lithologic attribute of most of these facies vary from clastic to carbonate or mixed, as indicated by well calibration, but the geometrical attributes are distinctive. For example, facies D represents turbidites, facies E clearly represents clinoforms, and facies F images channels.

Sayago et al. (2012, p. 1844) stated “It is known that 40 % or more of recoverable hydrocarbons in carbonate deposits are trapped at stratigraphic unconformities, and in most cases, they are of karst origin.” Their study is of a largely carbonate succession of Pennsylvanian-Permian age on the Barents Shelf in the Norwegian Sea. The analysis commenced with a multi-attribute classification study of the seismic volume. Eighteen seismic attributes covering the whole range of seismic information were computed (e.g., time, amplitude, frequency, and attenuation). Comparisons and crossplots between attributes were used to define the seismic facies. This classification was then applied to samples of the seismic survey volume. An initial “unsupervised” classification

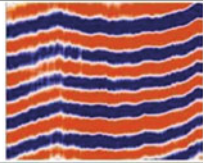
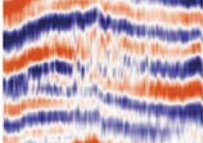
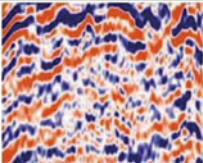
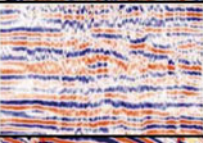
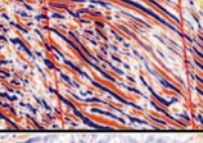
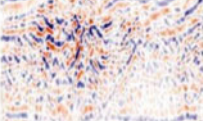
Seismic Facies	Reflection Attributes (a – external geometry, b – internal configuration, c – continuity, d) amplitude strength)
(a)	 <ul style="list-style-type: none"> a) sheet to wedge b) parallel to wavy c) high continuity d) moderate to high
(b)	 <ul style="list-style-type: none"> a) sheet to wedge b) parallel to wavy c) semi-continuous to high continuity d) low to moderate
(c)	 <ul style="list-style-type: none"> a) sheet to mound b) wavy to hummocky c) disrupted to discontinuous d) moderate to high
(d)	 <ul style="list-style-type: none"> a) sheet to wedge b) parallel to subparallel c) semi-continuous to disrupted d) low to moderate
(e)	 <ul style="list-style-type: none"> a) lens to wedge b) subparallel to convergent to oblique c) semi-continuous to high continuity d) low to moderate
(f)	 <ul style="list-style-type: none"> a) lens to channel-shaped b) wavy to chaotic c) discontinuous d) low to moderate

Fig. 6.26 A seismic facies classification for a mixed carbonate-clastic assemblage on the continental margin of the Philippines (Futral et al. 2012, Table 2). AAPG © 2012, reprinted by permission of the AAPG whose permission is required for further use

represents an automated analysis of the seismic data; a “supervised” classification includes some operator adjustments to better correlate the seismic data to information from core. The “training data” used in this classification is shown in Fig. 6.27. An example of a 2-D seismic cross-section analysed in this way is shown in Fig. 6.28a. Four seismic attributes have been calculated for the classification (instantaneous bandwidth, gradient magnitude, envelope, and dominant frequency), as shown in diagram B. Diagram C shows an “unsupervised classification” based entirely on numerical manipulations of the digital seismic data. Seismic facies 1 (SF1) is present not only in the flat-topped carbonate interval, but also in the vicinity of the main seismic reflectors occupying the outer slopes of the structural high, that is, top basement, top Gipsdalen, and top Bjarmeland (white arrows). Strongly chaotic patterns and complex alternation of seismic facies 2 (SF2), seismic facies 3 (SF3), seismic facies 4 (SF4),

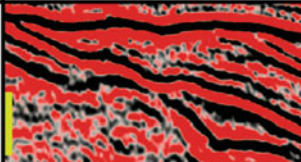
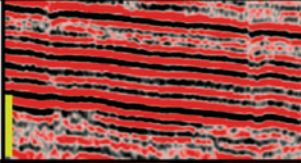
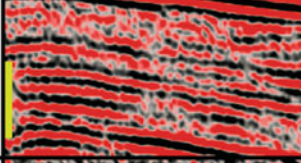
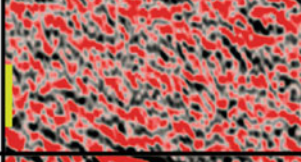
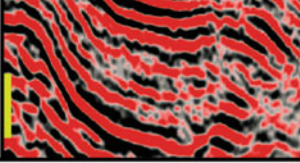
Seismic Facies	Reflection geometry	Amplitude characteristic	Spatial distribution	Example (Vertical bars represent 100 ms)
SF1	Parallel continuous	High amplitude	Occurs mainly at the crest of the structural high and at the top of basement	
SF2	Parallel continuous	Medium to low amplitude	Occurs mostly towards the flanks of the Loppa High	
SF3	Parallel discontinuous	Medium to low amplitude	In overlying Triassic clastics and some areas of the carbonate intervals	
SF4	Chaotic	Low amplitude	Present at the core of the buildups and in the basement	
SF5	Semiparallel dipping discontinuous	Medium amplitude	Occurs mostly in the slopes of buildups	

Fig. 6.27 A seismic facies classification for a carbonate succession, including paleokarst breccias. See text for explanation (Sayago et al. 2012, Table 4, p. 1860). AAPG © 2012, reprinted by permission of the AAPG whose permission is required for further use

and seismic facies 5 (SF5) are observed. “Supervised classification” results are shown in Diagram D. Seismic facies 1 is mostly concentrated in the topmost area (crest) of the Loppa High where it correlates with the parallel high-amplitude training points (the volumes selected by the user to fine-tune the classification). It is interpreted as consisting of paleokarst breccia units and its distribution in the supervised classification is associated with a major regional unconformity. Seismic facies 2 is restricted to the slopes of the structural high, high-lighting the main seismic boundaries.

An instructive clastic example of seismic-facies and sequence interpretation is that of Moscardelli et al. (2012) who examined the development of shelf-edge deltas on the Atlantic shelf margin off Trinidad, in an area where the continental-margin tectonic environment changes from transpressive to extensional within a space of 100 km. Figure 6.29 illustrates a composite northwest-southeast-oriented 3-D seismic line along strike, showing the shelf-edge region in eastern offshore Trinidad. Diagram (A) shows the seismic section; diagram (B) is a line drawing showing the seismic facies (SF) distribution and sequence-stratigraphic

interpretation of this section. The seismic character and distribution of the main sequence-stratigraphic units significantly vary from south to north; these variations are thought to be associated with underlying structural controls and changes in sedimentation rates across the margin. Contrasts in tectonic setting between the northern and southern parts of the project areas described in this study are marked. Steep thrust faults are important in the north; extensional growth faults are common in the south. These faults have guided the development of submarine canyons and therefore the downslope distribution of detritus. Tidal and along-shore currents are important in sediment dispersal, and gravity sliding and slumping have had a significant effect on the ultimate architecture of depositional units. This is clearly an example where the traditional 2-D approach to stratigraphic and sedimentological interpretation would not be successful. A seismic-facies classification developed for this area is shown in Fig. 6.30.

In this study and that of Safronova et al. (2014), analysis of the internal composition and architecture of clinoform units provides essential clues for the analysis of depositional

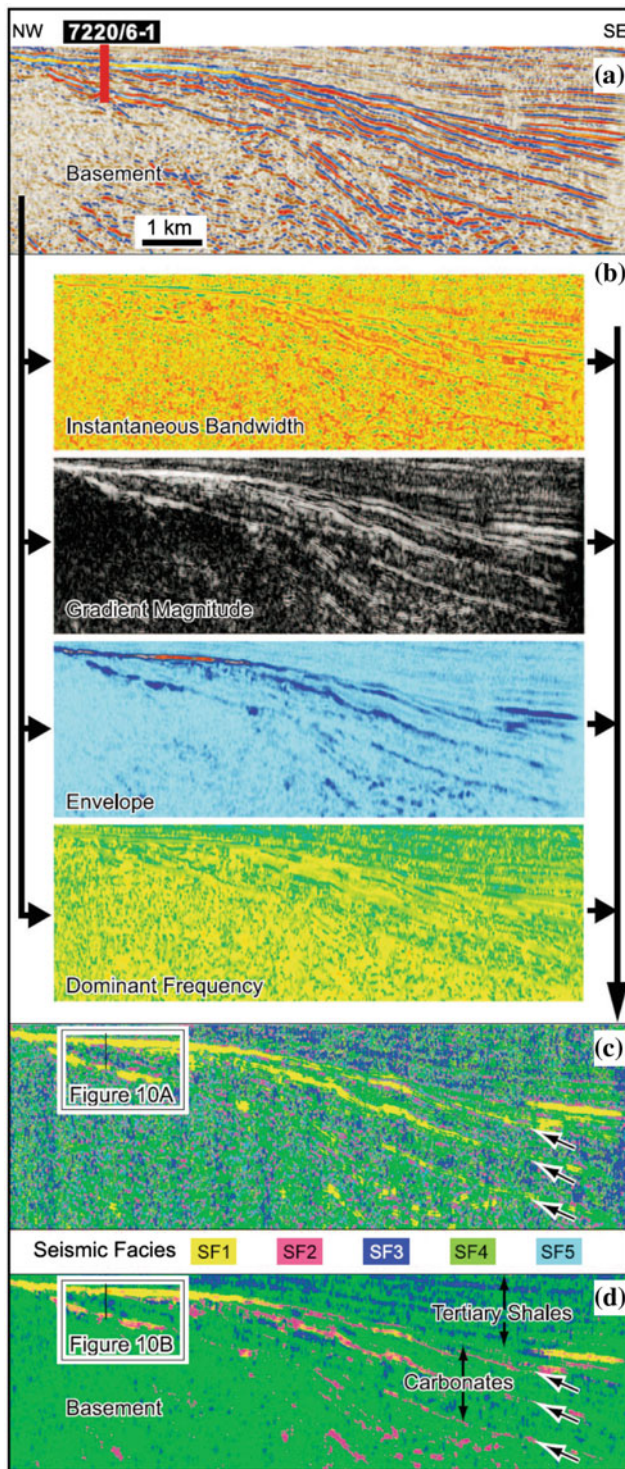


Fig. 6.28 Shelf-margin seismic section showing how the seismic facies classification is derived. **a** The uninterpreted seismic section; **b** Four seismic attributes calculated for the classification; **c** Unsupervised classification of the original seismic data; **d** supervised classification (Sayago et al. 2012, Fig. 9, p. 1858). AAPG © 2012, reprinted by permission of the AAPG whose permission is required for further use

and structural history. For example, in Fig. 6.25, the trajectory of the shelf-slope break is highlighted in the bottom diagram, providing insights into the changes in sediment supply and changes in relative sea-level through the accumulation of this unit.

Zeng et al. (2013) pointed out that seismic resolution may be a problem in the identification and mapping of clinoform sets, particularly those developed by deltaic progradation, which typically develop in shallow water and are much smaller than shelf-margin clinoforms.

It seems that the type of seismic clinoform configuration may also be related to data frequency. An oblique clinoform seismic configuration in higher frequency data ... tends to become a shingled configuration in the lower frequency data ... As a result, shingled facies observed in seismic data are not necessarily truly representative of geologic clinoform architecture. The merging of seismic responses of the thinner, low-angle downdip portion of clinoforms with that from underlying flat host rocks in low-frequency data appears to distort the seismic facies. (Zeng et al. 2013, p. SA45)

A process termed spectral balancing may be used to enhance the high-frequency end of the data spectrum, and this can reveal a subtle clinoform signature (Fig. 6.31).

The last example in this section is derived from the work of Burgess et al. (2013) who provided criteria for the identification of isolated carbonate buildups in the stratigraphic record. As they pointed out, these may be difficult to distinguish from volcanoes, erosional remnants and tilted fault blocks. In tropical and subtropical areas, such buildups may be common features of the continental shelf, but in many areas, such as continental margins off southeast Asia, characterized by rapid tectonism and a high sediment supply, local conditions may change over geologically rapid time scales, resulting in highly complex stratigraphic relationships. Aids to the identification of carbonate buildups (which can provide excellent petroleum reservoirs) have therefore been found useful. Figure 6.32 provides some examples of the distinctive seismic facies characteristics of carbonate buildups developed by Burgess et al. (2013) from a large seismic data bank assembled from offshore southeastern Asia. Key criteria include geometry (the vertical nature of the buildup, commonly with an overlying structural drape), seismic terminations (e.g., onlap of buildup margin by draping clastic units), and contrasts in reflection amplitude and continuity between the buildup and flanking strata.

6.3.4 Seismic Geomorphology

The development of seismic geomorphology represents a huge step forward in methods for petroleum exploration and development. High quality 3-D data are required, with

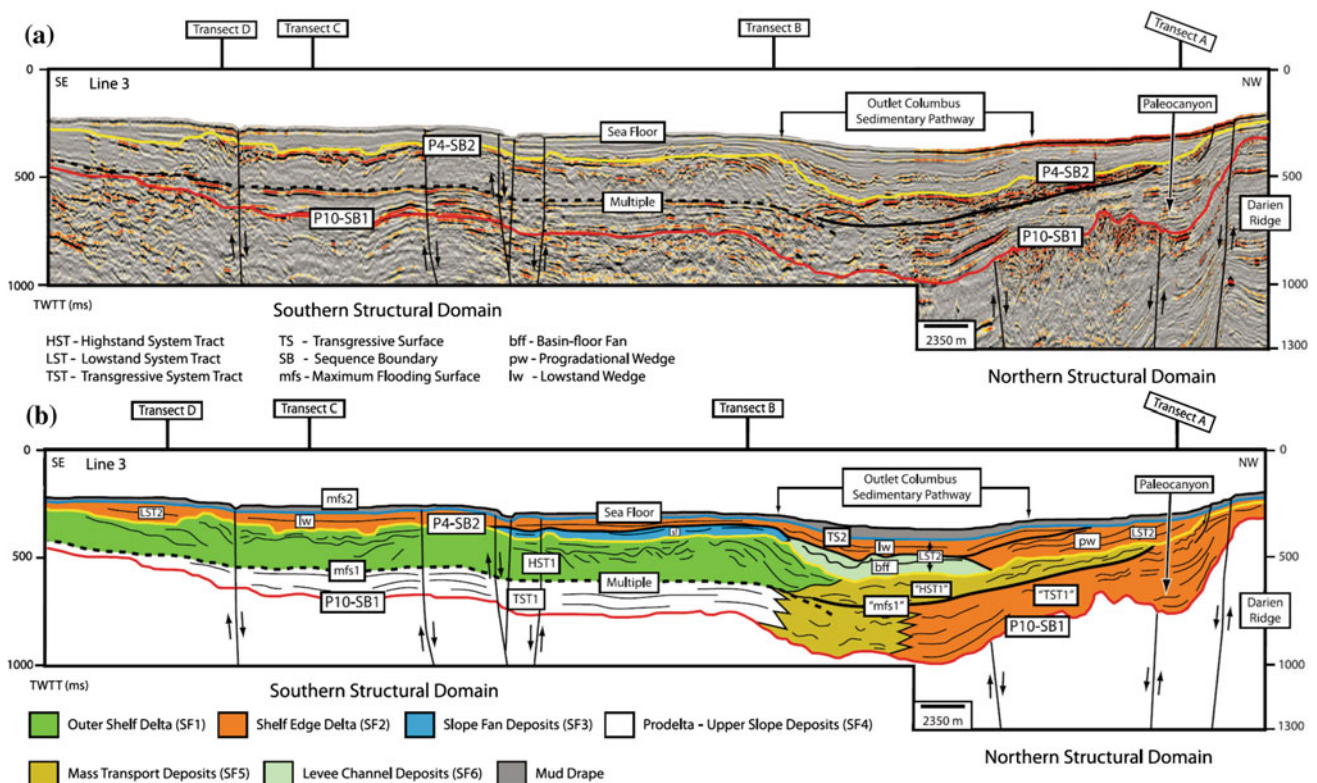


Fig. 6.29 Strike-oriented seismic section (a) and its interpretation (b), along the Atlantic shelf-margin of Trinidad. Terms in quotation marks indicate that the indicated units and surfaces do not present the typical seismic characteristics defined by the sequence-stratigraphic approach; however, these intervals are time equivalent to units to the south that fit the traditional sequence-stratigraphic definition for key surfaces and

system tracts. *TWTT* two-way traveltime; *LST* lowstand systems tract; *HST* highstand systems tract; *TST* transgressive systems tract; *mfs* maximum flooding surface; *lw* lowstand wedge; *bff* basin-floor fan (Moscardelli et al. 2012, Fig. 3, p. 1489). AAPG © 2012, reprinted by permission of the AAPG whose permission is required for further use

processing by skilled geophysicists, but a deep understanding of sequence stratigraphy and sedimentology is essential for in-depth interpretations of these data. Where such a combination of data and skillsets is available it may render all earlier sedimentological approaches to subsurface analysis obsolete. The simplistic facies models used through the 1960s to 1990s have been replaced by actual visualizations of entire depositional systems. However, the understanding of depositional processes that evolved during the facies-models era form an essential background to seismic analysis. For example, the earlier ideas about inner- mid- and outer-fan that were introduced in the 1970s (Mutti and Ricci-Lucchi 1972; Walker 1978) were still found to be useful when Bouma et al. (1985) compiled numerous studies of modern fans using side-scan sonar, and some of the defining elements of these three subdivisions do appear on seismic images of some submarine fans, a category of depositional system that we now know, through such studies, to be vastly more complex and varied than was imagined a few decades ago. For example, Fig. 6.33 illustrates three cross-sections through a fan complex on the Borneo continental margin, in which the three-fold subdivision that had

been proposed for fans appears to be applicable—an inner fan characterized by a prominent channel-levee complex (commonly a single main channel fed from a canyon point source), a mid-fan with a much more subdued distributary channel-level system, and an outer fan with a smooth, unchanneled, convex-up cross-section representing the accumulation of sheet-like turbidites.

The most spectacular 3-D interpretations of depositional systems are those of channelized environments, particularly fluvial and submarine fan settings, with their complexes of levees, crevasse splays, and overbank areas (e.g., Posamentier and Kolla 2003; see Figs. 6.34, 6.35, 6.36 and 6.37 of this book). For fluvial systems there is, of course, a virtually limitless suite of modern analogues for comparison with the ancient examples. Comparisons of horizontal seismic sections with selected images from Google Earth or some comparable source of aerial imagery make for very powerful and effective interpretations. Many such studies have now been published, many including quantitative analyses of channel and meander characteristics.

For submarine fans, imagery of modern fans is limited to what can be obtained from side-scan sonar data, and

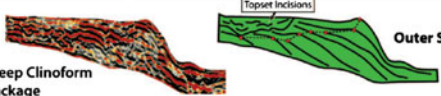
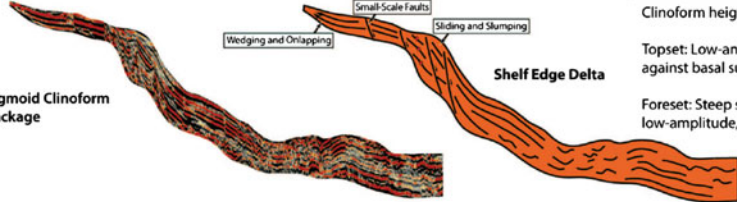



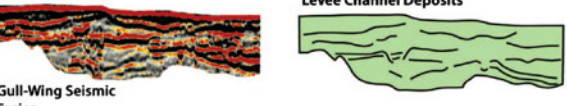
SF	Seismic Facies Description	
1	 <p>Steep Clinoform Package</p> <p>Outer Shelf Delta</p>	<p>Clinoform heights 10 s and 200 m</p> <p>Topset: Low-angle, high-amplitude, and relative continuous reflectors</p> <p>Topsets are incised by channelized-like features.</p> <p>Foreset: Steep slopes, medium- to low-amplitude reflectors</p> <p>Rollover points do not surpass outer shelf region and overall rollover trajectory is mostly progradational.</p>
2	 <p>Sigmoid Clinoform Package</p> <p>Shelf Edge Delta</p>	<p>Clinoform heights, >200 m</p> <p>Topset: Low-angle, high-amplitude and continuous reflectors; wedging and onlapping against basal surface</p> <p>Foreset: Steep slopes, high- and low-amplitude continuous reflectors that transition into low-amplitude, discontinuous, and sometimes chaotic reflectors</p> <p>Bottomset: Low-amplitude to discontinuous reflectors</p> <p>Rollover points are strongly progradational, sometimes displaced by sliding.</p>
3	 <p>Onlapping Wedge</p> <p>Slope Fan Deposits</p>	<p>Thickness of individual packages containing SF3 facies are in the range of 75 to 150 m.</p> <p>High-amplitude continuous reflectors that are arranged on an onlapping wedge against the slope.</p> <p>This facies is not volumetrically significant in the study area.</p>
4	 <p>Continuous and Parallel Reflectors</p> <p>Prodelta/Upper Slope Deposits</p>	<p>Thickness of individual packages containing SF4 facies are approximately 100 m.</p> <p>This facies is characterized by high-amplitude, continuous, and parallel seismic reflectors.</p> <p>Lateral or vertical variations within seismic reflectivity and continuity are limited.</p>
5	 <p>Chaotic Seismic Facies</p> <p>Mass Transport Deposits</p>	<p>Thickness of individual packages containing SF5 facies can reach up to 250 m</p> <p>This facies is characterized by low-amplitude, semitransparent, chaotic reflections that can transition into low- and high-amplitude semicontinuous reflections in some areas.</p> <p>This facies is volumetrically abundant on the lower slope region.</p>
6	 <p>Gull-Wing Seismic Facies</p> <p>Levee Channel Deposits</p>	<p>Thickness of individual packages containing SF6 facies can reach up to 250 m</p> <p>This facies is characterized by high- and low-amplitude reflectors with variable continuity. Packages within SF6 facies oftentimes dissect each other vertically and laterally.</p> <p>This facies is volumetrically abundant on the lower slope region.</p>

Fig. 6.30 A seismic-facies classification of the shelf-margin depositional systems, Atlantic margin of Trinidad (Moscardelli et al. 2012, Fig. 6, p. 1493). AAPG © 2012, reprinted by permission of the AAPG whose permission is required for further use

ancient-to-modern comparisons are less abundant. Descriptions and illustrations of some of the world's best outcrops of ancient deep-marine systems were collected in a large-format volume by Nilsen et al. (2007).

A few seismic-geomorphic studies of carbonate environments have been published, but few that make use of horizontal sections to image a carbonate system. It would appear that such sections are of limited usefulness, compared to traditional 2-D seismic.

The other major use of seismic geomorphology has been to image erosion surfaces, including unconformities and such features as incised valleys and paleokarst surfaces (Figs. 6.38, 6.39, 6.40 and 6.41). A range of examples of modern applications is contained in the volumes edited by Davies et al. (2004a, 2007).

Turning to fluvial examples, Ethridge and Schumm (2007) provided a discussion of modern concepts in fluvial geomorphology, focusing on what could be deduced from imagery of a random segment of a fluvial system. The use of modern aerial photographs or satellite imagery makes such

interpretations relatively straightforward. Figure 6.34 is one of the first illustrations of a horizontal seismic section through a fluvial system to be published. It shows a meandering system in the shallow subsurface of the Gulf of Thailand. False colour imagery is used to highlight the amplitude differences between the meandering channels and the overbank areas. Miall (2002) used successive time slices from a Pleistocene system to explore the architecture of an incised-valley system and its badland-style tributaries.

A recent example of the use of horizontal seismic sections to explore an ancient fluvial system was provided by Hubbard et al. (2011) from the Alberta Oil Sands (Fig. 6.35). The strata in this study area are between 300 and 400 m below the surface, and seismic resolution is less than 5 m. A modern analogue of the meandering fluvial style was suggested, in the form of an aerial photograph of the Sittang Estuary, Myanmar. The addition of a map of gamma-ray readings from wells that penetrate this section provides an essential cross-calibration between seismic and gamma-ray data that can then be used for the interpretation of lithofacies

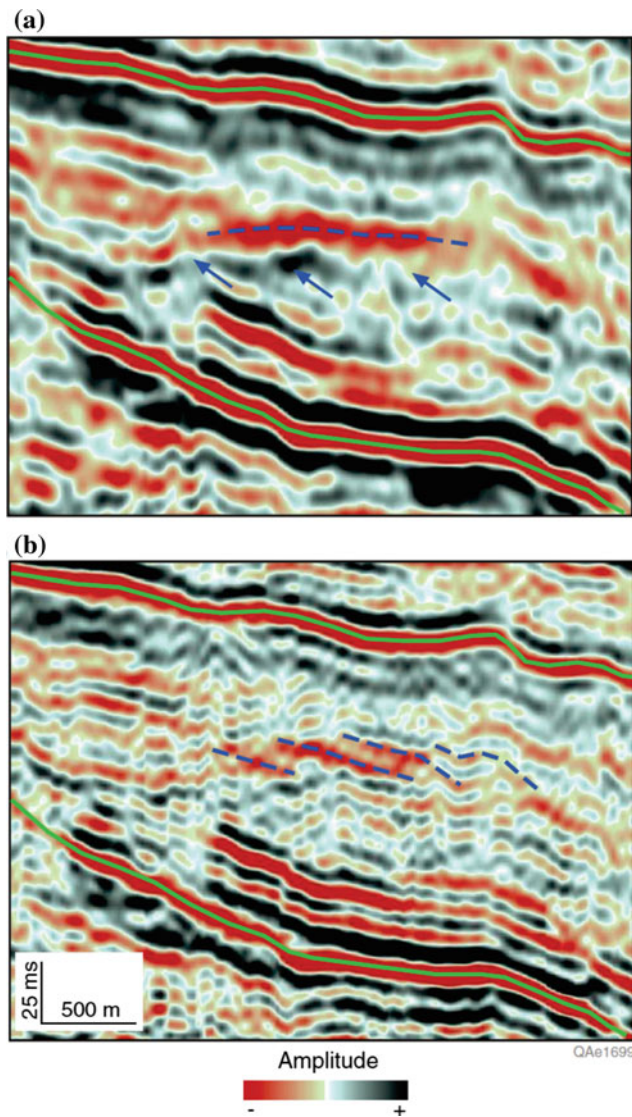


Fig. 6.31 Reducing ambiguity in interpreting clinoform prograding sequences by spectral balancing. **a** Original stacked and migrated seismic section in Abo Kingdom carbonate field of west Texas, with a flat (*dashed line*) event and some toplapped events (*arrows*) underneath. **b** The same section after spectral balancing processing. The flat event in the original data has been broken up into clinoforms (*dashed lines*) having slopes similar to those of surrounding events. The toplaps disappear (Zeng et al. 2013, Fig. 18, p. SA48). AAPG © 2013, reprinted by permission of the AAPG whose permission is required for further use

and reservoir properties in other areas. Hubbard et al. (2011) provided a detailed analysis of the lithofacies and architectural elements of this section, in terms of point bars, counterpoint bars and other features.

The use of perspective views of depositional systems can considerably enhance the visual effectiveness of 3-D seismic imagery. Figure 6.36 displays a turbidite channel in the Gulf of Mexico. The relevant portion of a vertical 2-D section that intersects the horizontal section provides the necessary

information on the vertical seismic characteristics of the succession. False colour variations, which display seismic amplitude variations, may be correlated locally to lithologic variability across the area, from channel-fill to overbank.

Another example of a submarine fan is shown in Fig. 6.37. This is a small fan, subdivided into upper-, mid- and lower-fan segments, according to Walker's (1978) model. The stratal slice image shown in Fig. 6.37b is not a structurally horizontal seismic section, but follows the synclinal dip of the strata, as shown by the dashed line in the vertical section, above. This image was derived from the top of a seismically chaotic section, which is interpreted by Zeng et al. (1998) as representing the lithologically heterogeneous assemblage characteristic of the fan setting.

The remaining examples in this section deal with the imaging of important surfaces in the subsurface. Unconformities may contain significant information about contemporary erosional patterns, and their topography may have useful implications for petroleum trapping configurations. A particularly interesting unconformity is the surface that marks the top of the Upper Miocene Messinian stage in the Mediterranean basin. Since the first deep-sea drilling project in the Mediterranean Sea in 1970 geologists have known about a prominent, widespread unconformity that spans most of the basin margins, and a thick evaporite section occupying the basin centre. During the Miocene the Mediterranean basin became isolated from the Atlantic Ocean, and evaporated to dryness several times (a drop in sea level of up to 2 km), leaving a deeply eroded basin margin cut by fluvial canyons (Ryan and Cita 1978). Figure 6.38 illustrates a seismic section across the basin margin off the Ebro delta in northeastern Spain. The erosional relief on what is interpreted as the Messinian unconformity is clear on this section, as is the truncation of the units below and the progradation of the Pliocene section that draped and buried the unconformity. A 3-D seismic survey of this area yielded the perspective map view shown in Fig. 6.39. The dendritic drainage pattern revealed by this map is very similar to that of "badland" topography in desert areas, such as that in southern Spain and parts of the southwest United States. About 400 m of erosional relief is visible in the seismic data from this area (Martinez et al. 2004).

As noted in the previous section, paleokarst deposits may be very important as petroleum traps, and 3-D seismic data has proved very successful in identifying and mapping these deposits (Sayago et al. 2012; Zeng et al. 2011; Ahlborn et al. 2014). Figure 6.40 is a 2-D seismic section through a succession of Lower Paleozoic carbonate deposits cut by several unconformities that are underlain by what are interpreted as paleokarst deposits. As each surface was developing by surface exposure and erosion, fluctuating water tables led to the development of subterranean drainage systems, with sinkholes, tunnels and caves, many of which underwent

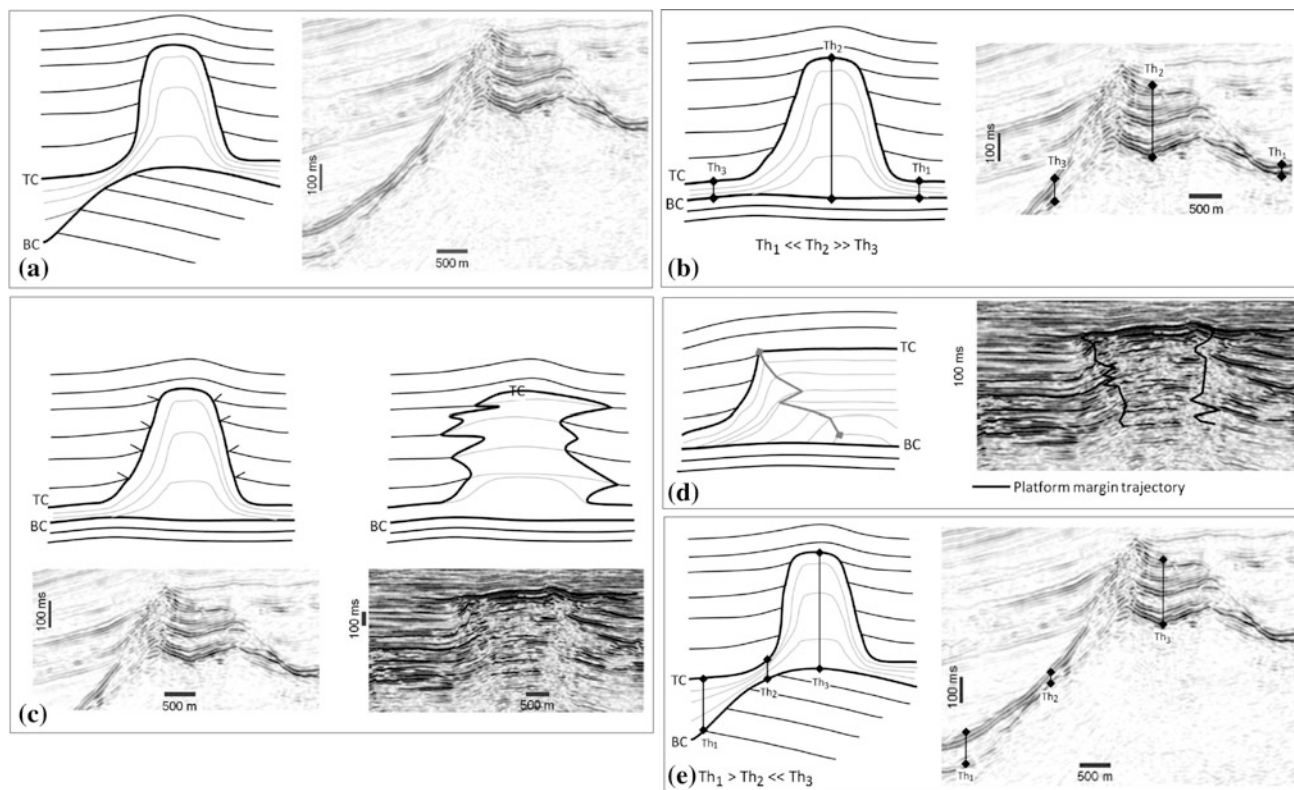


Fig. 6.32 Seismic facies of isolated carbonate builds. **a** An antecedent topographic high beneath an isolated carbonate buildup. **b** Significant localized thickening within an isolated carbonate buildup. **c** Onlap of overburden onto the margins of an isolated carbonate buildup (*left*), contrasted with a situation where depositional relief on the margins of the isolated carbonate buildup was lower because of contemporaneous infill of the adjacent basin (*right*). In this case, carbonate material from the platform top was transported away from the platform margin to produce depositional wings that interfinger

with the basin-fill strata. **d** Platform margin trajectories with phases of progradation, aggradation, and retrogradation, which can be indicative of an isolated carbonate buildup. **e** The thin-thick-thin pattern commonly developed on isolated carbonate builds that are shedding material from the platform top through a bypass zone to be redeposited in deeper water adjacent to the platform. *TC* top carbonate; *BC* base carbonate. (diagrams assembled from several illustrations in Burgess et al. 2013). AAPG © 2013, reprinted by permission of the AAPG whose permission is required for further use

significant collapse, resulting in disruption of the stratigraphic layering. Surface erosion, in some cases, ultimately led to the development of fluvial gullies and channels, with isolated karst towers left behind. An analogy with the karst topography of parts of the Guilin Province in southern China was suggested by Zeng et al. (2011, p. 2076). Extraction of stratal slice data from seismic volumes through these types of succession may provide detailed maps of the surface karst topography. Figure 6.41 provides an oblique view of such a surface, and contains graphic imagery of the surface erosional and collapse features of a paleokarst surface of Ordovician age.

6.4 Directional Drilling and Geosteering

Historically, most drill holes have been drilled vertically or as near vertically as possible, but for many reasons, directional drilling may have advantages, both geologically and

for practical reasons. For example, access to potential reservoir beneath environmentally sensitive lands, or under water, may be accessed by directional drilling, and the technology now allows multiple holes to be drilled in every direction from a single well pad, which reduces the surface impact of the operation. Geologically, the advantage of directional drilling is that it creates the possibility to access specific subsurface targets by the use of real-time downhole steering. In the 1980s the development of the technology permitted wells to be completed with horizontal segments that could be steered to penetrate a reservoir along its length, generating substantially greater exposure of a hydrocarbon-bearing unit to the producing well. Horizontal segments of up to 3 km are now possible. Drilling motors are mounted at the end of the drill pipe, driven by the drilling mud, and subsurface navigation is achieved by the use of gyroscopes, with steering achieved on the basis of navigational information sent electronically from the drill head in real time. Horizontal drilling has become widely used since the 1990s

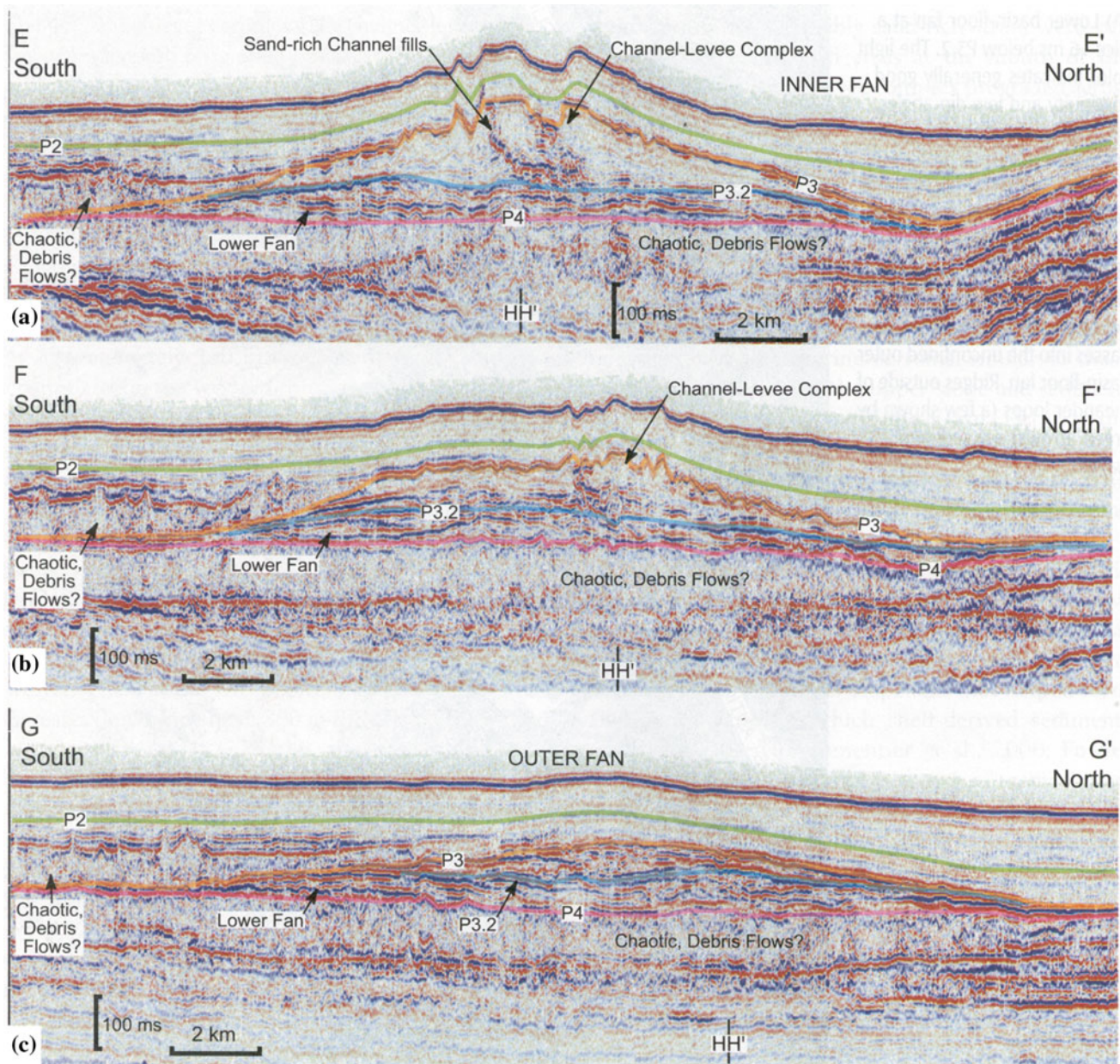


Fig. 6.33 Three strike-sections across the submarine fan formed on the basin floor, Borneo (Saller et al. 2004). AAPG © 2004, reprinted by permission of the AAPG whose permission is required for further use

in the production of shale gas and tight oil, and is also an integral part of the technique of in situ production of oil from the Alberta Oil Sands.

Geological mapping techniques may be used as an aid in subsurface navigation. This is termed **geosteering**, and may be carried out using detailed mapping information obtained before drilling commences, or may be done in real time, for example by using petrophysical log data recorded as the well is being drilled or by using well cuttings that may be monitored for lithological content, microfossils or palynomorphs that are known to characterize the target unit and the

overlying and underlying formations. The objective is to ensure that the well continues to penetrate the desired stratigraphic level as drilling proceeds, although allowance must be made for the delay caused by the travel time of the cuttings from the drill face. Three examples are briefly discussed here. In each case the operator stressed that considerable care needs to be taken to construct a very detailed and accurate three-dimensional model of the subsurface target volume before drilling commences, because the real-time data needs to be matched against the model as drilling proceeds.

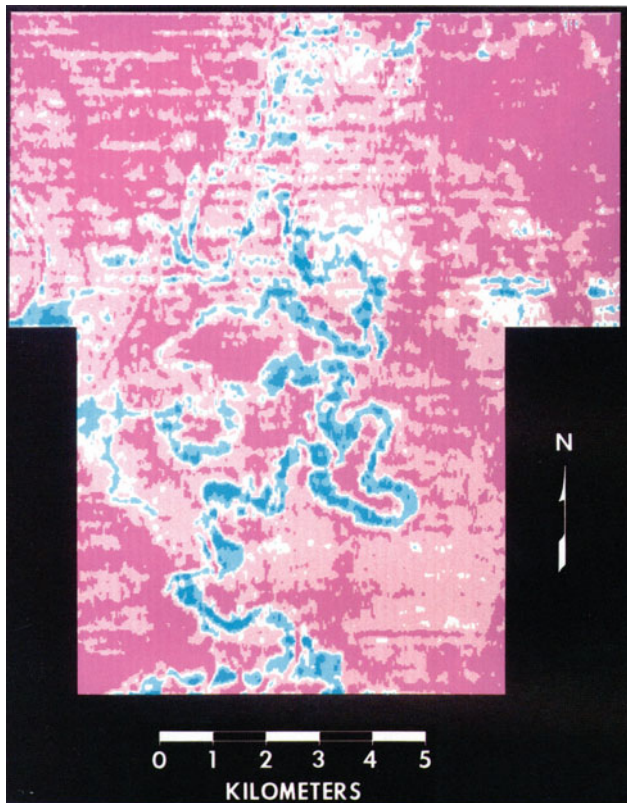


Fig. 6.34 A meandering fluvial channel in shallow sediments in the Gulf of Thailand. From the first (1986) edition of Brown's AAPG memoir (Brown 2011 is the latest edition). AAPG © 2011. Reprinted by permission of the AAPG whose permission is required for further use

Taylor (2010) described the use of real-time petrophysical monitoring during the drilling of a horizontal hole. The project began with the establishment of the petrophysical characteristics of the rocks to be drilled. From this information a model is developed of the petrophysical values to be predicted along the projected path of the hole, based on the three-dimensional reconstruction of the stratigraphic architecture (Fig. 6.42). Note how, in this diagram, the planned well path first passes nearly vertically through the stratigraphy, and is then designed to drill out straight legs at slightly different angles in order to follow the mapped structure, with the predicted petrophysical response along the course of the hole shown in the two graphs at the top. Figure 6.43 shows the results being obtained as drilling is in progress. Deviations from the modelled petrophysical responses may be fed back into the structural model of the target volume in order to permit corrections to be made, if necessary, to the path followed by the drill. Some earlier examples of the use of real-time "logging while drilling" were described by Bristow (2002).

Southcott (2014) described briefly how a 3-D seismic data volume was subjected to rigorous calibration and time-depth conversion with the use of relevant well

petrophysical and core data, and then used to plot the desired path of a projected lateral well.

In Sect. 6.6.3, brief reference is made to a study of "forensic chemostratigraphy" that was used by Hildred et al. (2014) to characterize the units that had been penetrated along a horizontal well through the Bakken petroleum system.

6.5 Older Methods: Isopleth Contouring

In the absence of seismic data, the explorationist and the basin analyst must maximize the data available from well or outcrop data. This was the situation after the Second World War, before the seismic technique had evolved to the point that stratigraphic information could be extracted from the data. As noted in Sect. 1.2.3, the need for a "big picture" of a sedimentary basin was the drive that underlay the work of W.C. Krumbein and his colleagues at Northwestern University (from which modern ideas about sequence stratigraphy emerged: see Sects. 1.2.9 and 1.2.10). Krumbein (1948) devised a suite of quantitative lithologic indices and ratios that could be calculated from the lithologic succession at each sample point. Contouring of the resulting data created "isopleths", which formed maps that could then be interpreted in terms of paleogeography. Some of these approaches have become part of the standard methodology of basin analysis. Net sand maps or sand-shale ratio maps are good examples. For example, Fig. 4.28 shows how the distribution of sand thicknesses may be used to define patterns that may be interpreted in terms of the sedimentary controls acting on deltas. Figure 4.47 shows how the ratio of clastic to carbonate lithologies defines the transition from a coastal clastic belt to a broad carbonate platform. The gamma-radiation map of Fig. 6.35c shows how petrophysical data may be used for a similar purpose, in this case the definition of net sand thickness, a parameter that could (in this case) be interpreted in terms of the patterns of channels and bars within a meandering fluvial system. Figure 6.44 illustrates the use of the net sand mapping technique to develop highly detailed facies interpretations, where adequate drill data are available. Figure 6.45 illustrates a modern example of the use of this technique. Seismic data were used to restore Middle Miocene topography in this basin in Trinidad. Net sand values reveal two major northeast to southwest sand trends and their relationship to growing structures. "Zones of absence of Middle Miocene Herrera sands coincided with paleo-highs on the restored Middle Miocene topography" (Moonan 2011).

Krumbein (1948) developed a clastic ratio parameter, calculated from the sum thickness of clastic lithologies divided by the sum thickness of carbonate and evaporite lithologies in a vertical section. Figure 6.46 is an example of the use of this ratio. He stated, of this map (p. 1913):

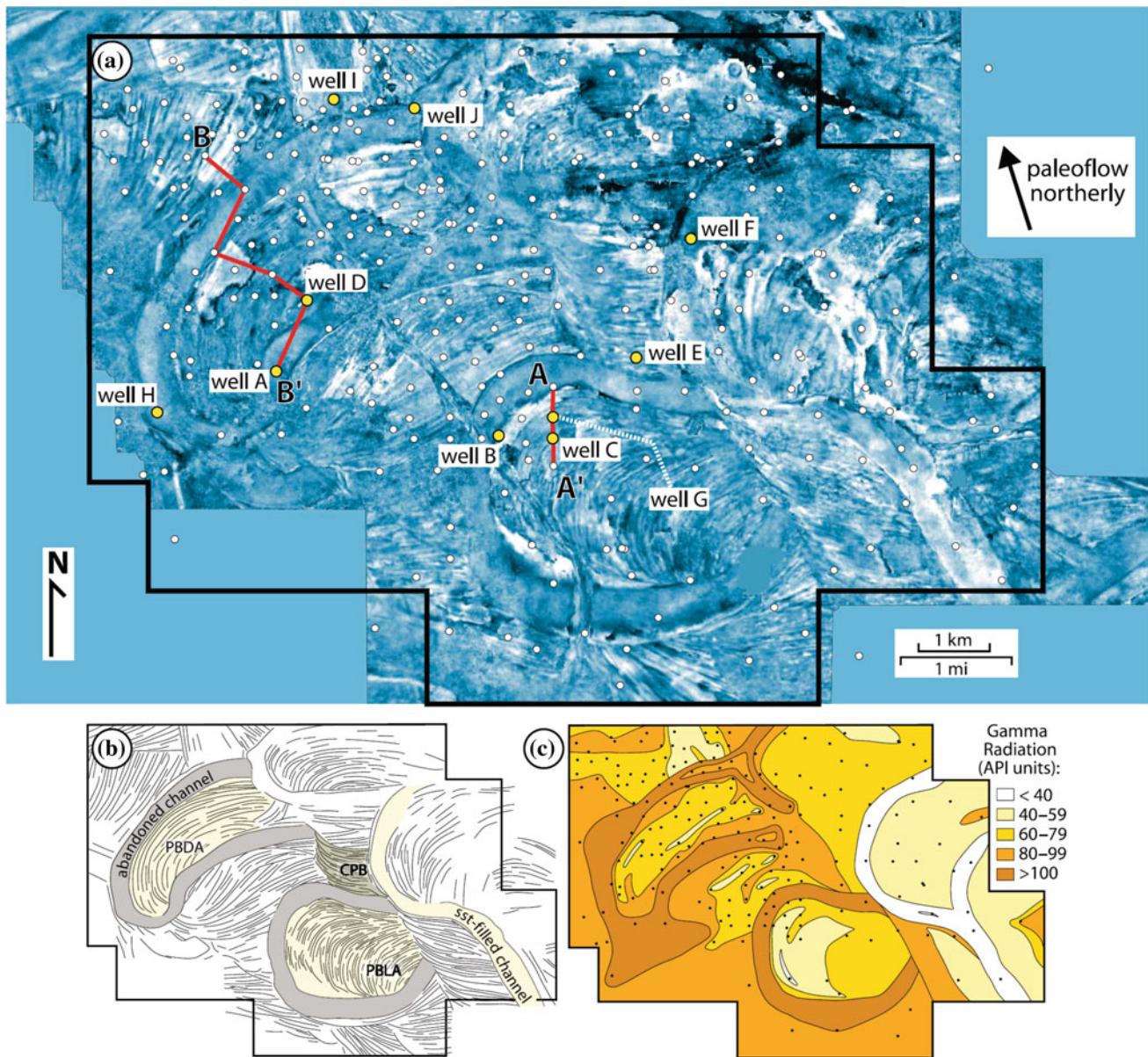


Fig. 6.35 Seismic exploration of the Alberta Oil sands. Mannville Group, south of Fort McMurray, Alberta. **a** Time slice taken at a horizon, 8 ms (approx. 8 m) below a flooding surface at the top of the oil-bearing unit; **b** Interpretation in terms of scroll bars, point bars and

channels; **c** Gamma-ray values at the selected horizon. From Hubbard et al. (2011, Fig. 2, p. 1126). AAPG © 2011. Reprinted by permission of the AAPG whose permission is required for further use

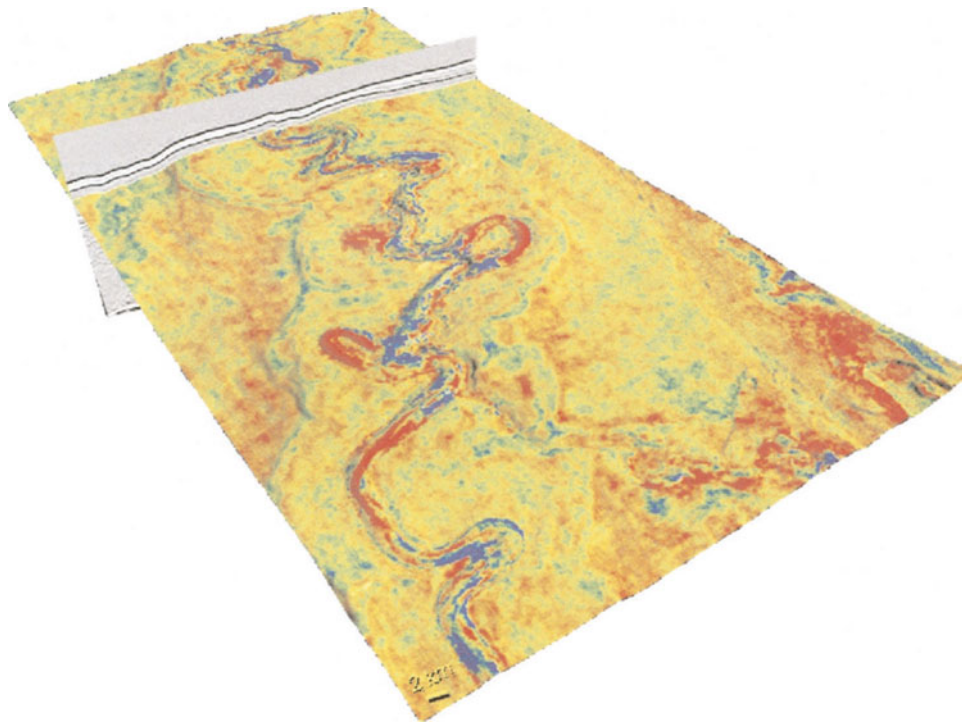
... the upper map shows generalized isopachs, clastic ratio lines, and sand-shale ratio lines. The three sets of lines render the map somewhat cumbersome, and in practice the clastic ratio may be used alone with the isopachs, if the section shows a balance between clastics and non-clastics. ... The lower map ... is a combination of the clastic and sand-shale ratios in the upper map, and it shows the statistical lithologic differentiations of the map area. The map is based on combinations of the clastic ratio and the sand-shale ratio in terms of certain limiting values.

The regional pattern revealed by this map is of a broad clastic belt in the east (Montana-Colorado) bordering the Canadian Shield, passing gradually westward into a

carbonate-dominated area near the continental margin, running north-south through Idaho. As an aid to constructing regional paleogeography this is a useful map, but clearly many data points would be required to plot individual depositional systems on a more local, 10^3 – 10^4 m scale.

Extensive use of these various isopleth maps was made in the early regional stratigraphic and sequence work of Sloss et al. (1949), but these techniques have largely fallen into disuse in recent decades, because of the more powerful methods of facies mapping that emerged in the 1960s and 1970s, and the seismic-stratigraphic and sequence-

Fig. 6.36 A map of amplitude variations draped on a gently dipping stratal surface, illustrating a meandering turbidite channel in shallow sediments in the Gulf of Mexico (Posamentier et al. 2007, Fig. 2, p. 3)



stratigraphic techniques that evolved more recently. An exception would be the net-sand map, which is still used to illustrate sand reservoirs in stratigraphic traps (e.g., Fig. 6.45).

6.6 Mapping on the Basis of Detrital Composition

Traditional methods of correlating petrophysical logs are discussed in Sect. 6.2. A wide range of additional techniques has evolved over the years for the examination of subsurface petrophysical, core and sample data. Compilations of such studies have been published by Hailwood and Kidd (1993) and Ratcliffe and Zaitlin (2010). These methods have several purposes: not just to aid in correlation, but to provide additional information, such as provenance studies, which can help in reconstructions of paleogeography, regional stratigraphic trends, and tectonic history. Some of these techniques provide information on numerical ages, and are discussed in Chaps. 7 and 8. Others are useful for local or regional correlation or provenance studies but do not necessarily provide such age information. A list of some of the latter follows:

Characterization by clastic petrofacies, including
 Heavy mineral stratigraphy
 Geochemical fingerprinting of sandstones and mudstones (chemostratigraphy)
 Magnetostratigraphic susceptibility
 Detrital zircon provenance studies

6.6.1 Clastic Petrofacies

The grain-size, grain shape, and composition of the clastic detritus present in a stratigraphic unit depends initially on the nature of the source, or **provenance**, of the detritus, but the detritus may undergo many modification processes during its derivation, transport, deposition, and burial, so that the characteristics of the original source become obscured. By careful study, the effects of some of these modification processes can be identified, providing much valuable information to a basin analysis.

Detrital composition depends on these main factors:

1. geological composition of the source area;
2. climate and relief of the source area and the area through which the detritus is transported;
3. detrital dispersal and mixing patterns brought about by the transport processes;
4. chemical and mechanical abrasion, winnowing, and breakdown that occur during transport and at the depositional site; and
5. diagenetic changes during burial.

Despite the many changes that the detritus undergoes during transport and deposition, the nature of the original source area can usually be identified. Certain compositional ranges are characteristic of particular types of tectonic source environment. This is the subject of **petrofacies analysis** and is not discussed here (see Miall 1999, Sect. 9.4). Without

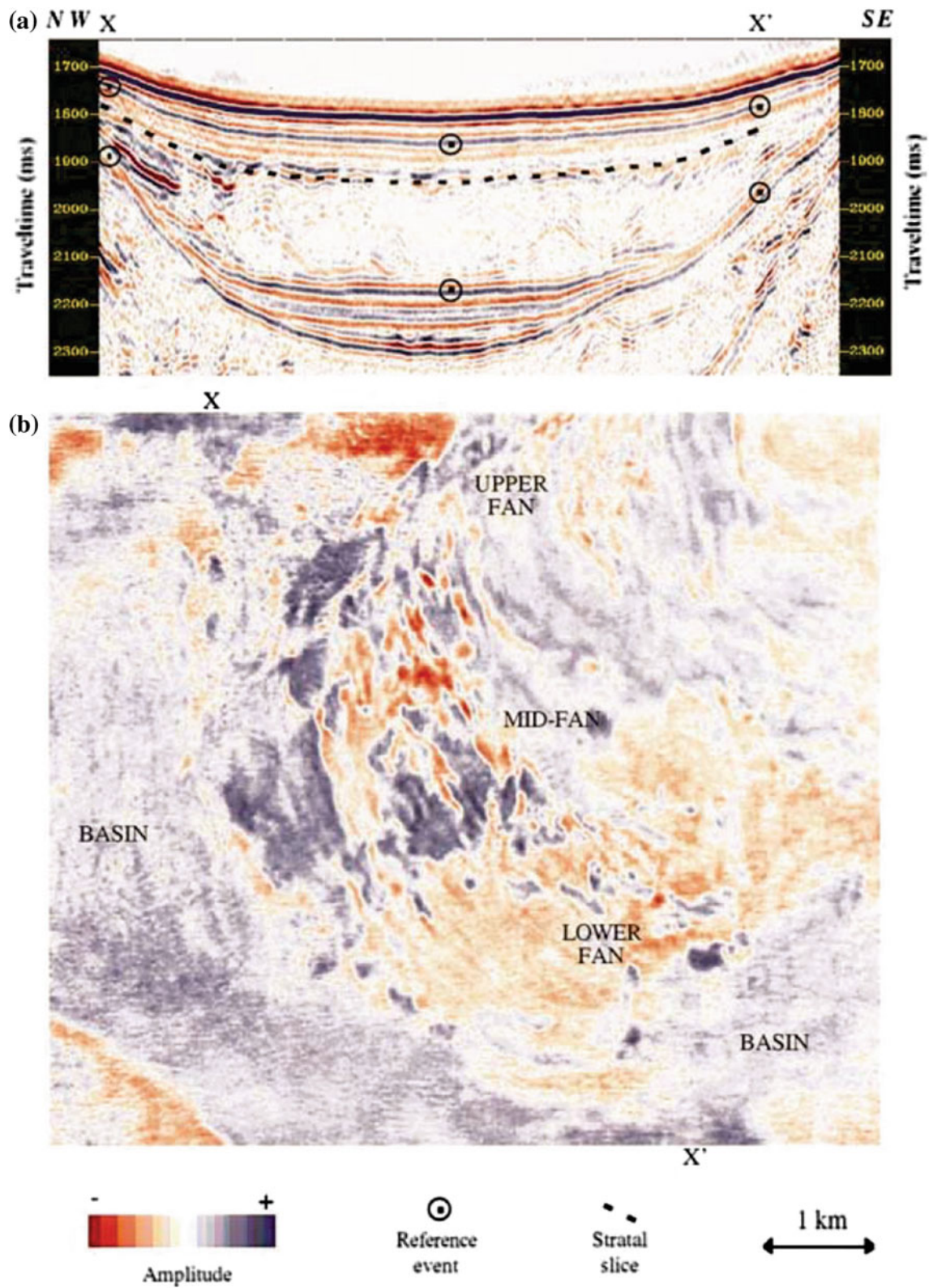


Fig. 6.37 A submarine fan shown on a stratal slice taken from the Pleistocene, deep water offshore Louisiana. **a** A vertical profile with a dominant frequency of 40 Hz; **b** A stratal slice from the 1400 to 1800 m (1750–1950 ms) interval, along the dashed line in (a) (Zeng et al. 1998, Fig. 6, p. 521)

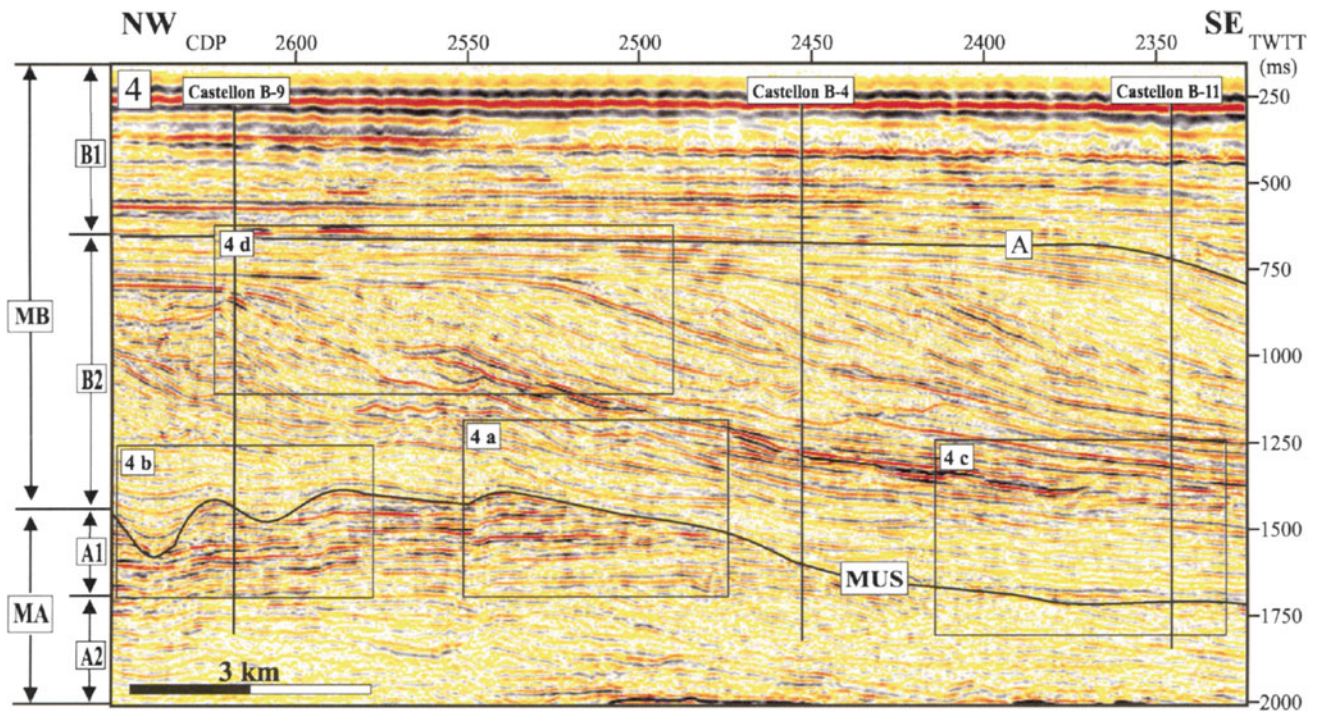
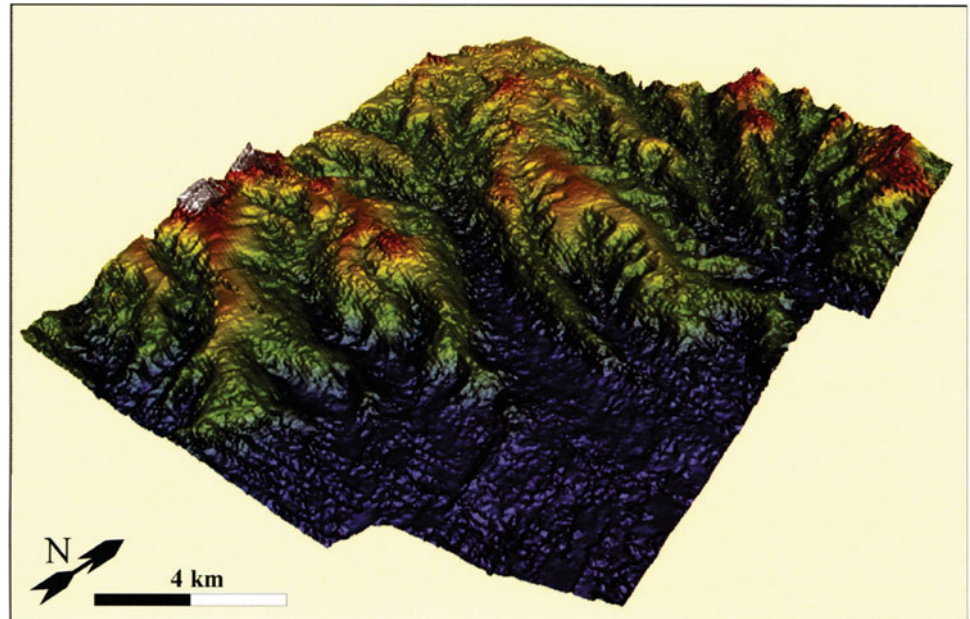


Fig. 6.38 Dip-oriented seismic cross-section across the Mediterranean continental margin off Northeastern Spain, showing the deeply incised Messinian unconformity (MUS). Megasquence A (MA) consists of a shallow-upward deep-marine to deltaic succession of Miocene age.

Megasquence B (MB) comprises a Prograding slope wedge of Pliocene age. The labelled rectangles refer to enlarged portions of this section that are not shown here (Martinez et al. 2004, Fig. 4, p. 93)

Fig. 6.39 A perspective view of the Messinian unconformity on the Mediterranean continental margin of northeastern Spain. The 2D section shown in the previous figure crosses this area from *centre-left* to *lower right* (Martinez et al. 2004, Fig. 8, p. 96)



going into the details of plate-tectonic setting, information regarding the geology of the local source area may be of considerable value in a basin analysis, because of the information it provides regarding transport directions, drainage areas, location of sources of economically valuable

minerals (such as those occurring in placer deposits), uplift and **unroofing history** of the source area, and so on. This is the main subject for discussion in this section.

Initially, of course, petrographic composition of primary detritus is similar to that of the rocks exposed in the

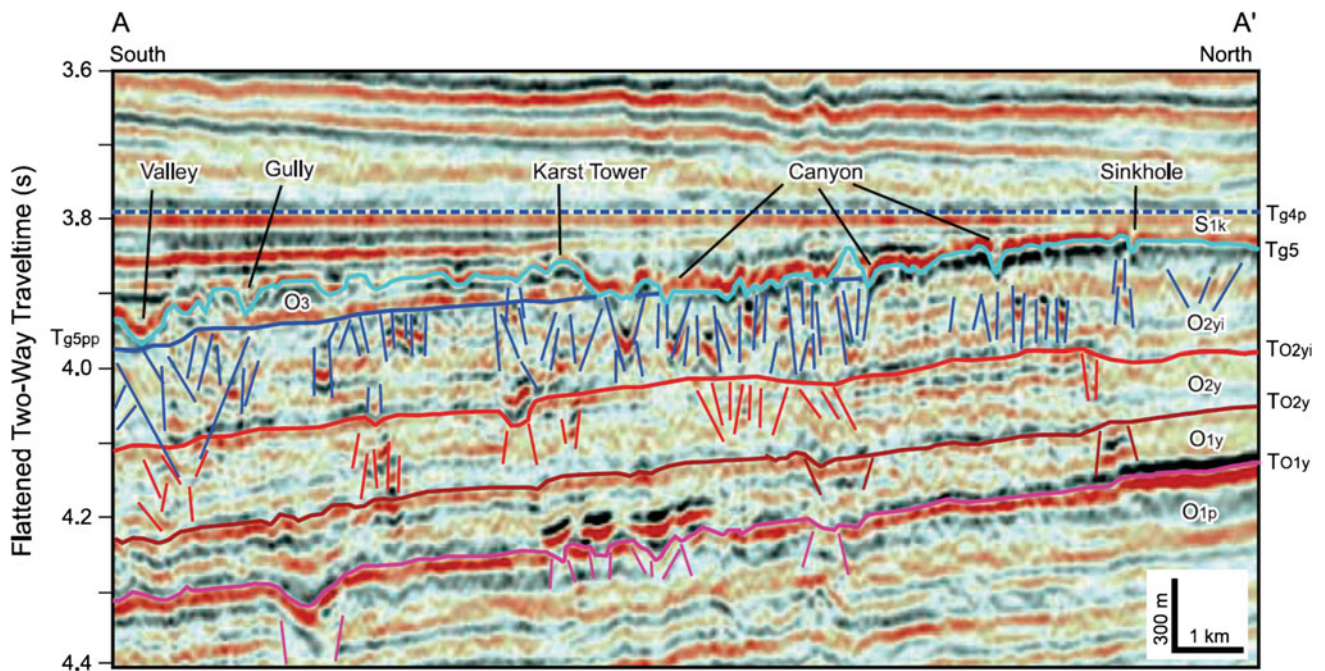


Fig. 6.40 Vertical seismic section through an Ordovician-Silurian carbonate succession in the Tarim Basin, western China, flattened on the Lower Silurian (Tg4p reflection) in order to show the original topography at the top of the Ordovician unconformity (Tg5). At this and older paleokarst surfaces, collapsed caves and sinkhole are shown

by the short coloured vertical lines, which mark disrupted or discontinuous reflections (Zeng et al. 2011, Fig. 10, p. 2074). AAPG © 2011, reprinted by permission of the AAPG whose permission is required for further use

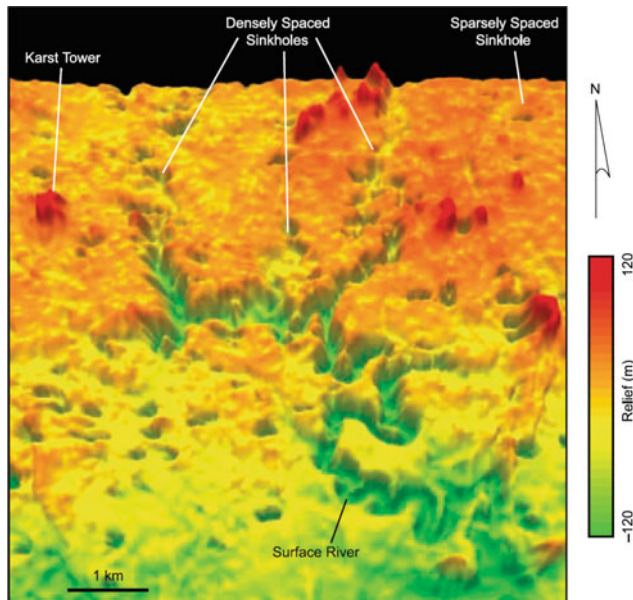


Fig. 6.41 A perspective view of the Ordovician unconformity extracted from 3-D seismic data, showing the morphology of the eroded, paleokarst surface (Zeng et al. 2011, Fig. 14, p. 2077). AAPG © 2011, reprinted by permission of the AAPG whose permission is required for further use

sediment source area, but changes begin to occur even as the rocks weather and become part of the subsoil. After only a short transport distance, the petrography of the detritus may not necessarily bear a simple relationship to that of the source area because of the destruction of unstable grains in transit, particularly in humid environments where chemical weathering may be rapid (e.g., Franzinelli and Potter 1983; Basu 1985). Nevertheless, studies of petrographic variation within the basin itself may provide much useful information. Downcutting by rivers reveals progressively older rocks, so that the derived sediments may display an **inverted stratigraphy**, older sediments containing detritus from the young cover rocks and the upper strata containing material derived from the local basement (Graham et al. 1986). Documentation of this unroofing sequence may help clarify the timing of orogeny, volcanism, plutonism, rates of uplift, etc. (Cerveny et al. 1988). Areal variations in petrographic composition depend on transport directions which, in turn, reflect tectonic control of the paleoslope. As clastic sediments are dispersed by currents or sediment-gravity flows, they are subjected to size sorting, abrasion, breakage, and rounding. They may retain a distinctive detrital composition, although easily weathered minerals, such as ferromagnesian grains, will gradually be destroyed. As a result of these

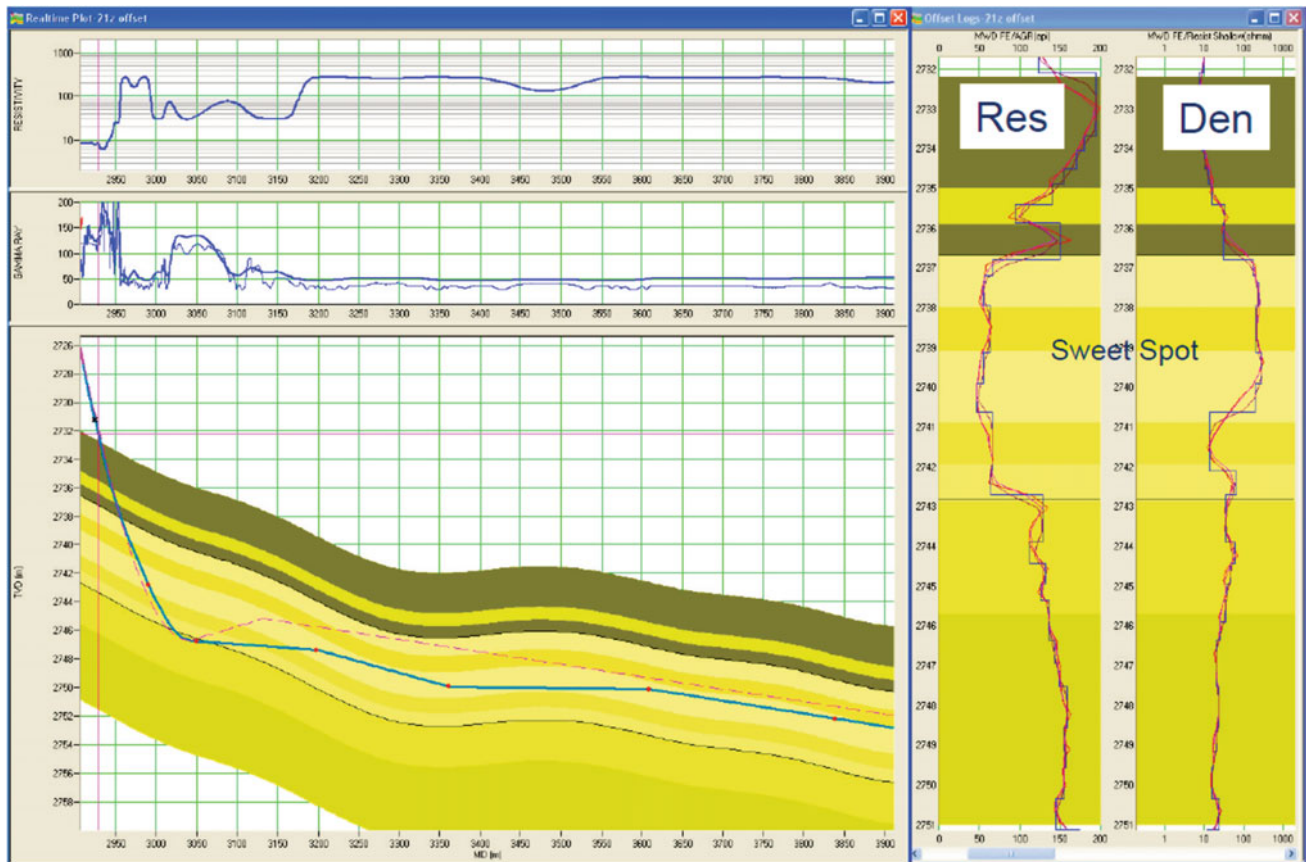


Fig. 6.42 At *right* density and resistivity logs through a target interval; at *lower left*, a two-dimensional cross-section of the modeled structure and the planned path of the directed well bore; at *top left* the expected

log response along the well (Taylor 2010). AAPG © 2010, reprinted by permission of the AAPG whose permission is required for further use

processes, a particular lithosome may become fingerprinted with a distinctive size range and composition, and down-current changes in the various petrographic parameters may be used as paleocurrent indicators. Interpretation of the source area for marine rocks may be a more complex procedure. For example, submarine fans may contain deltaic detritus plus shelf carbonate or siliciclastic material swept down to the continental rise via submarine canyons.

Petrographic data are simplest to use where the sediments have been deposited by unidirectional currents, as in fluvial, deltaic, and submarine-fan environments. Size and sorting parameters do not convey much, if any, directional information when the sediments have been formed by multidirectional currents, as in most shallow-marine and shelf environments. Few petrographic studies of this type have been carried out in submarine fans, in part because most such deposits contain abundant paleocurrent indicators such as sole markings (Sect. 2.2.2.7), and in part because most exposed fans are in complex structural belts where areal trends are difficult to reconstruct. Most of the remaining discussion in this section relates to fluvial and fluviodeltaic

deposits, for which petrographic studies may have uses in surface or subsurface exploration for petroleum, coal, uranium, or other economic deposits.

Grain-size changes caused by abrasion and breakage during downstream transport are rapid in gravel detritus, but the rate of change with distance of transport drops off asymptotically, becoming slow in coarse sand and negligible in fine sand to silt. Much experimental work has been carried out in an attempt to quantify the rate of change, so that grain-size in the field could be interpreted directly in terms of distance of transport. However, each detrital lithology responds differently to current transport, and rivers vary markedly in competency at any one point, so that research of this type is unlikely to meet with any success. Nevertheless, mapping of relative grain-size changes in conglomeratic and coarse sandy sediments has considerable use as a paleocurrent indicator.

What measurements should be made? For grain-size studies in conglomeratic rocks, the simplest and most useful mapping parameter is maximum clast size, which is usually given as the average of the intermediate clast diameter of the

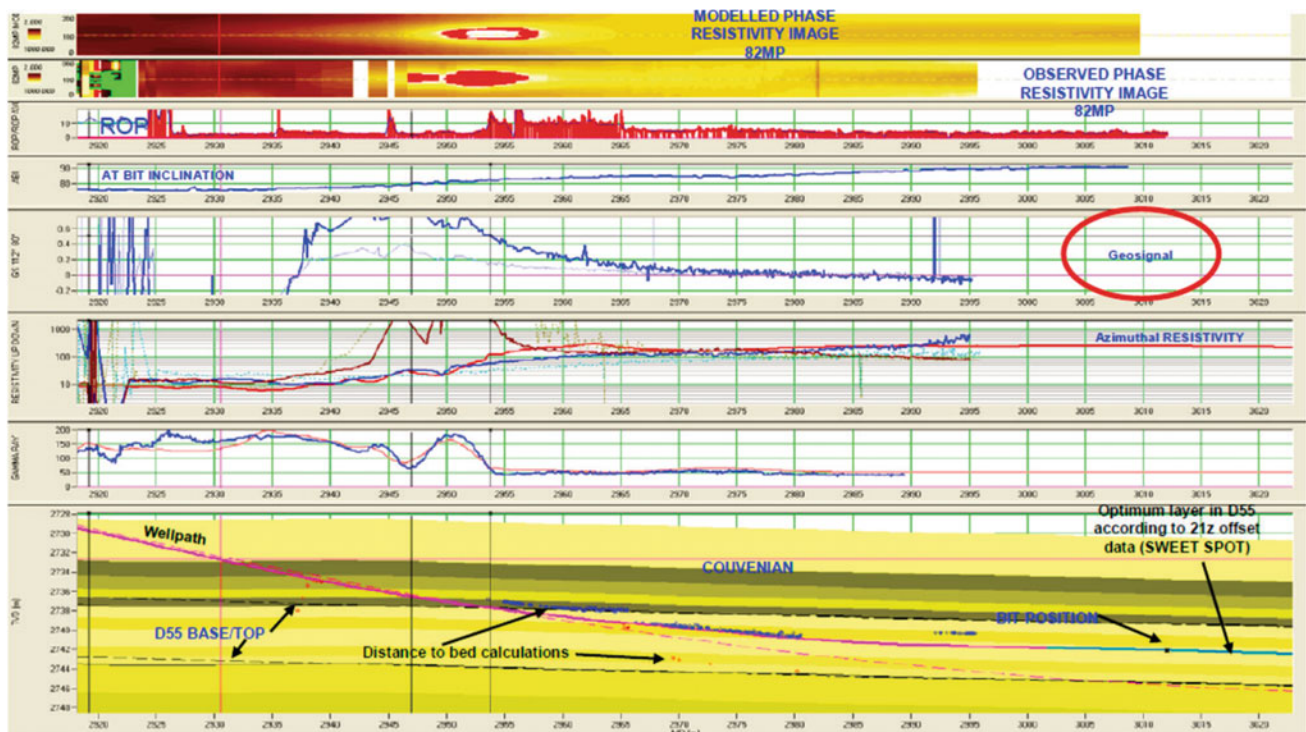


Fig. 6.43 Data being obtained in real time as the directional well planned in Fig. 6.42 was being drilled (Taylor 2010). AAPG © 2010, reprinted by permission of the AAPG whose permission is required for further use

10 largest clasts present at a sample point. For sand-sized grains mean or maximum grain-size may be used. Both can be measured in an outcrop or in a thin section by visual estimation against a grain-size chart (Fig. 2.5). This permits measurements to the nearest 0.5 ϕ , which is quite accurate enough for our purposes (sieve analyses and other laboratory studies are time consuming, and usually add little).

Detrital composition of conglomerates can be studied by counting and identifying 100 or more clasts at each sample point. Sandstone composition should be studied in thin-section using a moveable microscope stage and a point counter. It is recommended that at least 300 grains be identified and counted per sample point. The stage should be set to advance at each count by an amount equal to or slightly greater than the mean grain diameter. The number of points counted can be adjusted according to the compositional variability of the sample. Pure quartz arenites do not need such intensive study, but immature, lithic arenites with many varieties of rock fragments may need more detailed examination. Care should be taken to recognize and distinguish **extrabasinal** and **intra-basinal** detritus, particularly in the case of carbonate and volcanic fragments. Zuffa (1985b, 1987) discussed criteria for distinguishing these classes of particles. Mineral types have different densities and so they vary in their hydrodynamic behavior. They also have different fragmentation patterns. The detrital composition of a clastic rock may therefore vary markedly with grain-size (Fig. 6.47)

and so, for mapping purposes, it is advisable to control measurements according to a standard grain-size range, for example 1 ϕ class. These methods will usually result in a measurement repeatability of two or three percentage points or better, and this, again, is accurate enough for our purposes. Analytical methods are discussed in detail by Dickinson (1970), Pettijohn et al. (1973), and Zuffa (1985a, b, 1987). It is important to standardize laboratory procedures in order to facilitate comparisons between data sets. Zuffa (1985b, 1987) and Ingersoll et al. (1984) recommended use of the so-called **Gazzi-Dickinson point-counting method**, which counts coarse grains (>0.0625 mm) in terms of their component mineral grains rather than as rock fragments. The method also requires that the observer attempt to reconstruct the original composition of altered grains. This leads to a better clustering of data points and increased accuracy in provenance determinations. However, there is not universal agreement that the Gazzi-Dickinson method is suitable for all purposes. For example, Suttner and others (1985), in two separate discussions of the paper by Ingersoll et al. (1984), pointed out that the method of classifying coarse grains results in a loss of certain types of data, such as information regarding lithic grains. Careful study of these discussions and the replies by Ingersoll and his colleagues is recommended for anyone contemplating detailed petrographic work. Howard (1993) discussed the statistics of clast counting, sources of error, and field procedures.

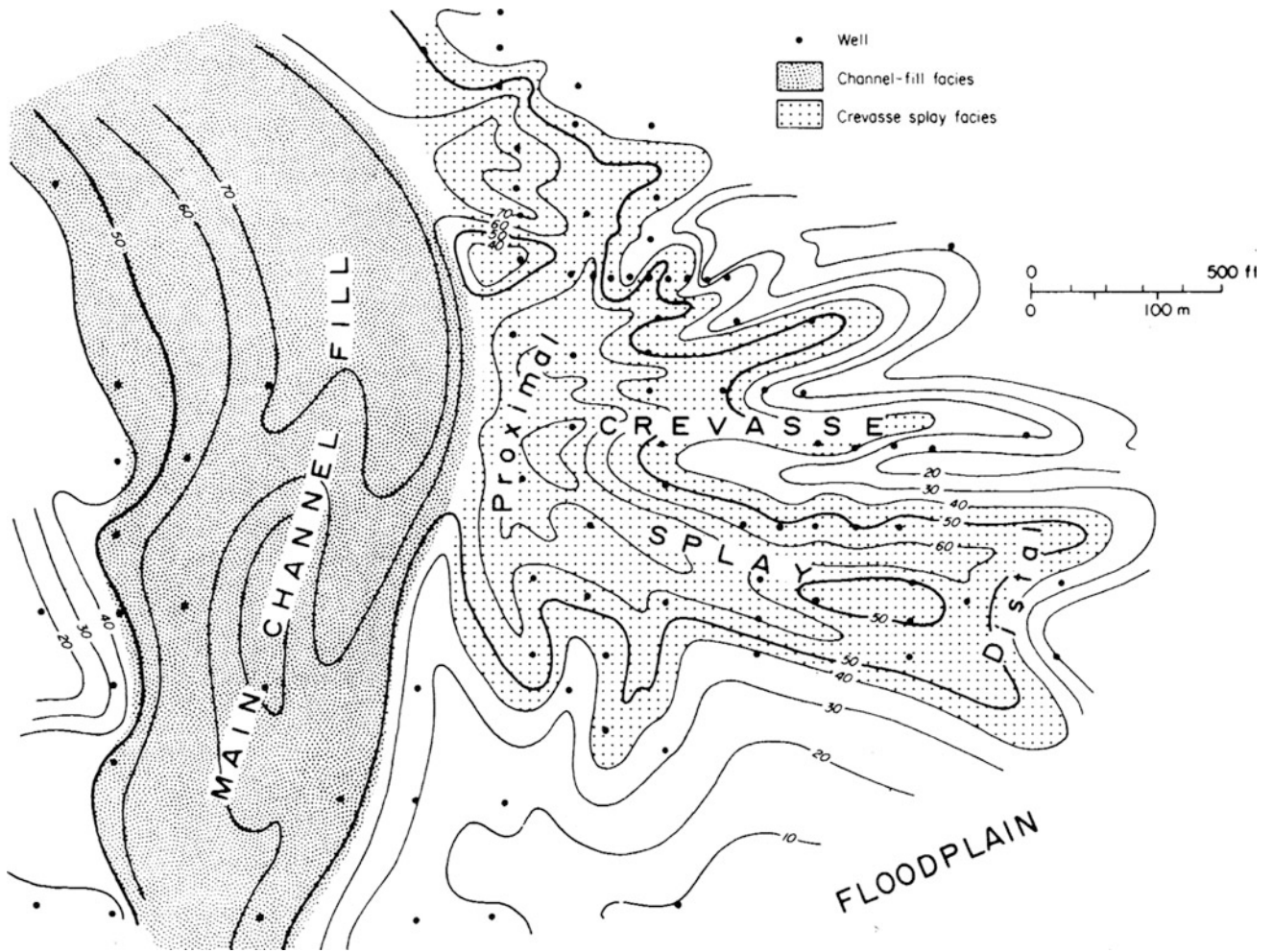
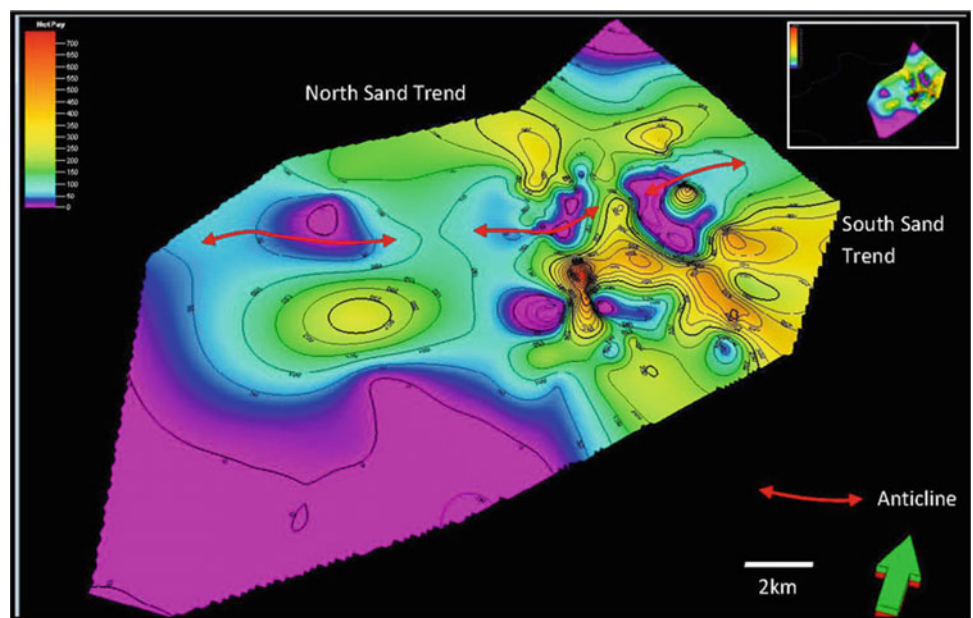


Fig. 6.44 Definition of a crevasse splay and a channel sand body by close-spaced drilling in Cenozoic fluvial deposits of the Gulf Coast (Galloway 1981)

Fig. 6.45 Net sand map, derived from well data in an oil field, southwest Trinidad (Moonan 2011). AAPG © 2011, reprinted by permission of the AAPG whose permission is required for further use



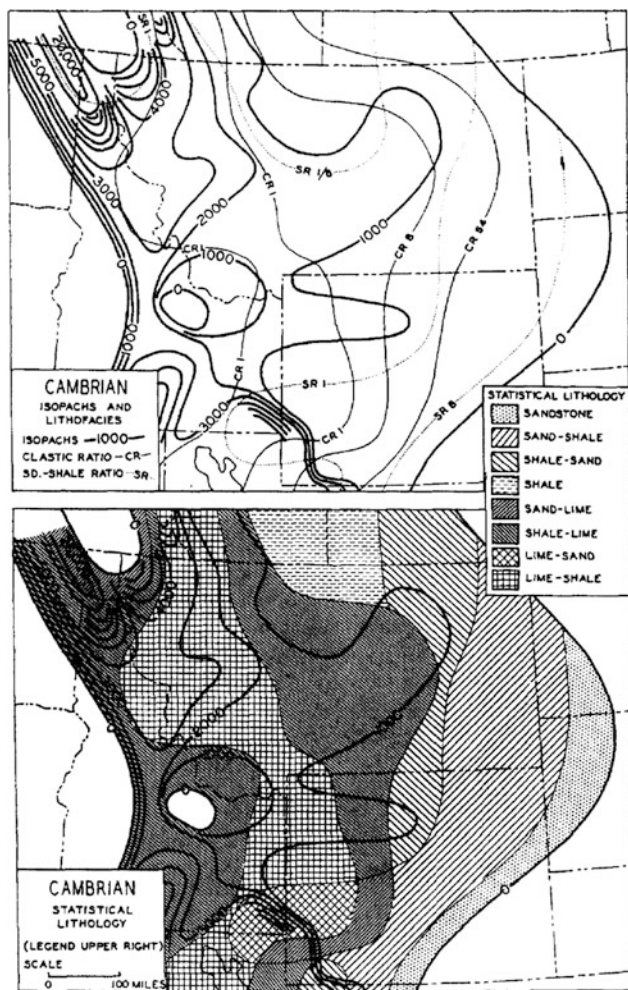


Fig. 6.46 A classic ratio map for Cambrian strata in the western United States (Krumbein 1948, Fig. 3, p. 1914). AAPG © 1948, reprinted by permission of the AAPG whose permission is required for further use

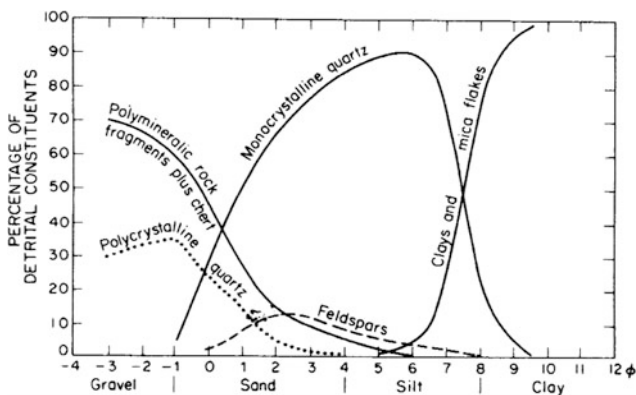


Fig. 6.47 Relationship between grain size and composition of the detrital fraction in siliciclastic sediments. (From Blatt, H., Middleton, G.V., and Murray, R.C., *Origin of sedimentary rocks*, 2nd ed., 1980, p. 321. Reprinted by permission of Prentice-Hall Inc., Englewood Cliffs, New Jersey.)

Much use has been made of heavy minerals (density greater than about 2.8) in provenance studies, even though most sands typically contain less than 1 % by weight. They are extracted from loose or disaggregated sand by separation in dense liquids, such as bromoform, and examined in grain mounts. Distribution is affected by hydraulic sorting during transport and by intrastratal solution following deposition (Morton 1985a). Considerable skill is needed to identify grain types correctly, and the technique is, in general, more difficult to use than thin-section analysis of the light fraction. We do not discuss this research theme further (see Morton and Hallworth 1994, 1999).

Grain-size and compositional measurements may be averaged over a vertical section at each mapping location or restricted to individual correlatable stratigraphic units. Plotting of both areal and vertical changes may provide useful paleogeographic information, and it is up to the basin analyst to exploit the data in the most effective way. Petrographic data may be analyzed manually, graphically, or statistically to define petrographic assemblages or provinces, typifying a particular source area geology (Suttner 1974). Alternatively, particular mineral species may be treated separately.

Some workers have concentrated on identifying and mapping varieties of quartz, feldspar, zircon, or other grain types, requiring a great deal of highly specialized research, but possibly providing provenance information unobtainable in any other way (Allen 1972; Heim 1974; Schnitzer 1977; Helmold 1985). Folk's (1968) work on quartz, chert, chalcedony and their varieties, is particularly noteworthy. Sophisticated analytical techniques are increasingly being used to define mineral varieties based on trace-element composition (Matter and Ramseyer 1985; Morton 1985a, b). For example, Morton (1985b) employed an electron microprobe to discriminate three populations of detrital garnets in a stratigraphic unit and related them to probable sources. Heller and Frost (1988) explored a huge new area: the study of stable and radiogenic isotope distributions in detrital grains and their use in fingerprinting source terranes.

Resistant grains, such as quartz and chert, plus the heavy minerals zircon, tourmaline, rutile, and garnet, are commonly recycled through several episodes of erosional derivation, sedimentation, lithification, uplift, and re-erosion. Usually, they show abundant evidence of this in the form of a high degree of rounding and the presence of authigenic overgrowths. It is usually difficult or impossible to determine the source of such grains because, in most cases, they could have come from several different stratigraphic units in the source area. Variations in color, crystal habit, or inclusions may help, but require more detailed research (Zuffa 1985b, 1987). Zircon studies have recently assumed a new importance as provenance indicators, as discussed in Sect. 6.6.2.

Extensive treatments of sandstone petrology and its application in sedimentological studies were given by

Pettijohn et al. (1973) and Blatt et al. (1980). Zuffa (1985a) edited a useful compilation of research and review papers, several of which are quoted above. In the remainder of this section, some examples of field studies are discussed to illustrate the kind of contribution petrography can make to regional basin analysis.

Two examples of the analysis of clastic detritus are provided here in order to illustrate the main uses of the method. Miall (1979) analyzed the petrography of the Isachsen Formation, a Lower Cretaceous braided river deposit in Banks Basin, Arctic Canada. The bulk of the formation consists of texturally and mineralogically mature medium to coarse sandstone, showing abundant evidence of a recycled origin. Samples were obtained from outcrops divided into two broad groups, from the north and south parts of the island. Paleocurrent evidence indicates northward flowing trunk rivers with tributaries entering from the east (the west side of the basin is covered by younger strata but may also have been a source area). Initial attempts to recognize petrographic provinces in the sandstone were unsuccessful. Ternary plots show that the samples from the north and south end of the basin contain essentially the same mineral composition. Cluster analysis revealed a weak trend for feldspar to be more common in the north, and sedimentary rock fragments are slightly more abundant in the south. This was then emphasized by re-plotting the thin-section data in terms of three minor components, which shows that chert is also slightly more abundant in the north. It was found that a few rare components, such as detrital quartz-feldspar intergrowths, quartz with mica, tourmaline, or zircon inclusions, and zoned quartz, are all present almost exclusively in the north end of the basin. Analyses of these data in terms of potential sediment sources resulted in the map shown in Fig. 6.48. The bulk of the quartz sand and the sedimentary rock fragments were derived from mature Proterozoic sediments, chert was fed into the north end of the basin from various Lower Paleozoic sources, and the feldspar plus rare quartz and feldspar components appear to have been derived from a small Archean granodiorite pluton. A Middle to Upper Devonian sandstone unit that outcrops over wide areas adjacent to the north end of the basin appears to have contributed little detritus. It is too fine grained and has the wrong texture and mineralogy.

Rahmani and Lerbekmo (1975) carried out a detailed heavy-mineral analysis of the Cretaceous-Paleocene molasse sandstones derived from the Canadian Rocky Mountains. Factor analysis was used to determine mineral associations, and these resulted in the definition of a series of petrographic provinces (Fig. 6.49). It was found, unexpectedly, that these provinces were distributed in belts subparallel to structural strike. It was concluded that the dominant fluvial systems flowed longitudinally down the depositional basin from source areas to the west and northwest, not transversely, as would initially have been expected. The mineral provinces

could be distinguished because of variations in source-area geology.

In southern Alberta the Lower Cretaceous stratigraphy is characterized by a suite of thin marine-nonmarine sequences featuring multiple cycles of incision, which have created a very complex stratigraphy in which it may be quite difficult to correctly correlate individual units. Petrographic and chemostratigraphic techniques have been employed to supplement conventional petrophysical log correlation work. We report here on a petrographic study by Zaitlin et al. (2002). Figure 6.50 was compiled from thin section studies of core samples. Zaitlin et al. (2002, p. 38) described this compilation as follows:

Summary lithostratigraphic comparison of the Basal Quartz as proposed in this study. A ternary diagram with quartz, chert, and clay-rich grains at the apices is effective in partitioning the petrographic data into distinctive populations. A second set of ternary diagrams, with intergranular, intragranular, and microporosity pore types at the apices is used to illustrate porosity fabric and reservoir quality. Key diagnostic grains and alteration features are used to exhibit the two cycles of mineralogical, textural, and reservoir quality cyclicity.

The stratigraphy is defined as two cycles, as shown in Fig. 6.50, but in practice the cycles consist of a complex of sheet sandstones with mutually erosive incised valleys. The petrographic work helps to differentiate these stratigraphic fragments. An example of the resulting reconstructions is shown in Fig. 6.51.

6.6.2 Provenance Studies Using Detrital Zircons

The heavy mineral zircon has been found to be a particularly valuable subject for provenance studies. It is highly resistant and survives multiple recycling events, which means that it can be used to identify the ultimate source of the detritus in which it is found. Zircon grains are now readily dated with the Uranium/Lead method, and the advent of sensitive high-resolution ion microprobe (SHRIMP) and laser-ablation-inductively coupled plasma-mass spectrometry (LA-ICP-MS), means that large populations of detrital zircon grains can be analyzed quickly (Thomas 2011). With care, it is possible to use zircon assemblages to map sediment sources as an aid to paleogeographic reconstruction. It is, of course, necessary to take into account the issue of recycling, which can be done by examining all aspects of a sandstone's detrital petrography. For example, in the case of the Banks Island study discussed briefly above (Fig. 6.48) it is highly relevant that the sand grains of the unit under discussion (the Isachsen Formation) are much coarser and more mature than those of the Devonian Melville Island Group, which is the immediately underlying unit around much of the basin margin, indicating that this unit could not

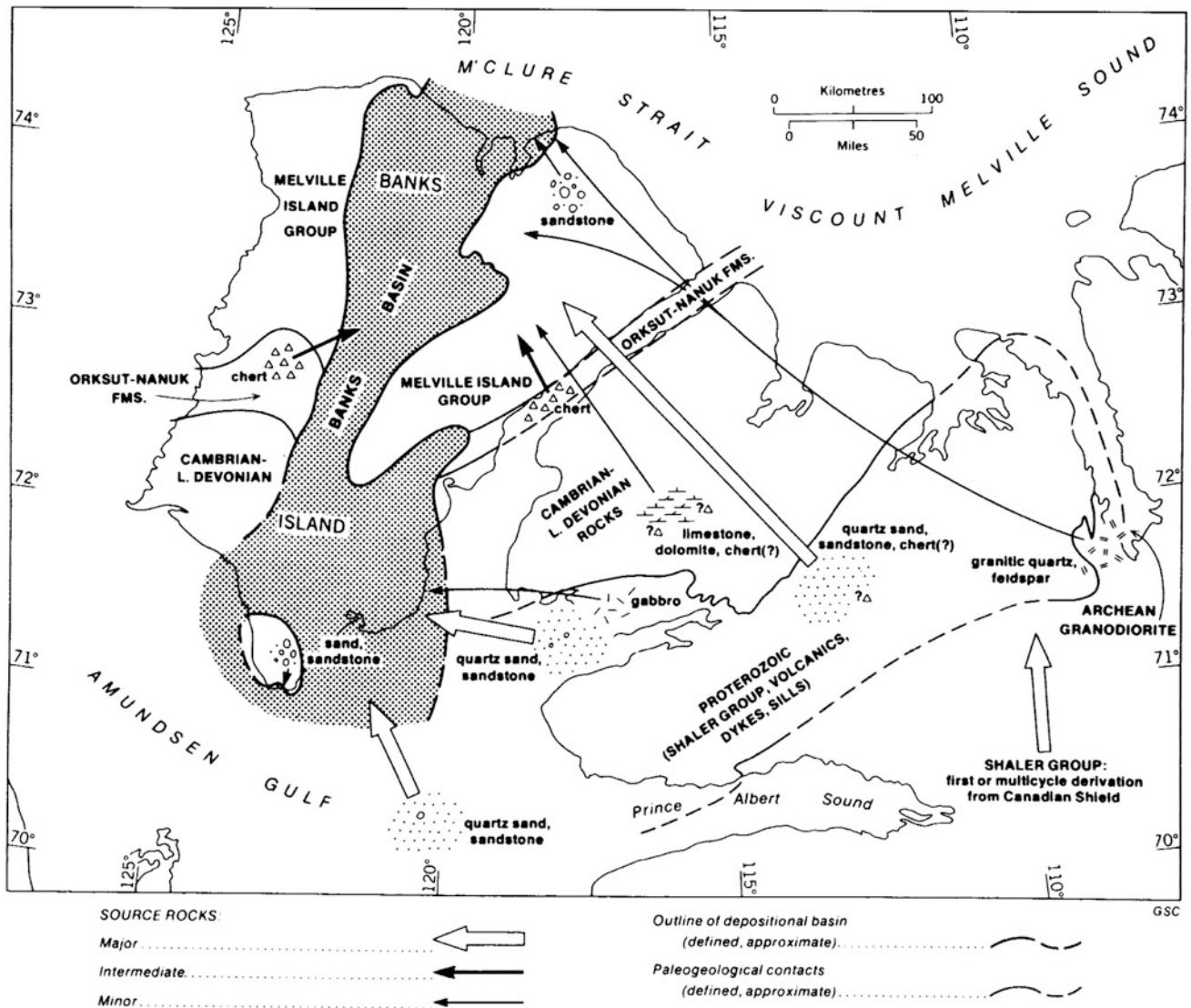


Fig. 6.48 The depositional basin (*shaded area*) of the Lower Cretaceous Isachsen Formation of the Banks Island area, Arctic Canada showing interpreted source rocks of the Isachsen sandstones (Miall 1979)

have provide the bulk of the sand in the Isachsen Formation. Given these types of caveats, zircon studies in North America have generated some surprising results, as discussed below.

Zircon studies on the North American continent began with a detailed study of the distribution and ages of zircons in potential sources terranes in the Cordilleran province along the western margin of the continent (Gehrels et al. 1995). Given the long-continued history of terrane accumulation that has built the continent, this information provides a quantitative basis for assigning zircons to ultimate sources based on their ages. In most sandstones, analysis demonstrates that there are several zircon populations exhibiting distinct age ranges, and it is usually a simple matter to relate these age populations to the age distributions of the ultimate sources. For example, Fig. 6.52 illustrates the

distribution of zircon ages in five samples from the Oil Sands of northern Alberta. This shows the importance of the Grenville as a sediment source, a feature of most zircon distributions from North American sources, and which indicates dramatic changes in sediment sources and the paleogeography of the major river systems through the Phanerozoic. Dickinson and Gehrels (2003) were amongst the first to realize the importance of distant sediment sources, such as the Grenville and Appalachian orogens, in the sourcing of much of the sand now constituting the Late Paleozoic and Mesozoic clastic successions of the Colorado Plateau area of the southwestern United States.

Raines et al. (2013) investigated the zircon geochronology of Upper Jurassic and lowermost Cretaceous strata in the Alberta foreland basin. Conventional petrographic and paleocurrent studies had long been interpreted in terms of

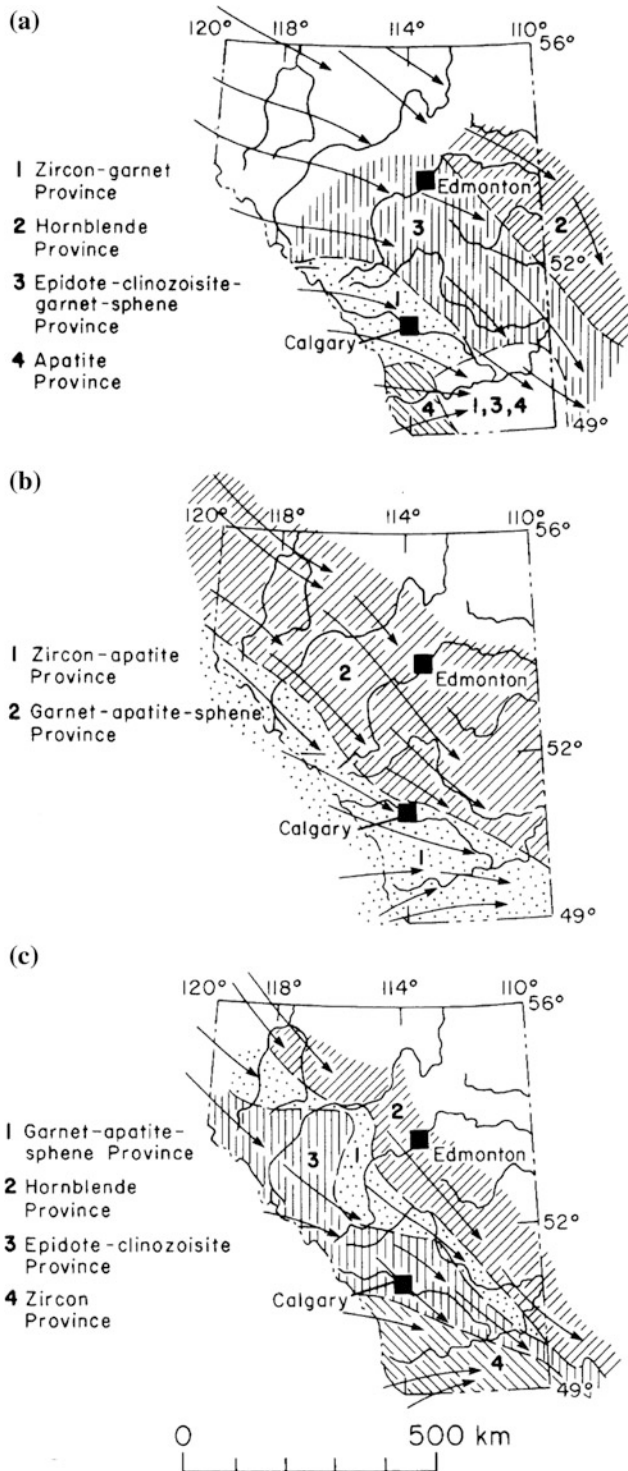


Fig. 6.49 Heavy mineral provinces, as determined by factor analysis, in three formations within the upper molasse wedge of Alberta. Arrows show interpreted dispersal directions. **a** Belly River Formation (Upper Cretaceous); **b** Edmonton Formation (Cretaceous-Tertiary); **c** Paskapoo Formation (Tertiary) (Rahmani and Lerbekmo 1975)

sources to the south and west, but considerable additional detail was obtained by these new methods. The zircon data indicate sediment in the early foreland basin was delivered via two principal sedimentary systems: a south-to-north axial river system, and transverse fluvial systems that emanated from the adjacent Cordillera (Fig. 6.53). Of particular interest are derived zircons from contemporary (Jurassic) strata preserved in the Michigan basin, which confirm the importance of an Appalachian source for some of the detritus. Speculating from this single data point, it is suggested that a network of tributaries fed sediment into the axial system flowing through the Alberta Basin from a wide area to the southeast (Fig. 6.53).

Combining these studies and others, of sands in the southern United States, Blum and Pecha (2014) generated two speculative maps that showed the likely complete re-organization of the interior drainage of the North American continent that evolved with the elevation of the Cordilleran orogen in the mid-Mesozoic (Fig. 6.54). Prior to this time, large-scale drainage systems appeared to have delivered abundant detritus from the Appalachian orogen to the west of the continent (Dickinson and Gehrels 2003). Large-scale river systems developed oriented in the reverse direction once significant sediment sources arose in the paths of these rivers, with significant transport eastward. Drainage into Hudson Bay, as outlined in the Paleocene map, was earlier suggested by McMillan (1973) and Duk-Rodkin and Hughes (1994).

6.6.3 Chemostratigraphy

The development of high-precision analytical methods in the last few decades has facilitated the development of a range of new techniques for supplementing lithostratigraphic correlations in regional studies, and several detailed studies have been reported.

Pearce et al. (1999) provided a general discussion of chemostratigraphic methods, based on the few published sources available at that time, and also drawing on unpublished, proprietary studies carried out in petroleum industry laboratories. They made a number of useful general points. For example, studies of sandstones need to take into account grain size effects. Absolute elemental concentrations decrease in coarser-grain size fractions owing to dilution by quartz. Also, it is difficult to develop homogenous samples in coarser sandstone fractions, and so finer sands are preferred. Diagenesis may modify compositions, with Ca, Na, K, Pb, Rb, Sr and certain REEs liable to reduce in concentration during the dissolution of feldspars. Therefore chemostratigraphic work makes preferential use of the more

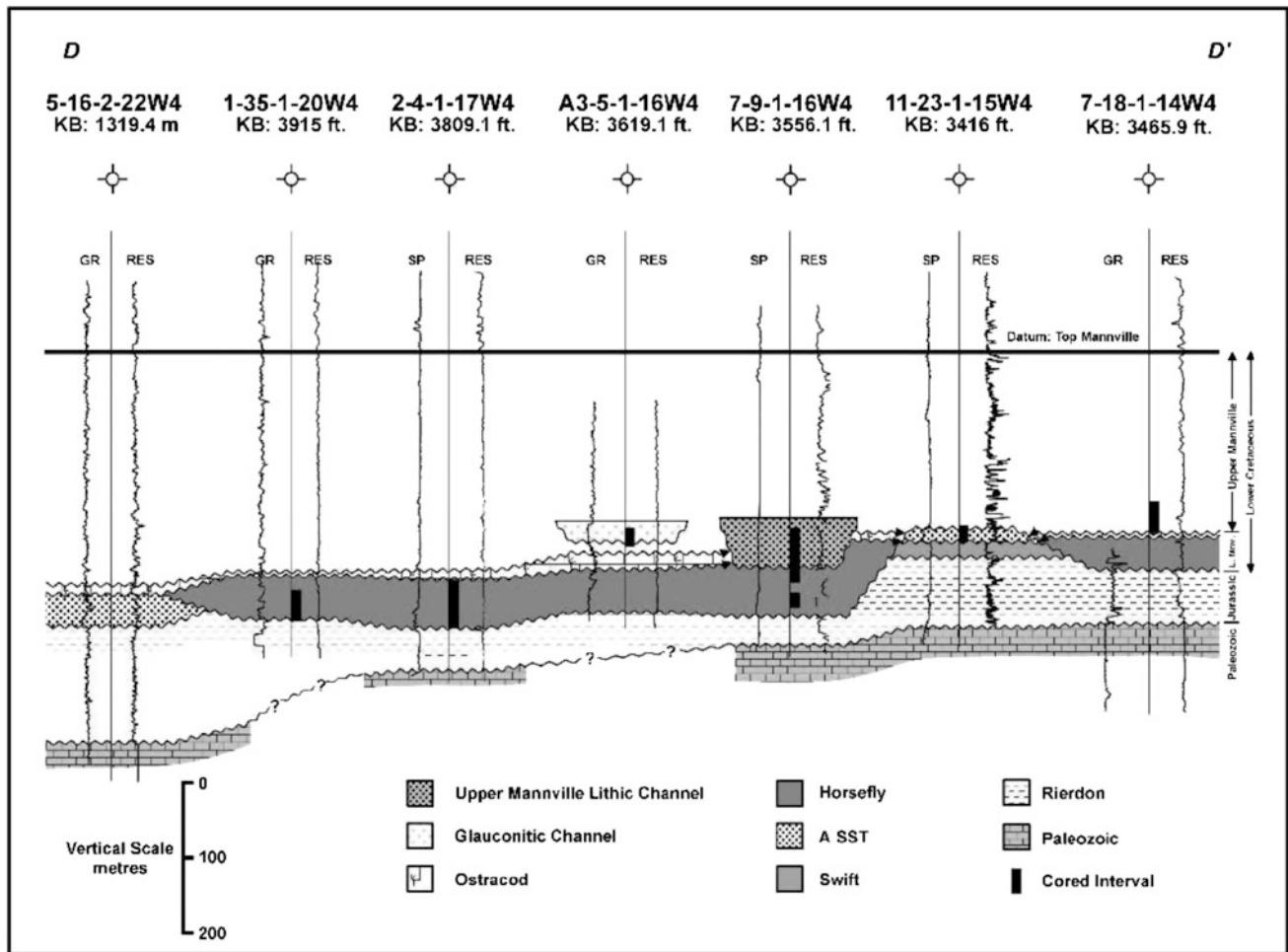


Fig. 6.51 An example of the complex Lower Cretaceous stratigraphy of southern Alberta. Individual lithosomes have been identified using the petrographic data shown in Fig. 6.50 (Zaitlin et al. 2002, Fig. 16, p. 50)

Experimental use of “forensic chemostratigraphy” has been used to map the path of a horizontal well. Hildred et al. (2014) used chemostratigraphic analysis of cuttings from vertical drill holes, to characterize four units, including a producing dolomite in the Bakken petroleum system of southwestern Alberta, and the formations that bracket it. They then took a series of cutting that had been generated along a horizontal well through this system, and were able to show how the hole had passed up and down through this stratigraphy, which contains several faulted offsets.

6.7 Paleocurrent Analysis

6.7.1 Introduction

The art of paleocurrent analysis was invented by the quintessential nineteenth century English amateur, Henry Clifton Sorby, who published his first paper on the subject in

1852. He understood the formation of “ripple drifted” and “drift bedded” structures (climbing ripples and large-scale crossbedding, respectively) and, in seven years, claimed to have made about 20,000 observations, a total that has probably never been equaled. Most of Sorby’s work remained unpublished. He was far ahead of his time, as paleocurrent work did not become a routine analytical procedure until the 1950s. His work remained unappreciated and largely unknown until exhumed by Pettijohn (1962) and reinterpreted by Allen (1963b) (see also Miall 1996, Chap. 2).

The technique could not become a routine component of basin analysis until proper attention was paid to the description and classification of sedimentary structures (McKee and Weir 1953; Pettijohn 1962; Allen 1963a, b), and a start was made on the investigation of bedform hydraulics. The major breakthrough here was the development of the flow-regime concept by Simons and Richardson (1961) and Simons et al. (1965). These two topics are discussed at some length in Sects. 1.2.5 and 3.5.4.

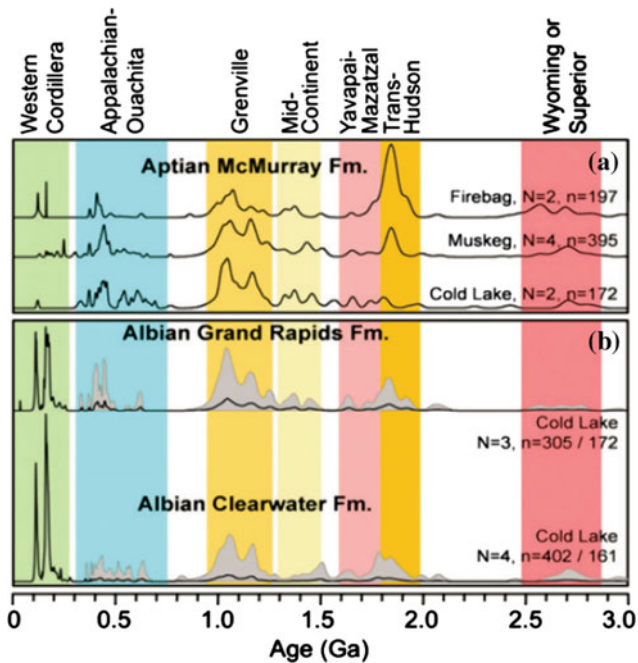


Fig. 6.52 Distribution of zircon ages in five sandstone samples from the Oil Sands of northern Alberta. Zircons of Grenville age (1.0–1.3 Ga) are particularly common, suggesting sources from the Grenville Province, which forms the edge of the Canadian Shield along the entire eastern margin of the continent (Blum and Pecha 2014)

Paleocurrent analysis is primarily an outcrop study. Oriented core can be used, but is rarely available. Subsurface information may also be obtained with the use of borehole imaging tools. The dipmeter, which makes use of four resistivity logs run at 90° around a borehole, may be used to reconstruct the attitude of surfaces intersecting the hole, including bedding planes, and fractures. The orientation of crossbedding is, theoretically, obtainable from such data, and service companies have promoted this use for the tool since the 1970s (see also Miall 1999, Chap. 5), but thin-bed resolution may be a problem, and the tool has not often been used. Modern digital imaging tools, including Schlumberger's Formation MicroScanner (FMS) and other, more recently developed tools, provide a full scan of the hole, and may be more practical (Pöppelreiter et al. 2010). In petroleum exploration wells, unoriented core may be oriented using a dipmeter, but correlation between the two is commonly difficult (Davison and Haszeldine 1984; Nelson et al. 1987). Figure 6.59 illustrates a modern borehole image of planar-tabular crossbedding and the dips calculated from it, indicating consistent westerly to northwesterly flow directions. Borehole imaging has not been widely used, mainly because of cost considerations, but as Fox et al. (2015) argued, this may be a false economy. For coal, metals, and other types of mining, where there may be large surface or underground outcrops, paleocurrent analysis may, in contrast, be extremely useful (e.g., Minter 1978; Long 2006).

Paleocurrent analysis can provide information on five main aspects of basin development:

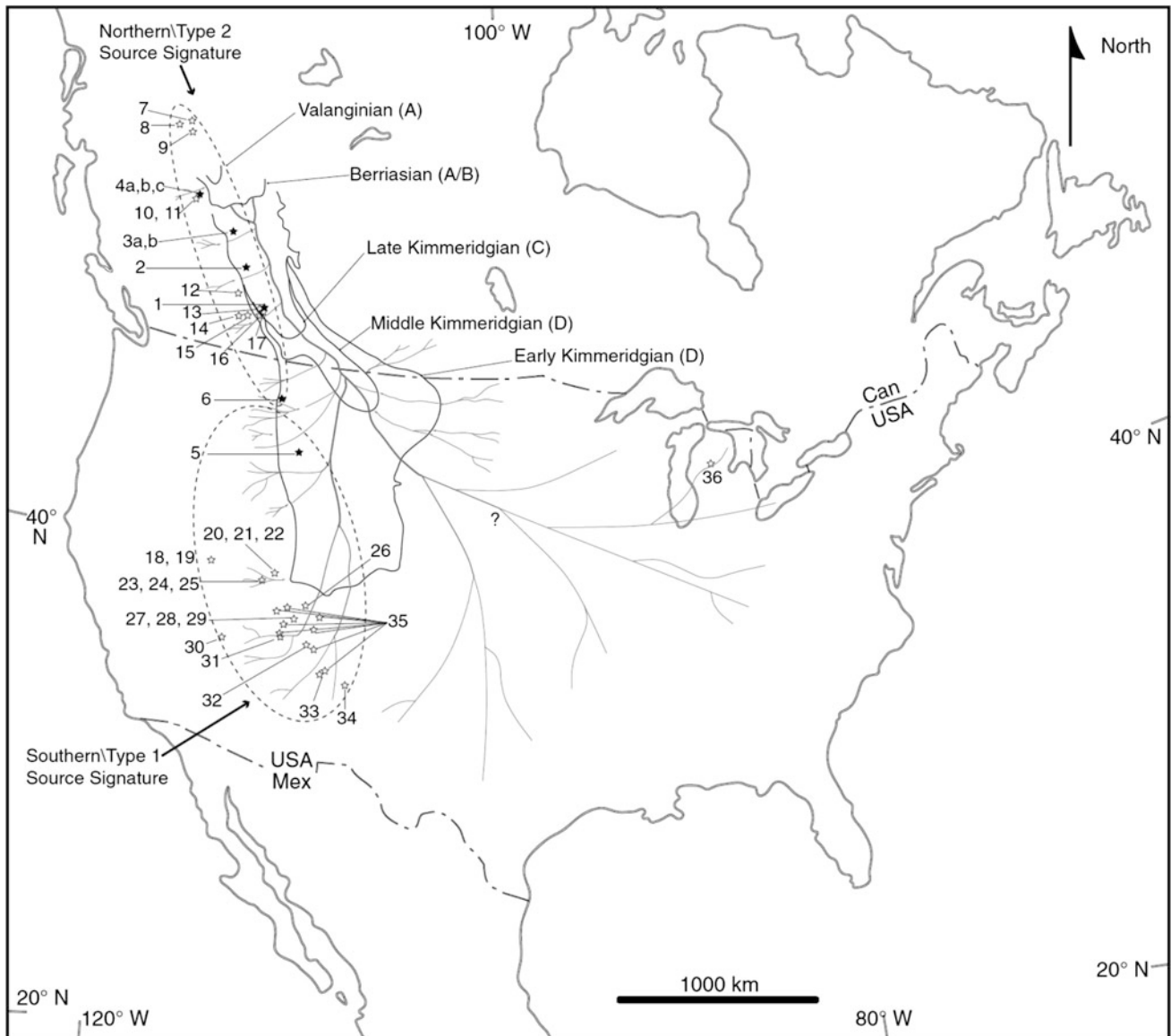
1. the direction of local or regional paleoslope, which reflects tectonic subsidence patterns,
2. the direction of sediment supply,
3. the geometry and trend of lithologic units,
4. the depositional environment,
5. the architecture of bars and bedforms at the outcrop scale.

Examples of these applications are discussed in the ensuing paragraphs.

6.7.2 Types of Paleocurrent Indicators

Sedimentary structures and fabrics used in facies and paleocurrent studies are described and illustrated in Sect. 2.2.6. The following notes explain briefly how they yield current directions.

1. For ripple marks and crossbedding (Figs. 2.8 and 2.9), the inclination of foreset directions is generally downcurrent, because of the grain avalanching mechanism. Needless to say, it is not always this simple. Smith (1972) demonstrated that planar-crossbed sets in rivers commonly advance obliquely to the flow direction. Trough crossbeds do not yield accurate flow directions unless the analyst can observe the orientation of the trough axis (see below). Hunter (1981) discussed the flow of air around large eolian dunes and suggested that these, too, commonly advance obliquely to the wind direction. The use of statistical procedures and appropriate facies data usually circumvents these problems (this is also discussed below).
2. Channels and scours (Fig. 2.13) occur in many environments and may indicate the orientation of major erosive currents, such as those generating river or tidal channels and delta or submarine fan distributaries. However, the larger channels, which are those most likely to be of regional significance, are usually too large to be preserved in outcrops. They may be readily apparent on seismic records, particularly 3-D, as discussed in this chapter (which obviates the need for paleocurrent studies!).
3. Parting lineation or primary current lineation, the product of plane-bed flow conditions (Fig. 2.9d), is only visible on bedding-plane exposures. It usually yields directional readings of low variance because it forms during high-energy flow in river, delta, or tidal channels, when bars or other obstructions to flow are under water and flow-sinuosity is low. The structure indicates orientation but not direction of flow, because of the ambiguity between two equally possible readings at 180° to each



Early Foredeep Deposits

- 1: Elbow Falls, AB (H*)
- 2: Cadomin townsite, AB (H*)
- 3: Grande Cache, AB (H*)
- 4: Williston Lake, BC (*)
- 5: Southern Montana (H)
- 6: Northern Montana (I)

Potential Northern Sandstone Sources

- 7: Devonian (E)
- 8: Cambrian (E)
- 9: Pennsylvanian/Permian (E)
- 10: Ordovician (E)
- 11: Triassic (F)
- 12: Ordovician (E)
- 13: Pennsylvanian/Permian (H)
- 14: Cambrian (E)
- 15: Neoproterozoic (E)
- 16: Triassic (F)
- 17: Pennsylvanian/Permian (E)

Potential Southern Sandstone Sources

- 18: Ordovician (K)
- 19: Ordovician (L)
- 20: Jurassic Eolianite, CP3 (M)
- 21: Permian (G)
- 22: Pennsylvanian (G)
- 23: Devonian (G)
- 24: Cambrian (G)
- 25: Neoproterozoic (G)
- 26: Jurassic Eolianite, CP16 (M)
- 27: Jurassic Eolianite, Wingate (M)
- 28: Jurassic Eolianite, Entrada (M)
- 29: Jurassic Eolianite, Navajo (M)
- 30: Jurassic Eolianite, CP20 (M)
- 31: Jurassic Eolianite, CP12 (M)
- 32: Jurassic Eolianite, CP20 (M)
- 33: Jurassic Eolianite, CP24 (M)
- 34: Jurassic Eolianite, CP54 (M)
- 35: Upper Jurassic Fluvial x8 (N)
- 36: Jurassic, Michigan - Fluvial (J)

Sources of Data

- * This study
- A: Stott, 1998
- B: Miles et al., 2012
- C: Hamblin and Walker, 1979
- D: Turner and Peterson, 2004
- E: Gehrels and Ross, 1998
- F: Ross et al., 1997
- G: Lawton et al., 2010
- H: Leier and Gehrels, 2011
- I: Fuentes et al., 2009
- J: Dickinson et al., 2010
- K: Smith and Gehrels, 1994
- L: Gehrels and Dickinson, 1995
- M: Dickinson and Gehrels, 2009
- N: Dickinson and Gehrels, 2010

Fig. 6.53 Proposed paleogeography showing the sediment sources and interpreted (schematic) rivers systems for the Western Interior Basin during the Late Jurassic and earliest Cretaceous (Raines et al. 2013, Fig. 11, p. 752)

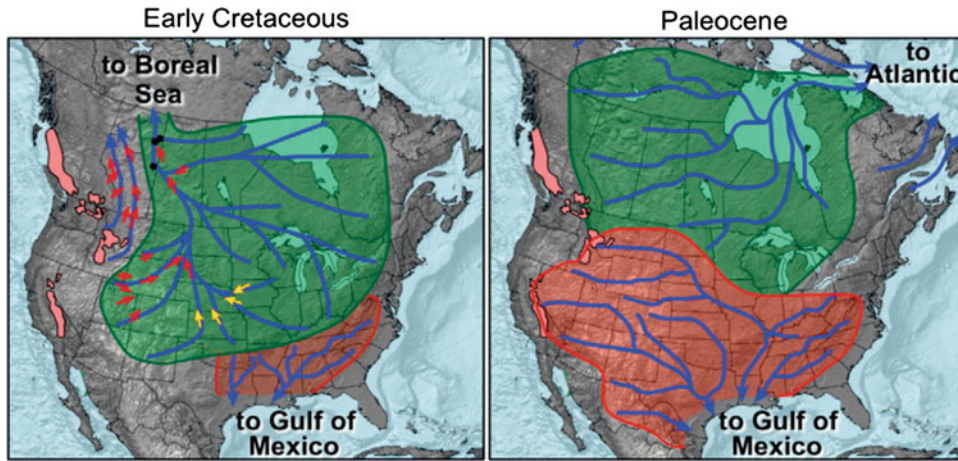
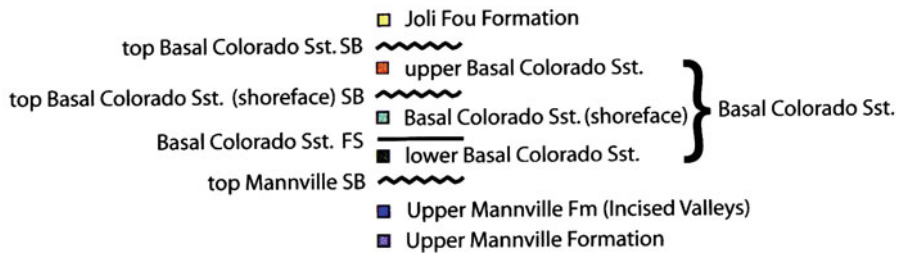
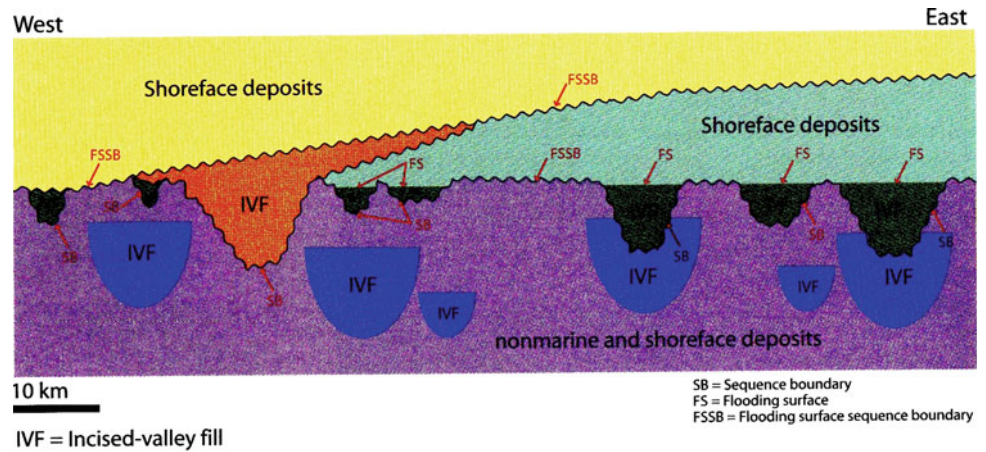


Fig. 6.54 Early Cretaceous to Paleocene continental-scale drainage reorganization. The major Early Cretaceous (Aptian ca. 125–113 Ma) drainage system was sourced in the Appalachian Mountains, and routed through the Assiniboia paleovalley to the Boreal Sea (*green*). Tributaries joined from the southwestern United States and eastern Canada. Only a small part of North America south of the Appalachian-Ouachita cordillera (*orange*) was routed to the Gulf of Mexico. A similar map for the early Albian (ca. 113–108 Ma) would include tributaries from arc-dominated terrains in the northwestern United States and southwestern Canada. *Red arrows* indicate

paleocurrents for basal Cretaceous fluvial deposits, whereas *yellow arrows* indicate orientations of bedrock paleovalleys that define the sub-Cretaceous unconformity. By the Paleocene, fluvial systems of the western United States were routed directly to the Gulf of Mexico, or to the Mississippi embayment, where they joined fluvial systems from the Appalachian Mountains: much of western Canada may have drained to the Atlantic. Locations of fluvial axes are schematic. *Pinkish areas* indicate locations of Cordilleran arc batholiths (after DeCelles 2004), (Blum and Pecha 2014, Fig. 4, p. 609)

Fig. 6.55 The stratigraphy of the Upper Mannville-Colored Group (Albian) of south-central Alberta, showing the complexity of the numerous incised valley systems that developed in this low-accommodation setting (Wright et al. 2010, Fig. 2, p. 96)



other. Usually, this can be resolved with reference to other structures nearby or to regional facies trends.

4. Clast transport by traction or in sediment-gravity flows commonly produces a measurable gravel fabric. Imbrication in traction current deposits occurs where platy

clasts are stacked up in a shingled pattern, with their flattest surface dipping upstream and resting on the next clast downstream (Fig. 2.12). Because gravel is only moved under high-energy flow conditions, it tends to show low directional variance, like parting lineation.

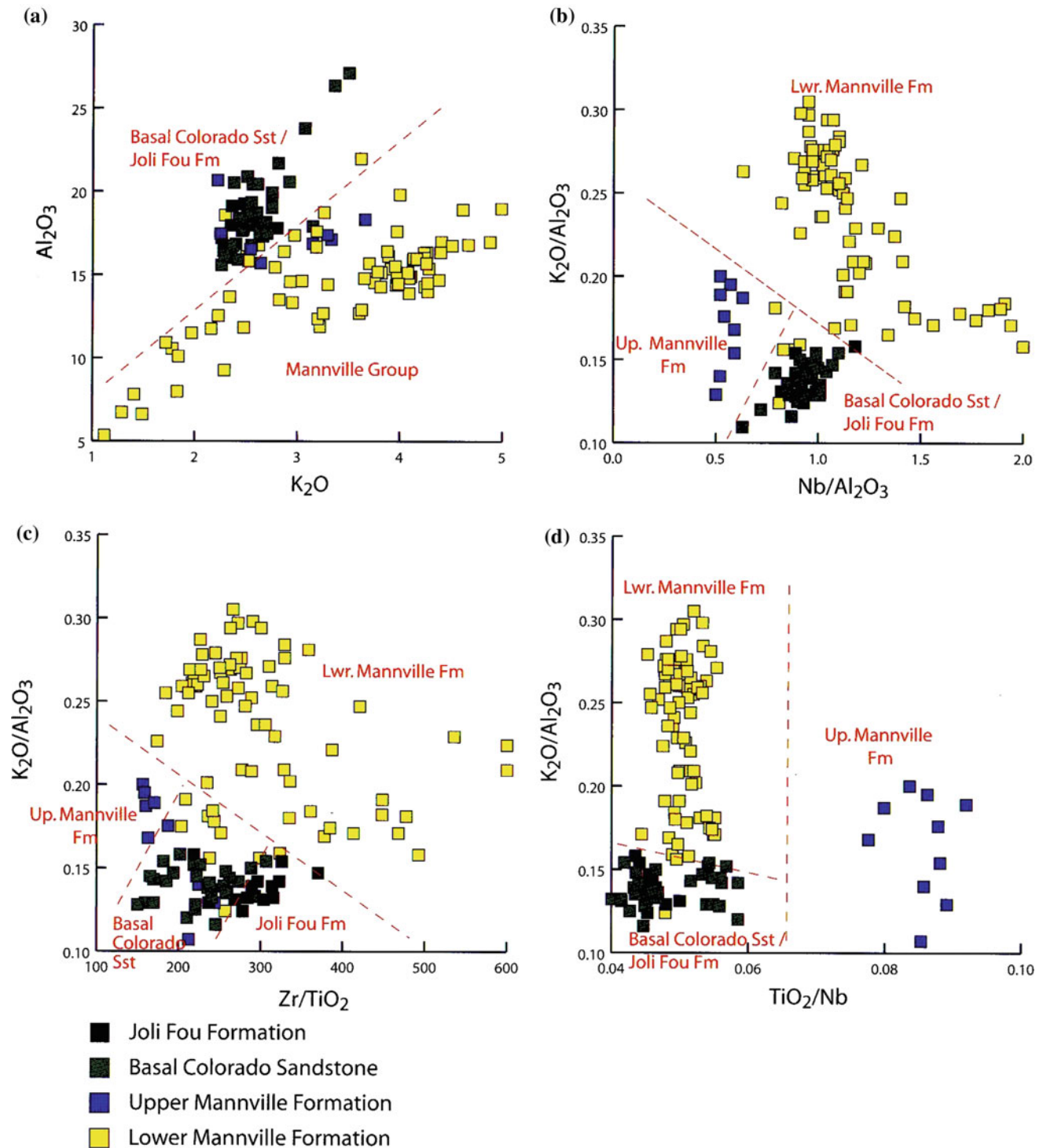


Fig. 6.56 Examples of the binary diagrams showing how whole-rock geochemistry may be used to characterize stratigraphic units in the Mannville-Colorado Group (Aptian-Albian) of south-central Alberta (Wright et al. 2010, Fig. 3, p. 97)

Rust (1975) found that in gravel rivers variance decreased with increasing clast size, suggesting reduced flow sinuosity with increased stream power. Interpretation of clast fabrics in subaqueous, poorly-sorted conglomerates (diamictites) can help distinguish depositional

mechanisms, such as debris flow, ice rain-out, and glacial lodgment, as well as provide paleocurrent information (Eyles et al. 1987).

- Sole markings (Fig. 2.15) are typically associated with the deposits of turbidity currents and fluidized or liquified

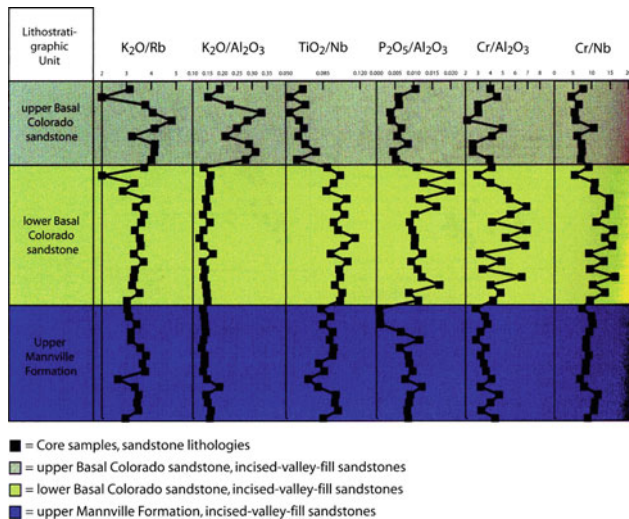


Fig. 6.57 “Synthetic chemical logs” developed from the sampling of cores through the Upper Mannville Formation and Colorado Group of south-central Alberta (Wright et al. 2010, Fig. 6, p. 100)

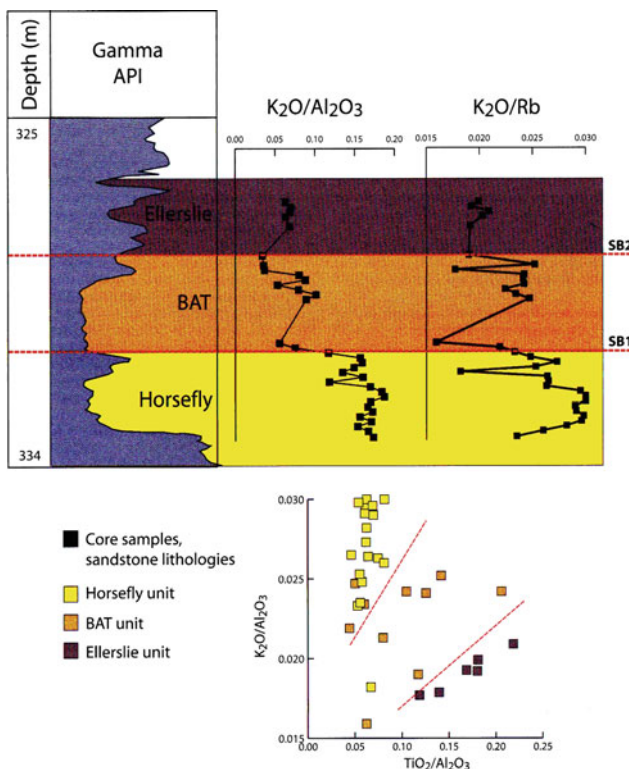


Fig. 6.58 Whole-rock geochemical data are used here to differentiate incised-valley-fill systems within a single well-bore through the Lower Mannville Formation, south-central Alberta (Wright et al. 2010, Fig. 9, p. 105)

flow, where vortex erosion may occur at the base of a flow, and “tools” can be swept down a bedding surface. They also occur less commonly in other clastic environments. Their greatest use, however, is in the

investigation of submarine-canyon and fan deposits. They are best seen on the undersides of bedding surfaces, where sandstone has formed a cast of the erosional feature in the underlying bed. Tool markings yield information on orientation but not direction, like parting lineation; flute marks are longitudinally asymmetric, with their deepest end lying upstream (Fig. 2.16).

- Oriented plants, bones, shells, etc., do not respond systematically to the aligning effects of currents unless they are elongated. There may be ambiguity as to whether they are oriented transverse or perpendicular to current patterns, and there are other difficulties, for example, the tendency of fossils such as high-spined gastropods to roll in an arc. Fossils are usually only useful for local, specialized paleocurrent studies.
- Slump structures generated on depositional slopes contain overfolds that may be aligned parallel to strike. They are therefore a potential paleoslope indicator, particularly on the relatively steep slopes of prodeltas and actively prograding continental margins. Friction at the margin of the slump may cause it to rotate out of strike alignment, so that a statistical approach to measurement is desirable. Potter and Pettijohn (1977, Chap. 6), Rupke (1978), and Woodcock (1979) reviewed their use as paleoslope indicators.

Several other paleocurrent indicators are reviewed by Potter and Pettijohn (1977), including some, such as sand-grain orientation and magnetic anisotropy, requiring detailed laboratory analysis of oriented samples. They are mainly of academic interest, where they may help solve a particular local problem, although laboratory techniques have improved in recent years to the point where studies of magnetic fabric could become routine (Hrouda and Stránik 1985; Eyles et al. 1987). The seven types of paleocurrent indicators listed above can be quickly and routinely measured in the field and have been widely used in basin studies.

6.7.3 Data Collection and Processing

Paleocurrent data should be carefully documented in the field. In the past, paleocurrent trends have sometimes been reported on the basis of a geologist’s mental estimates of the range of indicated directions, but even if this is correct, it may result in a significant loss of useful information. For every paleocurrent observation recorded in field notes, the following information should be included:

- location and (if relevant) precise position in a stratigraphic section;
- structure type;

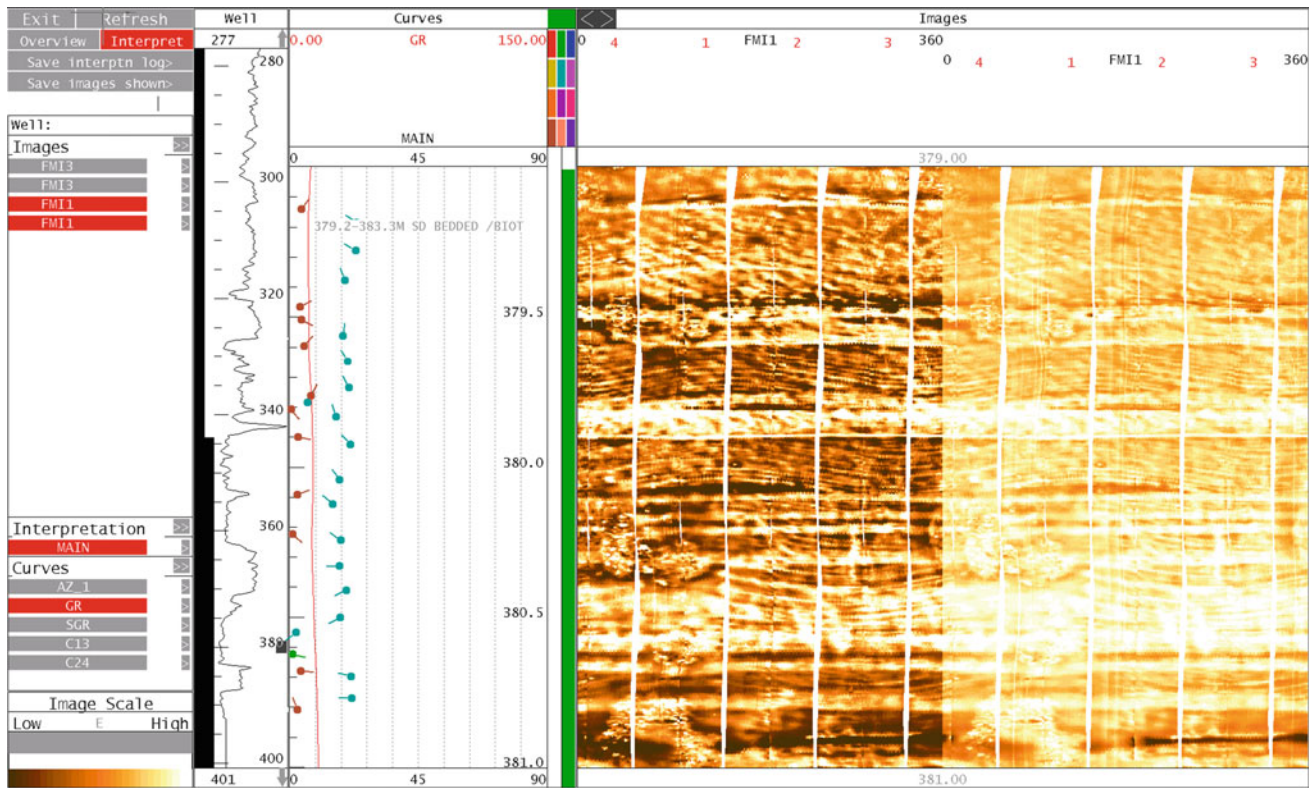


Fig. 6.59 A borehole image log, showing planar-tabular crossbedding and the dip readings obtained from image interpretation. The red tadpoles indicate stratification and the green tadpoles are from crossbed foresets. Two separate representations of the same scan are shown,

3. indicated current direction;
4. scale of structure (thickness of crossbed, depth and width of channel, mean or maximum clast size in imbricate gravels); and
5. local structural dip.

Current directions should be measured to the nearest 5° with a magnetic or sun-compass and corrected to true north wherever necessary. In the case of parting lineation and tool markings, the correct orientation of two possibilities at 180° can usually be identified by referring to other types of current structures nearby. Measurement accuracy greater than $\pm 5^\circ$ is difficult to achieve and is, in any case, rarely important. Difficulties in field measurement commonly arise because of incomplete exposure of crossbed sets. For example, two-dimensional exposures in flat outcrop faces cannot provide precise orientation information. DeCelles et al. (1983) and Bradley (1983) discussed the problem of incomplete or partial exposure of trough crossbed sets and ripple cross-lamination, and offered some solutions involving field measurement techniques and statistical treatment of the data.

Indicated current directions may need to be corrected for structural dip and fold plunge, otherwise significant

directional distortions may result. This should be carried out as soon as possible, preferably after every day's work, in order that possible errors can be detected while there is still time to rectify them in the field. For linear structures such as parting lineation or sole markings, structural dips as high as 30° can be safely ignored, as they result in errors of less than 4° . However, the foreset dip orientation of crossbedding is significantly affected by structural dip, and should be corrected wherever the structural dip exceeds 10° . This subject is discussed further by Potter and Pettijohn (1977, Chap. 10), who illustrated a correction technique using a stereonet. Ramsey (1961) provided graphical solutions. Parks (1970) presented computer routines for the necessary trigonometric calculations. Wells (1988) provided a practical guide to field procedures, and recommended the use of a pocket calculator to perform structural corrections and data synthesis in the field.

Sooner or later the question will arise as to how many readings should be made? There is no single or simple answer to this problem because it depends on how many measurable current indicators are available for observation and what the objectives of the study are. Olson and Potter (1954) discussed the use of grid-sampling procedures and random selection of structures to measure, followed by

calculation of reliability estimators to determine how many readings were necessary in order to be sure of determining correct directional trends. In this study, they were concerned only with determining regional paleoslope. We now understand a great deal about air and water flow patterns in different depositional environments, and a case could be made for measuring and recording every visible sedimentary structure. Such detailed data can be immensely useful in amplifying environmental interpretations and clarifying local problems, as discussed Sect. 6.7.5. Some selection may have to be made in areas of particularly good exposure. A practical compromise is to record every available structure along measured stratigraphic sections and to fill in the gaps between sections with spot (gridded or random) samples. This procedure permits the elaboration of both local and regional paleocurrent trends. When constructing lateral profiles of large outcrops, it is essential to document these with abundant paleocurrent determinations. Such data provide the third dimension to a two-dimensional outcrop and yield essential information regarding the shape and orientation of architectural elements (Sect. 3.5.11).

If the trend itself is important, 25 readings per sample station is commonly regarded as the minimum necessary for statistically significant small samples. However, the same or fewer readings plotted in map or section form can yield a great deal of environmental detail, whether or not their mean direction turns out to be statistically significant. Several hundred or a few thousand readings may be necessary for a thorough analysis of a complete basin.

A variety of statistical data-reduction and data-display techniques is available for paleocurrent work. The commonest approach is to group data into subsets according to stratigraphic or areal distribution criteria, display them visually in current-rose diagrams, and calculate their mean and standard deviation (or variance). The method of grouping the data into subsets has an important bearing on the interpretations to be made from them, as discussed in the next section. A current rose diagram is simply a histogram converted to a circular distribution. The compass is divided into 20, 30, 40 or 45° segments, and the rose is drawn with the segment radius proportional to number of readings or percent of total readings. A visually more correct procedure is to draw the radius proportional to the square root of the percent number of readings, so that the segment area is proportional to percent. Examples are given in Fig. 6.60. Wells (1988) warned that the choice of origin for rose diagrams and the method of subdivision of the segments can affect the visual appearance of the resulting diagram and the orientation of the modes. The calculation of means, which is done from raw data, is not affected, but Wells' warning indicates the need for caution in the visual interpretation of rose diagrams.

Potter and Pettijohn (1977) and Curray (1956) discussed arithmetic and vector methods for calculating mean, variance, vector strength, and statistical tests for randomness. Miall (1976) and Cant and Walker (1976) demonstrated the display and interpretation of data collected from vertical stratigraphic sections.

Statistical procedures, such as moving averages and trend analysis, are available for smoothing local detail and determining regional trends. An arbitrary grid may be drawn on the map; the mean current direction for the data in each group of four squares is then calculated and shown by an arrow at the center of this area. Each data point is thus used four times (except at the edges of the map). Examples of this method applied to paleocurrent data have been published by Potter and Pettijohn (1977).

The basin analyst should be wary of becoming too deeply enmeshed in the refinements of statistical methods. The use of probability tests is a useful curb on one's wilder flights of interpretive fancy, but there is a vast literature on the statistics of the circular distribution that seems to detract attention from very simple questions: Do the data make geological sense? Can they be correlated with trends derived from other methods, such as lithofacies mapping or petrographic data? Moving average and trend analyses are useful techniques for reducing masses of data to visually appealing maps, but they inevitably result in a loss of much interesting detail. The regional trends that emerge from such smoothing techniques are, in any case, usually readily deduced from modern stratigraphic data, such as grain-size trends, and the patterns of progradation and retrogradation within sequences. The more interesting approach is to relate individual readings to the architectural setting in which the structure resides, and to incorporate the data into an analysis of the bedform and lithosome hierarchy, as discussed in the next section.

6.7.4 The Bedform Hierarchy

A geologist collects paleocurrent measurements over individual bedding planes, through a local sequence in a quarry, along a lengthy dipping section in a river cut, or from several such sections throughout a map area. These readings differ from each other by varying amounts at different levels of this sampling hierarchy, but what do these differences mean? Statistically this is a classic example of a problem in analysis of variance (Olsen and Potter 1954; Kelling 1969). But what do the differences mean geologically? The larger the sampling area or the thicker the sampled section the greater will be the number of depositional events that contributed to the data set, and normally it will mean an increase in directional variance. This generalization can be systematized by the

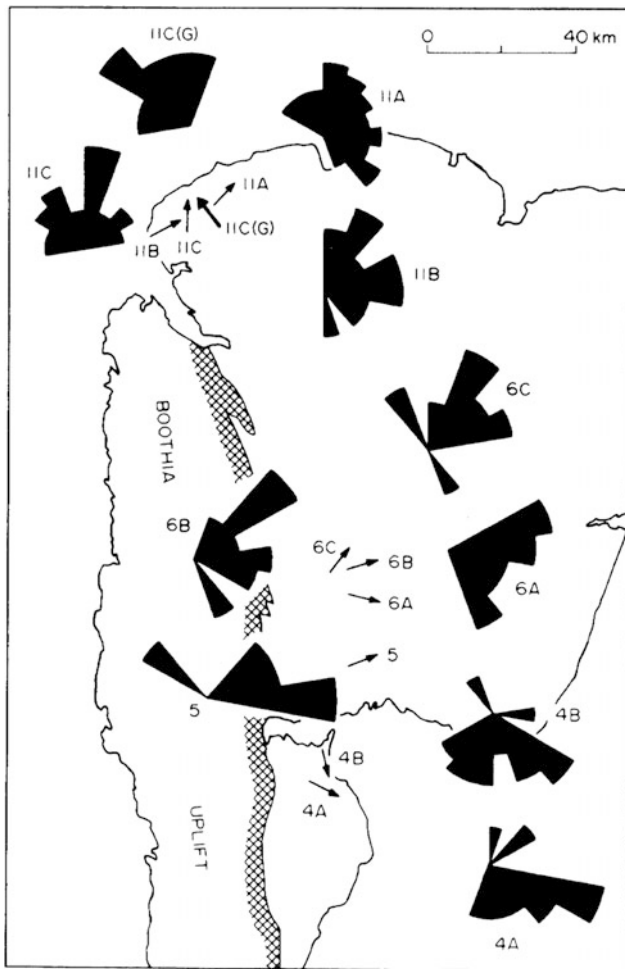


Fig. 6.60 Typical regional paleocurrent map, showing current rose diagrams and vector mean arrows for each of 10 outcrop areas, with station numbers. The map represents 165 field readings. Devonian fluvial sandstones, Somerset Island, Arctic Canada. Most readings are consistent with an interpretation of deposition taking place on ephemeral sandy alluvial fans radiating from multiple point sources along the front of the Boothia Uplift. Station 11C(G) represents giant crossbedding, interpreted as eolian dune stratification (Miall and Gibling 1978)

concept of the **bedform hierarchy**, as first noted by Allen (1966, 1967). Flow fields and the sedimentary structures arising from them are of up to six orders of magnitude, ranging from individual ripples to entire depositional systems. Allen (1966) and Miall (1974) applied this idea to river systems (Figs. 3.67 and 6.61). In Table 3.3 an attempt is made to expand it to other environments. Jackson (1975) showed that these ranks depend on three orders of time scale and physical scale, which we can now interpret as representing a range of Sedimentation Rate Scales (SRS) (See Sect. 8.4). Jackson (1975) proposed that they be grouped into three dynamic types:

1. **Microforms** are structures controlled by turbulent eddies in the fluid boundary layer. The time scale of variation is on the order of hours to seconds (deposits of SRS 1–3).
2. **Mesoforms** are structures that form in response to what Jackson (1975) termed **dynamic events**, such as hurricanes, seasonal floods, or eolian sand storms, when disproportionately large volumes of sediment are moved in geologically instantaneous time periods. The system may remain virtually unchanged between dynamic events (SRS 4–5).
3. **Macroforms** represent the long-term accumulation of sediment in response to major tectonic, geomorphic, and climatic controls, such as major bars and channels (SRS 6–7).

It is important for mapping purposes to attempt to relate the sampling scale to this hierarchy, so that the sources of directional variance can be interpreted intelligently. For example, a small quarry might be located entirely within the deposit of a single point bar or tidal delta, whereas a township (6 x 6 miles or 9.6 x 9.6 km) could encompass an entire delta lobe or barrier-inlet system. When interpreting microforms and mesoforms (the usual source of paleocurrent data) over large areas, it is important to remember that directional variance within each rank is summed to that of the higher ranks as far as is locally appropriate. Miall (1974) demonstrated the implications of this for fluvial-deltaic systems, such as those shown in Fig. 6.61, by compiling data for the various ranks summed to that of the single river or meander belt. A further discussion of the hierarchical nature of sedimentary facies is presented in Sect. 3.5.11.

6.7.5 Environment and Paleoslope Interpretations

A recommended first level of analysis is to plot current-rose diagrams and mean vectors for each outcrop or local outcrop group, if necessary separating the readings according to major facies variations. An example is illustrated in Fig. 6.60. If contemporaneous basin shape and orientation can be deduced from these data or from other mapping techniques, the paleocurrent data can be used interactively with lithofacies and biofacies criteria to interpret the depositional environment and to outline major depositional systems, such as deltas or submarine fan complexes. The geologist should examine the relationships between mean current directions in different lithofacies and in different outcrops. The number of modes in the rose diagrams (modality) and their orientation with respect to assumed

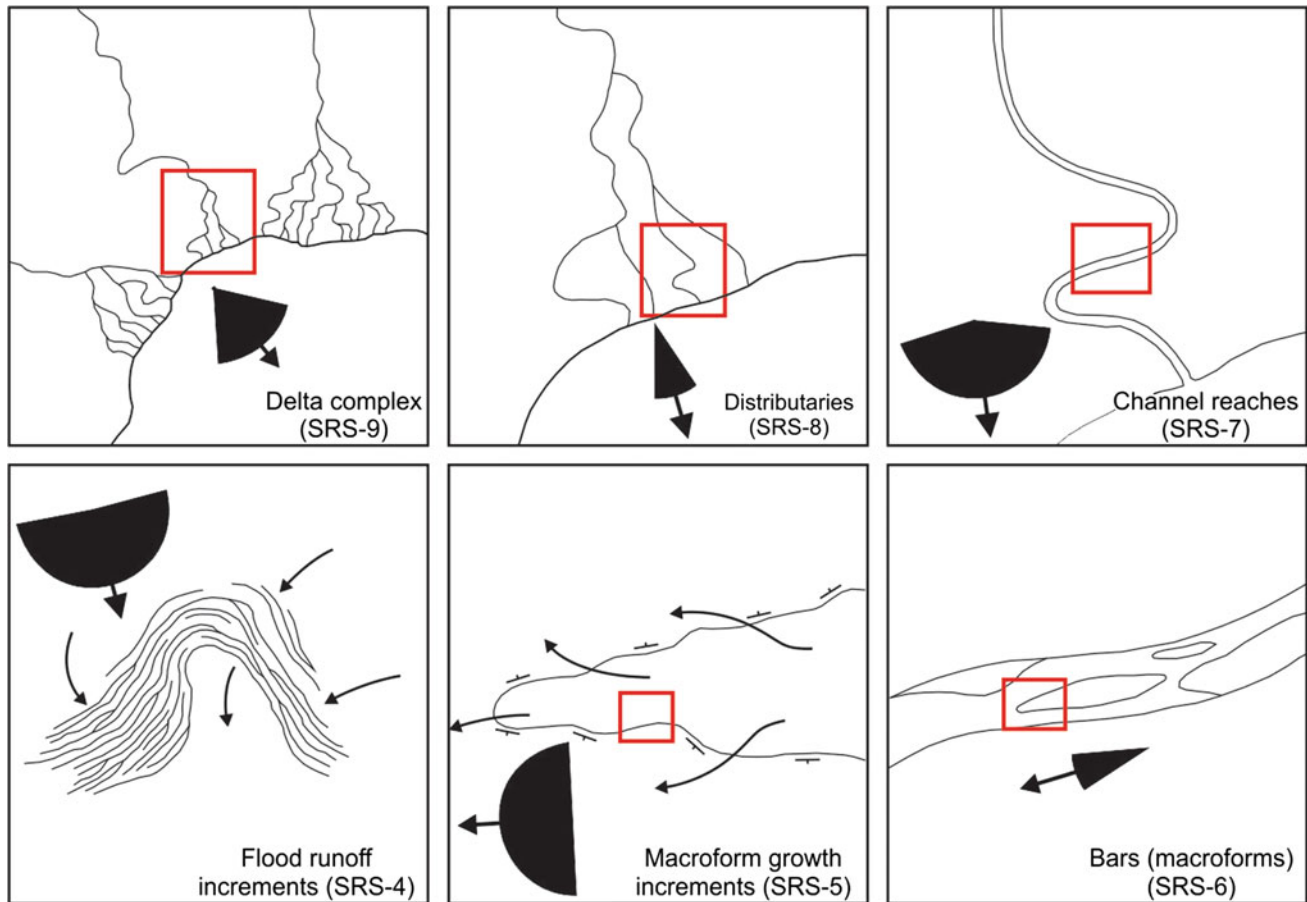


Fig. 6.61 Paleocurrent data plotted according to geographic scale, encompassing increasingly large areas moving anticlockwise from the *bottom left*. Each diagram corresponds to the area shown in the *red square* in the next diagram in an anticlockwise direction (adapted from Miall 1974)

shoreline or lithofacies contours are also important information. Another useful approach is to plot individual readings or small groups of readings collected in measured sections at the correct position in graphic section logs (e.g., Fig. 6.65). Some examples of how to use these data are discussed below. Potter and Pettijohn (1977) provided extensive examples and an annotated bibliography. Advanced methods for use in the analysis of fluvial systems are described by Miall (1996, Chap. 9).

Useful introductions to paleocurrent models have been published by Pettijohn (1962) and Selley (1968), but our increased understanding of clastic (siliciclastic, plus clastic-carbonate and evaporite) depositional systems requires a fresh look at the problem, because some of the earlier models are now seen to be simplistic. Many ideas are to be found in Reading (1996), although this book does not deal explicitly with paleocurrent models. Harms et al. (1975, 1982) provided several useful case studies.

Figure 6.62 provides examples of paleocurrent data plotted regionally according to stratigraphic position. They indicate

broad regional changes in dispersal directions that are interpreted in terms of changes in regional dispersal in response to tectonic tilting of the margin of the foreland basin.

Local paleocurrent distributions are commonly categorized as unimodal, bimodal, trimodal and polymodal. Each reflects a particular style of current dispersion. For example, the rose diagrams in Fig. 6.60 are unimodal to weakly bimodal, and vector mean directors are all oriented in easterly directions, roughly normal to the basin margin, with the exception of station 11C(G). The data were derived mainly from trough and planar crossbedding and parting lineation, and the environment of deposition is interpreted as braided fluvial (Miall and Gibling 1978). In some areas, for example, stations 6A, B, and C, there is a suggestion of a fanning out of the current systems, indicating possible deposition on large, sandy alluvial fans. The anomalous data set of station 11C(G) was derived from giant crossbed sets ranging from 1 to 6 m in thickness. They are interpreted as eolian dunes.

In high-sinuosity rivers, point bars dip at high angles to channel trends, whereas minor structures (mesoforms and

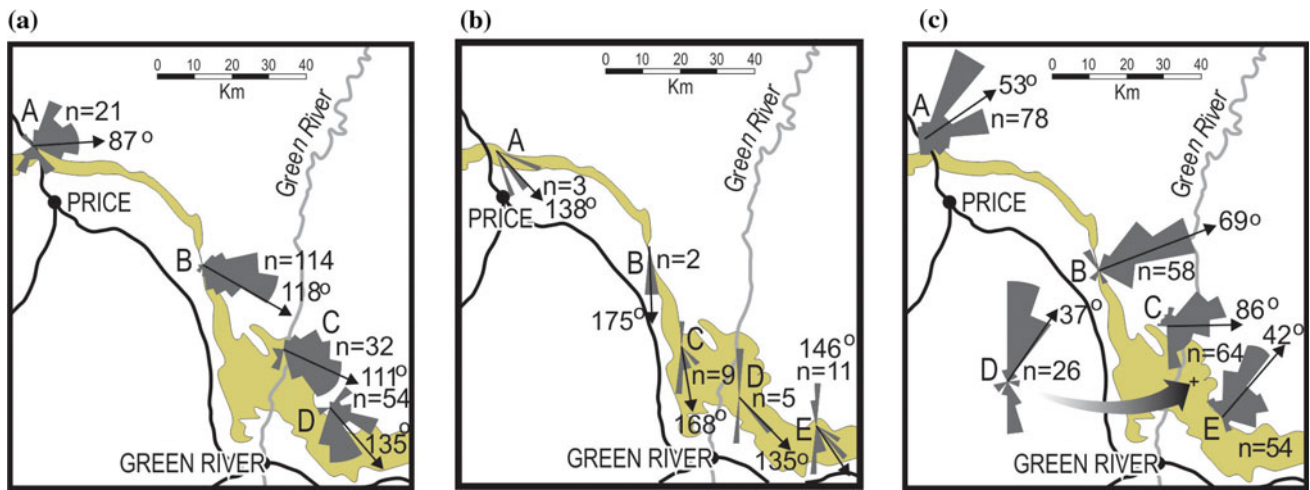


Fig. 6.62 An example of regional paleocurrent distributions. Each map shows outcrop summaries, and the variability between the maps indicates significant changes in regional paleocurrent dispersal, reflecting tectonic tilting (Willis 2000; Miall and Arush 2001a)

microforms) migrating down the point bars are oriented subparallel to channel direction and therefore parallel to the strike of point-bar (epsilon) crossbedding (Fig. 6.63). This paleocurrent pattern is a useful diagnostic criterion for recognizing point bars and distinguishing them from other large, low-angle crossbed types, such as Gilbertian deltas, or the downstream-accretion surfaces that are particularly common in braided rivers (e.g., Puigdefábregas 1973; Mossop and Flach 1983; Miall 1996). An example of how meticulous field measurements may be used to make detailed reconstructions of fluvial architecture is shown in Fig. 6.64. Such measurements are typically made as part of the analysis of large two- or three-dimensional outcrops (e.g., Fig. 2.3).

Although fluvial deposits typically yield unimodal paleocurrent patterns on an outcrop scale, on a larger scale they may show much more complex patterns, for example centripetal patterns indicating internal drainage (e.g., Friend and Moody-Stuart 1972) or bimodal patterns with the two modes at 90° and occurring in different lithofacies assemblages. Rust (1981) reported two examples of the latter case. In each case, one mode, occurring in coarse conglomerates, was interpreted as the product of alluvial fans prograding transversely out from the basin margin. The other mode, in interbedded sandstones, represented a trunk-river system draining longitudinally.

Coastal regions where rivers debouch into an area affected by waves and tides can give rise to very complex paleocurrent patterns (Fig. 4.14). Bimodal, trimodal, or polymodal distributions may result, for example, in the tide-swept offshore bar described by Klein (1970). However, time-velocity

asymmetry of tidal currents can result in local segregation of currents, so that they are locally unimodally ebb- or flood-dominated (Fig. 3.27). This could cause confusion at the outcrop level, because the tidal deltas showing such paleocurrent patterns may consist of lithofacies that are very similar to some fluvial deposits (although recent work has demonstrated the existence of a range of very subtle facies criteria that can be used to recognize a tidal signature: see Sect. 3.5.4). In wave-dominated environments, current reversals generate distinctive internal ripple-lamination patterns and herringbone crossbedding, as illustrated in Figs. 2.9 c and 3.27. Paleocurrent analyses of these bimodal crossbeds may yield much useful information on the direction of wave attack and hence on shoreline orientation. The term paleoslope means little in this environment because there are a diversity of local slopes and because waves and tides are only marginally influenced by the presence and orientation of bottom slopes.

Several examples of sandy shoreline deposits and their paleocurrent patterns are given by Harms et al. (1975, 1982). One of the most instructive is the section through the Cretaceous Gallup Sandstone, New Mexico, illustrated in Fig. 6.65. Individual trough and ripple orientations are shown at the left (north toward top). The shoreline is known from regional mapping to be oriented northwest-southeast. The top 2–3 m of section consists of low-angle, cross-stratified, beach-accretion sets dipping at a few degrees toward the northeast (offshore). This structure is typical of intertidal wave-swash zones (Fig. 4.14) Facies 2 (about 3–14 m in depth) consists of fine- to medium-grained sandstone with

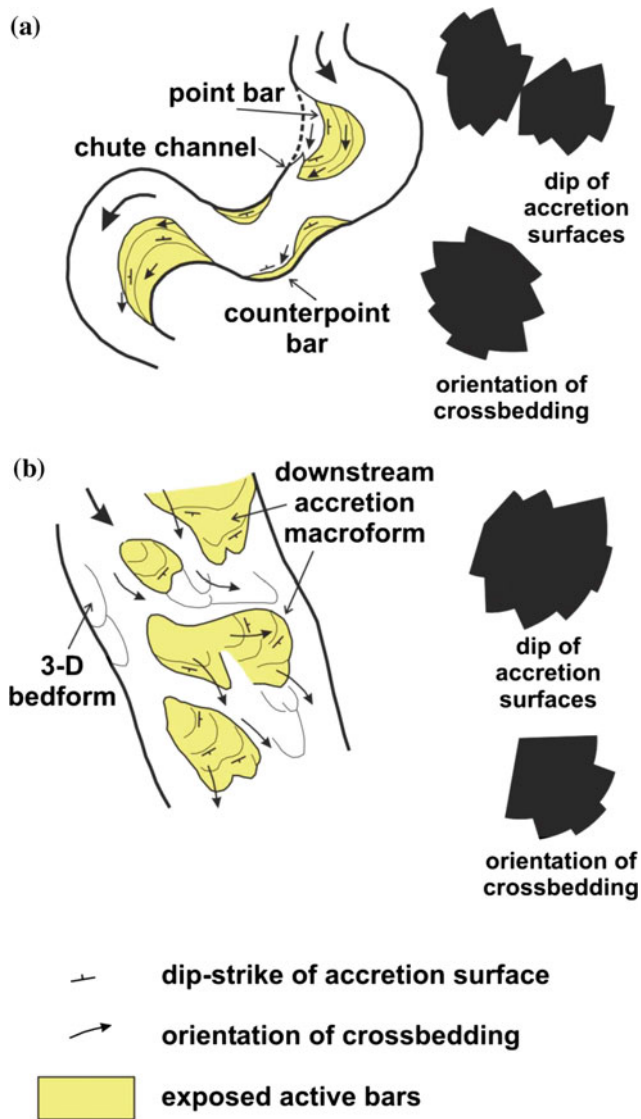


Fig. 6.63 Hypothetical examples of fluvial styles, indicating the range of orientations of dipping accretion surfaces and the variance of cross-bed orientations. **a** High-sinuosity river, such as a typical meandering river. Note that although there is a regional overlap of cross-bed and accretion-surface orientations, locally the two dips are oriented nearly perpendicular to each other, and the rose diagrams reflect this divergence. A counterpoint bar is shown. Such bars can be distinguished from the more common point bars by the fact that the accretion surfaces show curvature in plan view that is concave in a downdip direction, contrasting with the convex curvature of point-bar surfaces. Commonly such bars are characterized by finer grain sizes than other macroforms. **b** Low-sinuosity river—a typical sandy-braided river. Such rivers may show relatively high local channel sinuosity, in which case macroforms accreting downstream may also be oriented at a high angle to the regional trend. In the example shown here, mean directions are skewed to the southeast, diverging from the overall south-southeast channel orientation because of a major channel and bar complex (near the center of the reach) oriented in an eastward direction (Miall 1994b)

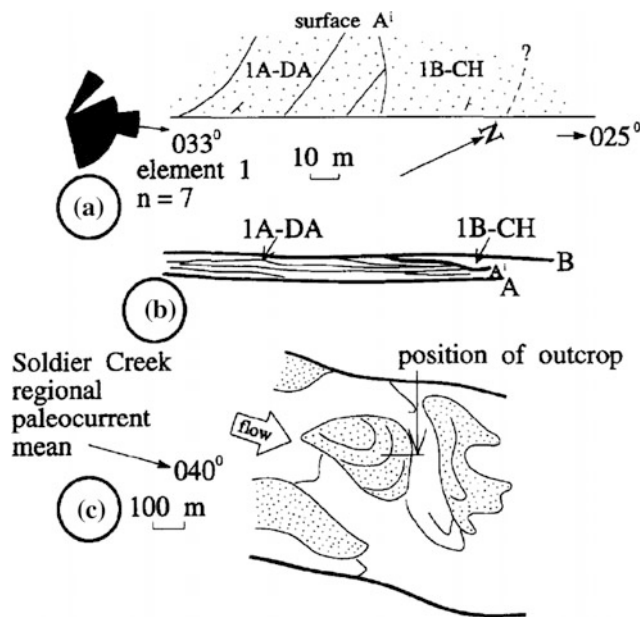


Fig. 6.64 An example of the type of architectural interpretation that may be made from the analysis of a vertical outcrop face, using paleocurrent data. A sketch of the relevant portion of the outcrop is shown in diagram B. Diagram A, above, shows a reconstruction of a plan view of the top bounding surface (surface B), with the suggested orientations of accretion surface, based on the measurements of dip and strike made at the outcrop face (dip-and-strike symbols). Diagram C shows the suggested interpretation of the outcrop, incorporating all orientation measurements of crossbedding (summarized in the rose diagram at top left). This is one of several worked examples provided by Miall (1994b)

trough and some planar cross-stratification. Foreset-dip and trough-axis orientations are mainly toward the northwest, southwest, and south to southeast, with the latter predominating, suggesting onshore-directed, wave-generated currents with local reversals and longshore currents directed toward the southeast. The same longshore-current pattern is apparent in the subtidal lower-shoreface deposits, which are dominated by storm-generated hummocky cross-stratification. Wave ripples are present in the lowest facies, again showing predominantly onshore-directed currents.

Submarine-fan and other deep-marine deposits show three main paleocurrent patterns:

1. Individual submarine fans prograde out from the continental slope and therefore show radial paleocurrent patterns with vector mean directions oriented perpendicular to the regional basin strike (e.g., Stow et al. 1996; see Fig. 6.66). This pattern is typical of many continental margins, particularly divergent margins.

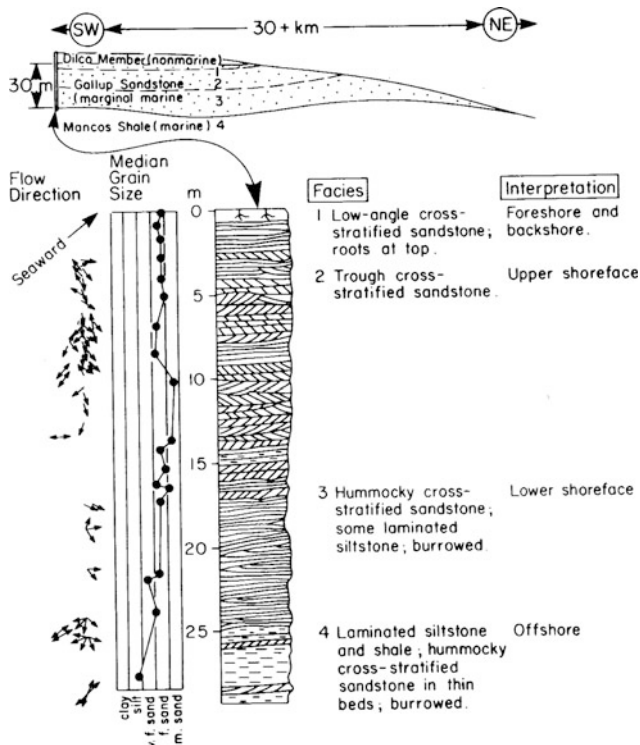


Fig. 6.65 Lithofacies profile, crossbed data, and interpreted depositional environments of the Gallup Sandstone (Cretaceous), New Mexico (Harms et al. 1975)

- In narrow oceans and many arc-related basins, deep-water sedimentation takes place in a trough oriented parallel to tectonic strike. Sediment-gravity flows, particularly low-viscosity turbidity currents, emerge from submarine fans and turn 90°, to flow longitudinally downslope, possibly for hundreds of kilometers. Current directions may be reversed by tilting of the basin. Many examples of this pattern have been published (e.g., Trettin 1970; Hesse 1974). Pickering and Hiscott (1985) used detailed grain-orientation measurements as a basis for reinterpreting anomalous paleocurrent measurements in a turbidite sequence. It was shown that supposed backset cross-lamination, attributed to upcurrent antidune migration, was in fact the product of turbidity currents that reversed direction as a result of deflection and reflection from the basin margins and internal topographic highs. Here is a case where subtle use was made of paleocurrent data to improve the sophistication of a basin-analysis case study.
- Contour currents or boundary undercurrents flow parallel to continental margins and generate paleocurrent patterns oriented parallel to basin margins. Stow and Lovell (1979) and Stow and Holbrook (1984) discussed the use of facies criteria and paleocurrent data in distinguishing these deposits.

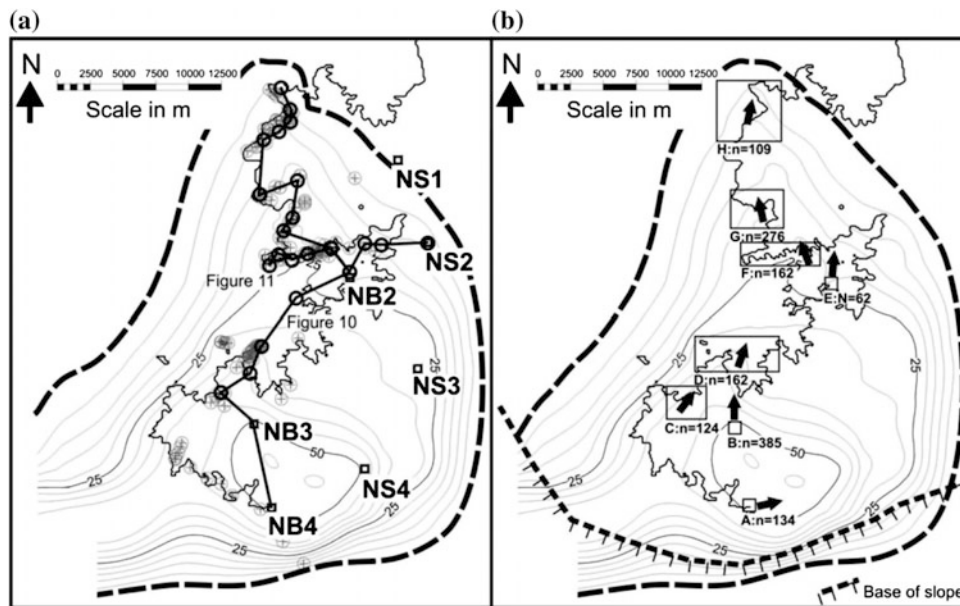


Fig. 6.66 a Isopach thickness map of Fan 3 constrained from integration of the core and outcrop data. Note the high rate of thinning to the south compared to the rest of the isopach map. Circles with crosses are outcrop logs, squares are borehole sites. **b** Paleocurrent arrows illustrate the general paleocurrent readings from Fan 3 across the entire study area from outcrop and Formation MicroImager

measurements from boreholes. Overall the trend is to the north; however, note the strong eastward trend in the south of the study area where stratigraphic thinning rates are highest. The east-directed readings are interpreted as turbidity-current directions prior to deflection northwards off an ENE–WSW trending slope, possibly the basin-margin slope (Hodgson et al. 2006, Fig. 9, p. 28)

References

- Ahlborn, M., Stemmerik, L., and Kalstø, T.-K., 2014, 3D seismic analysis of karstified interbedded carbonates and evaporites, Lower Permian Gipsdalen Group, Loppa High, southwestern Barents Sea: *Marine and Petroleum Geology*, v. 56, p. 16-33.
- Allen, J. R. L., 1963a, The classification of cross-stratified units, with notes on their origin: *Sedimentology*, v. 2, p. 93-114.
- Allen, J. R. L., 1963b, Henry Clifton Sorby and the sedimentary structures of sands and sandstones in relation to flow conditions: *Geologie en Mijnbouw*, v. 42, p. 223-228.
- Allen, J. R. L., 1966, On bed forms and paleocurrents: *Sedimentology*, v. 6, p. 153-190.
- Allen, J. R. L., 1967, Notes on some fundamentals of paleocurrent analysis, with reference to preservation potential and sources of variance: *Sedimentology*, v. 9, p. 75-88.
- Allen, P., 1972, Wealden detrital tourmaline: implications for north-western Europe: *Journal of the Geological Society of London*, v. 128, p. 273-294.
- Angulo, S., and Buatois, L. A., 2012, Integrating depositional models, ichnology, and sequence stratigraphy in reservoir characterization: The middle member of the Devonian-Carboniferous Bakken Formation of subsurface southeastern Saskatchewan revisited: *American Association of Petroleum Geologists Bulletin*, v. 96, p. 1017-1043.
- Bally, A. W., ed., 1987, Atlas of seismic stratigraphy: American Association of Petroleum Geologists Studies in Geology 27, in 3 vols.
- Basu, A., 1985, Influence of climate and relief on composition of sands released at source areas, in Zuffa, G. G., ed., *Provenance of arenites*: D. Reidel Publishing Company, Dordrecht, p. 1-18.
- Berg, R. R., 1968, point-bar origin of Fall River Sandstone reservoirs, northeastern Wyoming: *American Association of Petroleum Geologists Bulletin*, v. 52, p. 2116-2122.
- Bhattacharya, J. P., 2011, Practical problems in the application of the sequence stratigraphic method and key surfaces: integrating observations from ancient fluvial-deltaic wedges with Quaternary and modelling studies: *Sedimentology*, v. 58, p. 120-169.
- Blatt, H., Middleton, G. V., and Murray, R., 1980, *Origin of sedimentary rocks*; 2nd edition: Prentice-Hall Inc., Englewood Cliffs, New Jersey, 782 p.
- Blum, M., and Pecha, M., 2014, Mid-Cretaceous to Paleocene North American drainage reorganization from detrital zircons: *Geology*, v. 42, p. 607-610.
- Bohacs, K. M., Neal, J. E., and Grabowski, G. J., Jr., 2002, Sequence stratigraphy in fine-grained rocks: Beyond the correlative conformity: 22nd Annual Gulf Coast Section SEPM Foundation Bob F. Perkins Research Conference, p. 321-347.
- Bouma, A. H., Normark, W. R., and Barnes, N. E., eds., 1985, *Submarine fans and related turbidite systems*: Springer-Verlag Inc., Berlin and New York, 351 p.
- Bouma, A. H., Stelling, C. E., and Feeley, M. H., 1987, High-resolution seismic reflection profiles, in Bally, A. W., ed., *Atlas of seismic stratigraphy*: American Association of Petroleum Geologists Studies in Geology 27, v. 1, p. 72-94.
- Bradley, D. C., 1983, Paleocurrent directions from two-dimensional exposures of cross laminae in the Devonian flysch of Maine: *Journal of Geology*, v. 95, p. 271-279.
- Bridge, J. S., and Mackey, S. D., 1993, A theoretical study of fluvial sandstone body dimensions, in Flint, S. S., and Bryant, I. D., eds., *The geological modelling of hydrocarbon reservoirs and outcrop analogues*: International Association of Sedimentologists Special Publication 15, p. 213-236.
- Bridge, J. S., and Tye, R. S., 2000, interpreting the dimensions of ancient fluvial channel bars, channels, and channel belts from wire-line logs and cores: *American Association of Petroleum Geologists Bulletin*, v. 84, p. 1205-1228.
- Bristow, J. F., 2002, Real-time formation evaluation for optimal decision making while drilling: examples from the southern North Sea, in Lovell, M., and Parkinson, N., eds., *Geological applications of well logs*: American Association of Petroleum Geologists Methods in Exploration 13, p. 1-13.
- Brown, A. R., 1985, The role of horizontal seismic sections in stratigraphic interpretation, in Berg, O. R., and Woolverton, D. G., eds., *Seismic stratigraphy II*: American Association of Petroleum Geologists Memoir 39, p. 37-47.
- Brown, A. R., 1986, Interpretation of three-dimensional seismic data: *American Association of Petroleum Geologists Memoir 42*, 194 p.
- Brown, A. R., 2011, Interpretation of three-dimensional seismic data, seventh edition, *American Association of Petroleum Geologists Memoir 42*, 646 p.
- Burgess, P. M., Winefield, P., Minzoni, M., and Elders, C., 2013, Methods for identification of isolated carbonate buildups from seismic reflection data: *American Association of Petroleum Geologists*, v. 97, p. 1071-1098.
- Cant, D. J., 1992, Subsurface facies analysis, in Walker, R. G., and James, N. P., eds., *Facies models: response to sea level change*: Geological Association of Canada, St. John's, Newfoundland, p. 27-45.
- Cant, D. J., and Walker, R. G., 1976, Development of a braided-fluvial facies model for the Devonian Battery Point Sandstone, Quebec: *Canadian Journal of Earth Sciences*, v. 13, p. 102-119.
- Cervený, P. F., Naeser, N. D., Zeitler, P. K., Naeser, C. W., and Johnson, N. M., 1988, History of uplift and relief of the Himalaya during the past 18 million years: evidence from fission-track ages of detrital zircons from sandstones of the Siwalik Group, in Kleinspehn, K. L., and Paola, C., eds., *New perspectives in basin analysis*: Springer-Verlag Inc., Berlin and New York, p. 43-61.
- Cross, T. A., and Lessenger, M. A., 1988, *Seismic stratigraphy*: Annual Review of Earth and Planetary Sciences, v. 16, p. 319-354.
- Curry, J. R., 1956, The analysis of two-dimensional orientation data: *Journal of Geology*, v. 64, p. 117-131.
- Davies, R. J., Cartwright, J. A., Stewart, S. A., Lappin, M., and Underhill, J. R., eds., 2004a, 3D Seismic technology: Application to the exploration of sedimentary Basins: Geological Society, London, Memoir 29, 355 p.
- Davies, R. J., Stewart, S. A., Cartwright, J. A., Lappin, M., Johnston, R., Fraser, S. I., and Brown, A. R., 2004b, 3D seismic technology: are we realising its full potential? In Davies, R. J., Cartwright, J. A., Stewart, S. A., Lappin, M., and Underhill, J. R., eds., 3D Seismic technology: Application to the exploration of sedimentary Basins: Geological Society, London, Memoir 29, p. 1-9.
- Davies, R. J., Posamentier, H. W., Wood, L. J., and Cartwright, J. A., eds., 2007, *Seismic geomorphology: applications to hydrocarbon exploration and production*: Geological Society, London, Special Publication 277, 274 p.
- Davison, I., and Haszeldine, R. S., 1984, Orienting conventional cores for geological purposes: a review of methods: *Journal of Petroleum Geology*, v. 7, p. 461-466.
- DeCelles, P. G., 2004, Late Jurassic to Eocene evolution of the Cordilleran thrust belt and foreland basin system, western USA: *American Journal of Science*, v. 304, p. 105-168.
- DeCelles, P., Langford, R. P., and Schwartz, R. K., 1983, Two new methods of paleocurrent determination from trough cross-stratification: *Journal of Sedimentary Petrology*, v. 53, p. 629-642.
- Dickinson, W. R., 1970, Interpreting detrital modes of graywacke and arkose: *Journal of Sedimentary Petrology*, v. 40, p. 695-707.
- Dickinson, W. R., and Gehrels, G. E., 2003, U-Pb ages of detrital zircons from Permian and Jurassic eolian sandstones from the

- Colorado Plateau, USA: paleogeographic implications: *Sedimentary Geology*, v. 163, p. 29-66.
- Duk-Rodkin, A., Hughes, O.L., 1994. Tertiary–Quaternary drainage of the pre-glacial Mackenzie Basin. *Quaternary International* v. 22/ 23, p. 221 – 241.
- Ethridge, F. G., and Schumm, S. A., 2007, Fluvial seismic geomorphology: a view from the surface, in Davies, R. J., Posamentier, H. W., Wood, L. J., and Cartwright, J. A., eds., *Seismic geomorphology: applications to hydrocarbon exploration and production*: Geological Society, London, Special Publication 277, p. 205-222.
- Eyles, N., Day, T. E., and Gavican, A., 1987, Depositional controls on the magnetic characteristics of lodgement tills and other glacial diamict facies: *Canadian Journal of Earth Sciences*, v. 24, p. 2436-2458.
- Fielding, C. R., Whittaker, J., Henrys, S. A., Wilson, T. J., and Naish, T. R., 2008, Seismic facies and stratigraphy of the Cenozoic succession in McMurdo Sound, Antarctica: implications for tectonic, climatic and glacial history, *Palaeogeography, Palaeoclimatology, Palaeoecology*, v. 260, p. 8-29.
- Folk, R. L., 1968. *Petrology of Sedimentary Rocks*. Hemphill's, Austin, 170 p.
- Fox, A., and Vickerman, K., 2015, The value of borehole image logs: Reservoir, Canadian Society of Petroleum Geologists, January, p. 30-34.
- Franzinelli, E., and Potter, P. E., 1983, Petrology, chemistry and texture of modern river sands, Amazon river system: *Journal of Geology*, v. 91, p. 23-40.
- Friend, P.F., and Moody-Stuart, M., 1972, Sedimentation of the Wood Bay Formation (Devonian) of Spitsbergen: regional analysis of a late orogenic basin: *Norsk Polarinstitutt Skrifter* Nr. 157.
- Futalan, K., Mitchell, A., Amos, K., and Backe, G., 2012, Seismic facies analysis and structural interpretation of the Sandakan sub-basin, Sulu Sea, Philippines: *American Association of Petroleum Geologists, Search and Discovery Article* 30254.
- Galloway, W. E., 1981, Depositional architecture of Cenozoic Gulf Coastal Plain fluvial systems, in Ethridge, F. G., and Flores, R. M., eds., *Recent and ancient nonmarine depositional environments: models for exploration*: Society of Economic Paleontologists and Mineralogists Special Publication 31, p. 127-156.
- Gehrels, G. E., Dickinson, W. R., Ross, G. M., Stewart, J. H., Howell, D. G., 1995. Detrital zircon reference for Cambrian to Triassic miogeoclinal strata of western North America. *Geology* v. 23, p. 831-834.
- Gennaro, M., Wonham, J. P., Gawthorpe, R. and Saalen, G., 2013, Seismic stratigraphy of the Chalk Group in the Norwegian Central Graben, North Sea: *Marine and Petroleum Geology*, v. 45, p. 236-266.
- Graham, S. A., Tolson, R. B., DeCelles, P. G., Ingersoll, R. V., Bargar, E., Caldwell, M., Cavazza, W., Edwards, D. P., Follo, M. F., Handschy, J. F., Lemke, L., Moxon, I., Rice, R., Smith, G. A., and White, J., 1986, Provenance modeling as a technique for analyzing source terrane evolution and controls on foreland sedimentation, in Allen, P. A., and Homewood, P., eds., *Foreland basins: International Association of Sedimentologists Special Publication* 8, p. 425-436.
- Hailwood, E. A., and Kidd, R. B., eds., 1993, *High resolution stratigraphy*: Geological Society, London, Special Publication 70, 357 p.
- Hardage, B. A., 1985, Vertical seismic profiling—measurement that transfers geology to geophysics, in Berg, O. R., and Woolverton, D. G., eds., *Seismic stratigraphy II*: American Association of Petroleum Geologists Memoir 39, p. 13-34.
- Harms, J. C., Southard, J. B., Spearing, D. R., and Walker, R. G., 1975, Depositional environments as interpreted from primary sedimentary structures and stratification sequences: *Society of Economic Paleontologists and Mineralogists Short Course* 2, 161 p.
- Harms, J. C., Southard, J. B., and Walker, R. G., 1982, Structures and sequences in clastic rocks: *Society of Economic Paleontologists and Mineralogists Short Course* 9, Calgary.
- Hart, B. S., 2013, Whither seismic stratigraphy: Interpretation: A journal of subsurface characterization: *Society of Exploration Geophysicists and American Association of Petroleum Geologists*, v. 1, p. SA3-SA20.
- Heim, D., 1974, Über die feldspate in Germanischen Buntsandstein, ihre Korngrößenabhängigkeit, verbreitung und paleogeographische bedeutung: *Geol. Rundschau*, v. 63, p. 943-970.
- Heller, P. L., and Frost, C. D., 1988, Isotopic provenance of clastic deposits: applications of geochemistry to sedimentary provenance studies, in Kleinspehn, K. L., and Paola, C., eds., *New perspectives in basin analysis*: Springer-Verlag, New York, p. 27-42.
- Helmold, K. P., 1985, Provenance of feldspathic sandstones—the effect of diagenesis on provenance interpretations: a review: in Zuffa, G. G., ed., *Provenance of arenites*: D. Reidel Publishing Company, Dordrecht, p. 139-163.
- Hesse, R., 1974, Long-distance continuity of turbidites: possible evidence for an Early Cretaceous trench-abyssal plain in the East Alps: *Geological Society of America Bulletin*, v. 85, p. 859-870.
- Hildred, G. V., Martinez-Kulikowski, N., and Zaitlin, B. A., 2014, forensic chemostratigraphy: A tool to determine lateral wellbore placement: *Search and Discovery Article* 41359.
- Hodgson, D. M., Flint, S. S., Hodgetts, D., Drinkwater, N. J., Johannessen, E. P., and Luthi, S. M., 2006, Stratigraphic evolution of fine-grained submarine fan systems, Tanqua depocenter, Karoo Basin, South Africa: *Journal of Sedimentary Research*, v. 76, p. 20-40.
- Howard, J. L., 1993, The statistics of counting clasts in rudites: a review, with examples from the upper Paleogene of southern California, USA: *Sedimentology*, v. 40, p. 157-174.
- Hrouda, F., and Stránik, Z., 1985: The magnetic fabric of the Zdanice thrust sheet of the Flysch belt of the West Carpathians: sedimentological and tectonic implications: *Sedimentary Geology*, v. 45, p. 125-145.
- Hubbard, S. M., Smith, D. G., Nielsen, H., Leckie, D. A., Fustic, M., Spencer, R. J., and Bloom, L., 2011, Seismic geomorphology and sedimentology of a tidally influenced river deposit, Lower Cretaceous Athabasca oil sands, Alberta, Canada: *American Association of Petroleum Geologists Bulletin*, v. 95, p. 1123-1145.
- Hunter, R. E., 1981, Stratification styles in eolian sandstones: some Pennsylvanian to Jurassic examples from the Western Interior U.S. A., in Ethridge, F. G., and Flores, R., eds., *Recent and ancient nonmarine depositional environments: models for exploration*: Society of Economic Paleontologists and Mineralogists Special Publication 31, p. 315-329.
- Ingersoll, R. V., Bullard, T. F., Ford, R. L., Grimm, J. P., Pickle, J. D., and Sares, S. W., 1984, The effect of grain size on detrital modes: a test of the Gazzi-Dickinson point-counting method: *Journal of Sedimentary Petrology*, v. 54, p. 103-116.
- Jackson, R. G., II, 1975, Hierarchical attributes and a unifying model of bed forms composed of cohesionless material and produced by shearing flow: *Geological Society of America Bulletin*, v. 86, p. 1523-1533.
- Kauffman, E. G., 1986, High-resolution event stratigraphy: regional and global bio-events, in Walliser, O. H. ed., *Global bioevents: Lecture Notes on Earth History*: Springer-Verlag, Berlin, p. 279–335.
- Kauffman, E. G., 1988, Concepts and methods of high-resolution event stratigraphy: *Annual Reviews of Earth and Planetary Sciences*, v. 16, p. 605-654.

- Kelling, G., 1969: The environmental significance of cross-stratification parameters in an Upper Carboniferous fluvial basin: *Journal of Sedimentary Petrology*, v. 39, p. 857-875.
- Klein, G. deV., 1970, Depositional and dispersal dynamics of intertidal sand bars: *Journal of Sedimentary Petrology*, v. 40, p. 1095-1127.
- Krumbein, W. C., 1948, Lithofacies maps and regional sedimentary-stratigraphic analysis: *American Association of Petroleum Geologists*, v. 32, p. 1909-1923.
- Locklair, R. E., and Sageman, B. B., 2008, Cyclostratigraphy of the Upper Cretaceous Niobrara Formation, Western Interior, U.S.A.: A Coniacian-Santonian timescale: *Earth and Planetary Science Letters*, v. 269, p. 539-552.
- Long, D. G. F., 2006, Architecture of pre-vegetation sandy-braided perennial and ephemeral river deposits in the Paleoproterozoic Athabasca Group, northern Saskatchewan, Canada as indicators of Precambrian fluvial style: *Sedimentary Geology*, v. 190, p. 71-95.
- Leckie, D. A., Bhattacharya, J., Gilboy, C. F. and Norris, B., 1994, Colorado-Alberta Group strata of the Western Canada Sedimentary Basin, in: Mossop, G. D., and Shetsen, I., eds., *Geological Atlas of the Western Canada Sedimentary Basin*: Canadian Society of Petroleum Geologists and Alberta Research Council, Calgary, p. 335-352.
- Martin, J. H., 1993, A review of braided fluvial hydrocarbon reservoirs: the petroleum engineer's perspective, in: Best, J. L., and Bristow, C. S., eds., *Braided rivers*: Geological Society, London, Special Publication 75, p. 333-367.
- Martinez, J. F., Cartwright, J. A., Burgess, P. M., and Bravo, J. V., 2004, 3D seismic interpretation of the Messinian unconformity in the Valencia Basin, Spain, in Davies, R. J., Cartwright, J. A., Stewart, S. A., Lappin, M., and Underhill, J. R., eds., *3D Seismic technology: Application to the exploration of sedimentary Basins*: Geological Society, London, Memoir 29, p. 91-100.
- Matter, A., and Ramseyer, K., 1985, Cathodoluminescence microscopy as a tool for provenance studies of sandstones, in Zuffa, G. G., ed., *Provenance of arenites*: D. Reidel Publishing Company, Dordrecht, p. 191-211.
- McCrossan, R. G., 1961, Resistivity mapping and petrophysical study of Upper Devonian inter-reef calcareous shales of central Alberta, Canada: *American Association of Petroleum Geologists Bulletin*, v. 45, p. 441-470.
- McKee, E. D., and Weir, G. W., 1953, Terminology for stratification in sediments: *Geological Society of America Bulletin*, v. 64, p. 381-389.
- McMillan, N.J., 1973, Shelves of Labrador Sea and Baffin Bay, Canada, in: McCrossan, R. G., ed., *The Future Petroleum Provinces of Canada; Their Geology and Potential*, Canadian Society of Petroleum Memoir 1, p. 473-517.
- Miall, A. D., 1974, Paleocurrent analysis of alluvial sediments: a discussion of directional variance and vector magnitude: *Journal of Sedimentary Petrology*, v. 44, p. 1174-1185.
- Miall, A. D., 1976, Palaeocurrent and palaeohydrologic analysis of some vertical profiles through a Cretaceous braided stream deposit: *Sedimentology*, v. 23, p. 459-483.
- Miall, A. D., 1979, Mesozoic and Tertiary geology of Banks Island, Arctic Canada: the history of an unstable craton margin: *Geological Survey of Canada Memoir* 387.
- Miall, A. D., 1994b, Reconstructing fluvial macroform architecture from two-dimensional outcrops: examples from the Castlegate Sandstone, Book Cliffs, Utah: *Journal of Sedimentary Research*, v. B64, p. 146-158.
- Miall, A. D., 1996, *The geology of fluvial deposits: sedimentary facies, basin analysis and petroleum geology*: Springer-Verlag Inc., Heidelberg, 582 p.
- Miall, A. D., 1999, *Principles of sedimentary basin analysis*, Third edition: New York, N. Y.: Springer-Verlag Inc., 616 p.
- Miall, A. D., 2002, Architecture and sequence stratigraphy of Pleistocene fluvial systems in the Malay Basin, based on seismic time-slice analysis: *American Association of Petroleum Geologists Bulletin*, v. 86, p. 1201-1216.
- Miall, A. D., 2006, Reconstructing the architecture and sequence stratigraphy of the preserved fluvial record as a tool for reservoir development: a reality check; *American Association of Petroleum Geologists Bulletin* v. 90, p. 989-1002.
- Miall, A. D., 2014a, *Fluvial depositional systems*: Springer-Verlag, Berlin 316 p.
- Miall, A. D., and Arush, M., 2001a, The Castlegate Sandstone of the Book Cliffs, Utah: sequence stratigraphy, paleogeography, and tectonic controls: *Journal of Sedimentary Research*, v. 71, p. 536-547.
- Miall, A. D., and Gibling, M. R., 1978, The Siluro-Devonian clastic wedge of Somerset Island, Arctic Canada, and some regional paleogeographic implications: *Sedimentary Geology*, v. 21, p. 85-127.
- Minter, W. E. L., 1978, A sedimentological synthesis of placer gold, uranium and pyrite concentrations in Proterozoic Witwatersrand sediments, in Miall, A. D., ed., *Fluvial Sedimentology*: Canadian Society of Petroleum Geologists Memoir 5, p. 801-829.
- Moonan, X. R., 2011, 4-D understanding of the evolution of the Penal/Barrackpore Anticline, southern sub-basin, Trinidad: *American Association of Petroleum Geologists, Search and Discovery Article* 90135.
- Morton, A. C., 1985a, Heavy minerals in provenance studies, in Zuffa, G. G., ed., *Provenance of arenites*: D. Reidel Publishing Company, Dordrecht, p. 249-277.
- Morton, A. C., 1985b, A new approach to provenance studies: electron microprobe analysis of detrital garnets from Middle Jurassic sandstones of the northern North Sea: *Sedimentology*, v. 32, p. 553-566.
- Morton, A. C., and Hallsworth, C. R., 1994, identifying provenance-specific features of detrital heavy mineral assemblages in sandstones: *Sedimentary Geology*, v. 90, p. 241-256.
- Morton, A. C., and Hallsworth, C. R., 1999, Processes controlling the composition of heavy mineral assemblages in sandstones: *Sedimentary Geology*, v. 124, p. 3-29.
- Moscardelli, L., Wood, L. J., and Dunlap, D. B., 2012, Shelf-edge deltas along structurally complex margins" A case study from eastern offshore Trinidad: *American Association of Petroleum Geologists*, v. 96, p. 1483-1522.
- Mossop, G. D., and Flach, P. D., 1983, Deep channel sedimentation in the Lower Cretaceous McMurray Formation, Athabasca Oil Sands, Alberta: *Sedimentology*, v. 30, p. 493-509.
- Mutti, E., and Ricci-Lucchi, F., 1972, Le turbiditi dell'Appennino settentrionale: introduzione all'analisi di facies: *Soc. Geol. Ital. Mem.* 11, p. 161-199.
- Myhr, D. W., and Meijer-Drees, N. C., 1976, Geology of the southeastern Alberta Milk River gas pool; in Lerand, M. M., ed., *The sedimentology of selected clastic oil and gas reservoirs in Alberta*: Canadian Society of Petroleum Geologists, p. 96-117.
- Nelson, R. A., Lenox, L. C., and Ward, B. J., Jr., 1987, Oriented core: its use, error, and uncertainty: *American Association of Petroleum Geologists Bulletin*, v. 71, p. 357-367.
- Nilsen, T., Shew, R., Steffens, G., and Studlick, J., eds., 2007, *Atlas of deep-water outcrops*: American Association of Petroleum Geologists, *Studies in Geology* 56, 504 p.
- Oliver, T. A., and Cowper, N. W., 1963, Depositional environments of the Ireton Formation, central Alberta: *Bulletin of Canadian petroleum Geology*, v. 11, p. 183-202.
- Oliver, T. A., and Cowper, N. W., 1965, Depositional environments of the Ireton Formation, central Alberta: *Bulletin of the American Association of Petroleum Geologists*, v. 49, p. 1410-1425.

- Olson, J. S., and Potter, P. E., 1954, Variance components of crossbedding direction in some basal Pennsylvanian sandstones of the eastern Interior Basin: statistical methods: *Journal of Geology*, v. 62, p. 26-49.
- Parks, J. M., 1970, Computerized trigonometric solution for rotation of structurally tilted sedimentary directional features: *Geological Society of America Bulletin*, v. 81, p. 537-540.
- Pearce, T. J., Besly, N. M., Wray, D. S., and Wright, D. K., 1999, Chemostratigraphy: a method to improve interwell correlation in barren sequences — a case study using onshore Duckmantian/Stephanian sequences (West Midlands, U.K.): *Sedimentary Geology*, v. 124, p. 197-220.
- Pettijohn, F. J., 1962, Paleocurrents and paleogeography: *American Association of Petroleum Geologists Bulletin*, v. 46, p. 1468-1493.
- Pettijohn, F. J., Potter, P. E., and Siever, R., 1973, *Sand and sandstone*: Springer-Verlag, New York, 618 p.
- Pickering, K. T., and Hiscott, R. N., 1985, Contained (reflected) turbidity currents from the Middle Ordovician Cloridorme Formation, Quebec, Canada: an alternative to the antidune hypothesis: *Sedimentology*, v. 32, p. 373-394.
- Pirmez, C., Prather, B. E., Mallarino, G., O'Hayer, W. W., Droxler, A. W., and Winker, C. D., 2012, Chronostratigraphy of the Brazos-Trinity depositional system, western Gulf of Mexico: implications for deepwater depositional models, in *Applications of the Principles of seismic geomorphology to continental slope and base-of-slope systems: case studies from seafloor and near-seafloor analogues*: Society for Sedimentary Geology Special Publication 99, p. 111-143.
- Pöppelreiter, M., Garcia-Carballido, C., and Kraaijveld, M. A., eds., 2010, Dipmeter and borehole image log technology, *American Association of Petroleum Geologists, Memoir 92*.
- Posamentier, H. W., 2000, Seismic stratigraphy into the next millennium: a focus on 3-D seismic data: *American Association of Petroleum Geologists, Annual Conference, New Orleans*, p. 16-19.
- Posamentier, H. W., and Kolla, V., 2003, Seismic geomorphology and stratigraphy of depositional elements in deep-water settings: *Journal of Sedimentary Research*, v. 73, p. 367-388.
- Posamentier, H. W., Davies, R. J., Cartwright, J. A., and Wood, L., 2007, Seismic geomorphology — an overview, in Davies, R. J., Posamentier, H. W., Wood, L. J., and Cartwright, J. A., eds., *Seismic geomorphology: applications to hydrocarbon exploration and production*: Geological Society, London, Special Publication 277, p. 1-14.
- Potter, P. E., and Pettijohn, F. J., 1977, *Paleocurrents and basin analysis*, 2nd edition: Academic Press, San Diego, California, 296 p.
- Puigdefábregas, C., 1973, Miocene point-bar deposits in the Ebro Basin, northern Spain: *Sedimentology*, v. 20, p. 133-144.
- Rahmani, R. A., and Lerbekmo, J. F., 1975, Heavy mineral analysis of Upper Cretaceous and Paleocene sandstones in Alberta and adjacent areas of Saskatchewan, in Caldwell, W. G. E. ed., *The Cretaceous system in the Western Interior of North America*: Geological Association of Canada Special Paper 13, p. 607-632.
- Raines, M. K., Hubbard, S. M., Kukulski, R. B., Leier, A. L., and Gehrels, G. E., 2013, Sediment dispersal in an evolving foreland: detrital zircon geochronology from Upper Jurassic and lowermost Cretaceous strata, Alberta Basin, Canada, *Geological Society of America Bulletin*, v. 125, p. 741-755
- Ramsey, J. G., 1961, The effects of folding upon the orientation of sedimentation structures: *Journal of Geology*, v. 69, p. 84-100.
- Ratcliffe, K. T., and Zaitlin, B. A., eds., 2010, *Application of modern stratigraphic techniques: theory and case histories*: Society for Sedimentary Geology (SEPM) Special Publication 94, 241 p.
- Reading, H. G., ed., 1996, *Sedimentary environments: processes, facies and stratigraphy*, third edition: Blackwell Science, Oxford, 688 p.
- Rich, J. L., 1951, Three critical environments of deposition and criteria for recognition of rocks deposited in each of them: *Geological Society of America Bulletin*, v. 62, p. 1-20.
- Rosenthal, L. R. P. and Walker, R. G., 1987, Lateral and vertical facies sequences in the Upper Cretaceous Chungo Member, Wapiabi Formation, southern Alberta: *Canadian Journal of Earth Sciences*, v. 24, p. 771-783.
- Rosenthal, L. R. P., Leckie, D. A. and Nadon, G., 1984, Depositional cycles and facies relationships within the Upper Cretaceous Wapiabi and Belly River formations of west-central Alberta: *Canadian Society of Petroleum Geologists, Field Trip Guide Book*, 54.
- Rupke, N. A., 1978, Deep clastic seas, in Reading, H. G., ed., *Sedimentary environments and facies*: Blackwell, Oxford, p. 372-415.
- Rust, B. R., 1975, Fabric and structure in glaciofluvial gravels, in Jopling, A. V., and McDonald, B. C., eds., *Glaciofluvial and glaciolacustrine sedimentation*: Society of Economic Paleontologists and Mineralogists Special Publication 23, p. 238-248.
- Rust, B. R., 1981, Alluvial deposits and tectonic style: Devonian and Carboniferous successions in eastern Gaspe, in Miall, A. D., ed., *Sedimentation and tectonics in alluvial basins*: Geological Association of Canada Special Paper 23, p. 49-76.
- Ryan, W. B. F., and Cita, M. B., 1978, The nature and distribution of Messinian erosional surfaces — indicators of a several-kilometres-deep Mediterranean in the Miocene: *Marine geology*, v. 27, p. 193-230.
- Safronova, P. A., Henriksen, S., Andreassen, K., Laberg, J. S., and Vorren, T. O., 2014, Evolution of shelf-margin clinofolds and deep-water fans during the middle Eocene in the Sørvestsnaget Basin, southwest Barents Sea: *American Association of Petroleum Geologists Bulletin*, v. 98, p. 515-544.
- Sageman, B. B., Singer, B. S., Meyers, S. R., Siewert, S. E., Walaszczyk, I., Condon, D. J., Jicha, B. R., Obradovich, J. D., and Sawyer, D. A., 2014, Integrating $^{40}\text{Ar}/^{39}\text{Ar}$ and astronomical clocks in the Cretaceous Niobrara Formation, Western Interior Basin, USA: *Geological Society of America Bulletin*, v. 126, p. 956-973.
- Saller, A. H., Noah, J. T., Ruzuar, A. P., and Schneider, R., 2004, Linked lowstand delta to basin-floor fan deposition, offshore Indonesia: an analog for deep-water reservoir systems: *American Association of Petroleum Geologists Bulletin*, v. 88, p. 21-46.
- Sangree, J. B., and Widmier, J. M., 1977, Seismic stratigraphy and global changes of sea level, part 9: Seismic interpretation of clastic depositional facies, in Payton, C. E., ed., *Seismic stratigraphy — applications to hydrocarbon exploration*: American Association of Petroleum Geologists Memoir 26, p. 165-184.
- Savit, C. H., and Changsheng, W. V., 1982, Geophysical characterization of lithology—application to subtle traps; in Halbouty, M. T., ed., *The deliberate search for the subtle trap*: American Association of Petroleum Geologists Memoir 32, p. 11-30.
- Sayago, J., Di Lucia, M., Mutti, M., Cotti, A., Sitta, A., Broberg, K., Przybylo, A., Buonaguro, R. and Zimina, O., 2012, Characterization of a deeply buried paleojarst terrain in the Loppa High using core data and multiattribute seismic facies classification: *American Association of Petroleum Geologists*, v. 96, p. 1843-1866.
- Schnitzer, W. A., 1977, Die quarkornfarben-methoden und ihre Bedeutung für die stratigraphische und palaeogeographische erforschung psammitischer sedimente: *Erlanger Geol. Abh., Heft 103*, 28 p.
- Selley, R. C., 1968, A classification of paleocurrent models: *Journal of Geology*, v. 76, p. 99-110.
- Shank, J. A., and Plint, A. G., 2013, Allostratigraphy of the Upper Cretaceous Cardium Formation in subsurface and outcrop in southern Alberta, and correlation to equivalent strata in

- northwestern Montana: *Bulletin of Canadian Petroleum Geology*, v. 61, p. 1-40.
- Sharma, P. V., 1986, *Geophysical methods in geology: 2nd Edition*: Elsevier Scientific Publications, Amsterdam, 442 p.
- Sheriff, R. E., 1985, Aspects of seismic resolution, in Berg, O. R., and Woolverton, D. G., eds., *Seismic stratigraphy II: American Association of Petroleum Geologists Memoir 39*, p. 1-10.
- Simons, D. B., and Richardson, E. V., 1961, Forms of bed roughness in alluvial channels: *American Society of Civil Engineers Proceedings*, v. 87, No. HY3, p. 87-105.
- Simons, D. B., Richardson, E. V., and Nordin, C. F., 1965, Sedimentary structures generated by flow in alluvial channels, in Middleton, G. V., ed., *Primary sedimentary structures and their hydrodynamic interpretation: Society of Economic Paleontologists and Mineralogists Special Publication 12*, p. 34-52.
- Sloss, L. L., Krumbain, W. C., and Dapples, E. C., 1949, Integrated facies analysis; in Longwell, C. R., ed., *Sedimentary facies in geologic history: Geological Society of America Memoir 39*, p. 91-124.
- Smith, N. D., 1972, Some sedimentological aspects of planar cross-stratification in a sandy braided river: *Journal of Sedimentary Petrology*, v. 42, p. 624-634.
- Smith, T., and Leone, J., 2014, Shallow onlap model for Ordovician and Devonian organic-rich shales, New York State: *American Association of Petroleum Geologists Search and Discovery Article #50911*.
- Southcott, A., 2014, 3D seismic proves its value in Bakken geosteering: *Search and Discovery article 41435*.
- Stark, T. J., Zeng, H., and Jackson, A., 2013, An introduction to this special section: *Chronostratigraphy: The Leading Edge*, v. 32, p. 132-138.
- Stow, D. A. V., and Holbrook, J. A., 1984, North Atlantic contourites: an overview, in Stow, D. A. V., and Piper, D. J. W., eds., *Fine-grained sediments: deep-water processes and facies: Geological Society of London Special Publication 15*, p. 245-256.
- Stow, D. A. V., and Lovell, J. P. B., 1979, Contourites: their recognition in modern and ancient sediments: *Earth Science Reviews*, v. 14, p. 251-291.
- Stow, D. A. V., Reading, H. G., and Collinson, J. D., 1996, Deep seas, in Reading, H. G., *Sedimentary environments: processes, facies and stratigraphy*, 3rd edition: Blackwell Science, Oxford, p. 395-453.
- Suttner, L. J., 1974, Sedimentary petrographic provinces: an evaluation, in Ross, C. A., ed., *Paleogeographic provinces and provinciality: Society of Economic Paleontologists and Mineralogists Special Publication 21*, p. 75-84.
- Suttner, L. J., Basu, A., Decker, J., Helmhold, K. P., Ingersoll, R. V., et al., 1985: The effect of grain size on detrital modes: a test of the Gazzi-Dickinson point-counting method: discussions and replies: *Journal of Sedimentary Petrology*, v. 55, p. 616-621.
- Taylor, M. S. G., 2010, Visualization and the use of real time data while geosteering – onshore Algeria: *Search and Discovery Article 40592*.
- Thomas, W. A., 2011, detrital-zircon geochronology and sedimentary provenance: *Lithosphere, Geological Society of America*, v. 3, p. 304-308.
- Trettin, H. P., 1970, Ordovician-Silurian flysch sedimentation in the axial trough of the Franklinian Geosyncline, northeastern Ellesmere Island, Arctic Canada, in Lajoie, J., ed., *Flysch sedimentology in North America: Geological Association of Canada Special Paper 7*, p. 13-35.
- Tye, R. S., 1991, Fluvial-sandstone reservoirs of the Travis Peak Formation, East Texas Basin, in Miall, A. D., and Tyler, N., eds., *The three-dimensional facies architecture of terrigenous clastic sediments, and its implications for hydrocarbon discovery and recovery: Society of Economic Paleontologists and Mineralogists Concepts and Models Series*, v. 3, p. 172-188.
- Vail, P. R., Mitchum, R. M., Jr., Todd, R. G., Widmier, J. M., Thompson, S., III, Sangree, J. B., Bubba, J. N., and Hatlelid, W. G., 1977, Seismic stratigraphy and global changes of sea-level, in Payton, C. E., ed., *Seismic stratigraphy - applications to hydrocarbon exploration: American Association of Petroleum Geologists Memoir 26*, p. 49-212.
- Veeken, 2007, *Seismic stratigraphy, basin analysis and reservoir characterization*: Elsevier, Amsterdam, *Seismic Exploration*, v. 37, 509 p.
- Visher, G. S., 1965, Use of vertical profile in environmental reconstruction; *American Association of Petroleum Geologists Bulletin*: v. 49, p. 41-61.
- Walaszczyk, I., Shank, J. A., Plint, A. G., and Cobban, W. A., 2014, Interregional correlation of disconformities in Upper Cretaceous strata, Western Interior Seaway: Biostratigraphic and sequence-stratigraphic evidence for eustatic change: *Geological Society of America Bulletin*, v. 126, p. 307-316.
- Walker, R. G., 1978, Deep-water sandstone facies and ancient submarine fans: models for exploration for stratigraphic traps: *American Association of Petroleum Geologists Bulletin*, v. 62, p. 932-966.
- Wells, N. A., 1988, Working with paleocurrents: *Journal of Geological Education*, v. 35, p. 39-43.
- Willis, A. J., 2000, Tectonic control of nested sequence architecture in the Sego Sandstone, Neslen Formation, and Upper Castlegate Sandstone (Upper Cretaceous), Sevier Foreland Basin, Utah, U.S. A.: *Sedimentary Geology*, v. 136, p. 277-318.
- Woodcock, N. H., 1979, The use of slump structures as palaeoslope orientation estimators: *Sedimentology*, v. 26, p. 83-99.
- Wray, D. S., and Gale, A. S., 1993, Geochemical correlation of marl bands in Turonian chalks of the Anglo-Paris basin, in Hailwood, E. A., and Kidd, R. B., eds., *High resolution stratigraphy: Geological Society, London, Special Publication 70*, p. 211-226.
- Wright, A. M., Ratcliffe, K. T., Zaitlin, B. A., and Wray, D. S., 2010, The application of chemostratigraphic techniques to distinguish compound incised valleys in low-accommodation incised-valley systems in a foreland-basin setting: an example from the Lower Cretaceous Mannville Group and Basal Colorado Sandstone (Colorado Group), Western Canadian Sedimentary Basin, in Ratcliffe, K. T., and Zaitlin, B. A., eds., *Application of modern stratigraphic techniques, Society for Sedimentary geology, Special Publication 94*, p. 93-107.
- Zaitlin, B. A., Warren, M. J., Potocki, D., Rosenthal, L., and Boyd, R., 2002, depositional styles in a low accommodation foreland basin setting: an example from the Basal Quartz (Lower Cretaceous), southern Alberta: *Bulletin of Canadian Petroleum Geology*, v. 50, p. 31-72.
- Zeng, H., Backus, M., Barrow, K. T., and Tyler, N., 1996, Facies mapping from three-dimensional seismic data: potential and guidelines from a Tertiary sandstone-shale sequence model, Powderhorn field, Calhoun County, Texas: *American Association of Petroleum Geologists Bulletin*, v. 80, p. 16-46.
- Zeng, H., Henry, S. C., and Riola, J. P., 1998, Stratal slicing, Part II: Real 3-D seismic data: *Geophysics*, v. 63, p. 514-522.
- Zeng, H., Loucks, R., Janson, X., Wang, G., Xia, Y., Yuan, B., and Xu, L., 2011, Three-dimensional seismic geomorphology and analysis of the Ordovician paleokarst drainage system in the central Tabei Uplift, northern Tarim Basin, western China: *American Association of Petroleum Geologists*, v. 95, p. 2061-2083.
- Zeng, H., Zhu, X., and Zhu, R., 2013, new insights into seismic stratigraphy of shallow-water progradational sequences: subseismic clinoforms: *Interpretation: A journal of subsurface characterization*:

- Society of Exploration Geophysicists and American Association of Petroleum Geologists, v. 1, p. SA35-SA51.
- Zuffa, G. G., ed., 1985a, Provenance of arenites: D. Reidel Publishing Company, Dordrecht, 408 p.
- Zuffa, G. G., 1985b, Optical analyses of arenites: influence of methodology on compositional results; in Zuffa, G. G., ed., Provenance of arenites: D. Reidel Publishing Company, Dordrecht, p. 165-189.
- Zuffa, G. G., 1987, Unravelling hinterland and offshore paleogeography from deep-water arenites, in Leggett, J. K., and Zuffa, G. G., eds., Marine clastic sedimentology, concepts and case studies: Graham and Trotman, London, p. 39-61.